Institute of Bioorganic Chemistry
Polish Academy of Sciences in Poznan
Integrative Biology Team

The *C. elegans* “hibernation”: surviving cold through ferritin-mediated iron detoxification

Alicja Komur

A dissertation supervisor: **Dr. hab. Rafał Ciosk, prof. IBCh PAS**

A dissertation co-supervisor: **Dr. Daria Sobańska**

Poznan, 2022

I would like to thank:

My supervisor, Dr. hab. Rafał Ciosk

for giving me the opportunity to work on this challenging but interesting and meaningful project

My co-supervisor, Dr. Daria Sobańska

for understanding, invaluable help in writing this dissertation, and all of the scientific support

All of the laboratory members

for support and valuable scientific discussions

My family and friends

for invaluable faith in me during all hard times

My fiancé, Szymon

who always knew what to do to, how to support me and convenience me to not give up. Thank you for limitless faith in my skills, understanding and invaluable patience

Founding:

- This work resulted from the implementation of the research project number POIR.04.04.00-00-203A/16 carried out within the Team program of the Foundation for Polish Science, co-financed by the European Union under the European Regional Development Fund.
- This work resulted from the implementation of the research project number 2019/34/A/NZ3/00223 funded by the National Science Center

LIST OF FIGURES

LIST OF TABLES

LIST OF ABBREVIATIONS

A - adenine

ACO - aconitase

ACT - actin

AGE - ageing alternation

AKT - AKT kinase family

APS - ammonium persulfate

ATAD - ATPase family with AAA domain homolog

BAT - brown adipose tissue

BPB - bromophenol blue

BSA - bovine serum albumin

C - cytosine

C. elegans - *Caenorhabditis elegans*

CAT - catalase

cDNA - complementary DNA

CEBP - C/EBP (CCAAT/enhancer-binding protein) homolog

CGC - Caenorhabditis Genetics Center

cGMP - cyclic guanosine monophosphate

CRISPR/Cas9 - clustered regularly interspaced short palindromic repeats and CRISPR-associated protein 9

Ct - cycle threshold

CTL - catalase

DAF - abnormal dauer formation

DBE - DAF-16 binding element

DEG - degeneration of certain neurons

DFO - deferoxamine

DHE - dihydroethidium

DIC - differential interference contrast

DMSO - dimethyl sulfoxide

DMT - divalent metal transporter

DNA - deoxyribonucleic acid

DNase - deoxyribonuclease

DPY - dumpy: shorter than wild-type

DTT - dithiothreitol

E – glutamic acid

EDTA - ethylenediaminetetraacetic acid

EGL - egg laying defective

ELT - erythroid-like transcription factor family

ENDU - endonuclease, poly(U) specific

E. coli - *Escherichia coli*

ETS - E twenty six

F - forward

FAC - ferric ammonium citrate

Fer1HCH - ferritin 1 heavy chain homologue

Fer2LCH - ferritin 2 light chain homologue

FO-dead - ferroxidase inactive

FOXO - forkhead box class O

FoxO3a - Forehead box O3

FPN - ferroportin

FSHR - mammalian follicle stimulating hormone receptor

FTH - ferritin heavy chain

FTHL17 - ferritin heavy chain like 17

FTL - ferritin light chain

FTN - ferritin

FTT - fourteen-three-three family

G - guanine

G (amino acid) - glycine

GCS - gamma glutamylcysteine synthetase

GFP - green fluorescent protein

GLO - gut granule loss

Glu – glutamic acid

GPX - glutathione peroxidase

GST - glutathione S-transferase

H (amino acid) - histidine

HCF - human host cell factor related

HIF – hypoxia-inducible factor

His - histidine

HLH - helix loop helix

HRE - hypoxia-response element

HSF - heat shock factor

HSP - heat shock protein

IDE – iron-dependent element

IGFR - insulin-like growth factor receptor

IIS - insulin/insulin-like growth factor (IGF)-1 signaling

ILP - insulin-like peptide

INS - insulin related

IPTG - isopropyl β- d-1-thiogalactopyranoside

IRE - iron response element

IRP - iron-regulatory protein

K - lysine

LB - Luria Broth

LIPS - lipase related

M - middle

MCPIP - monocyte chemotactic protein-induced protein

MDL - Mad-like

MFN - mitoferrin

MFRN - mitoferrin

MosSCI - mos1 mediated single copy insertion

mRNA - messenger RNA

mTOR - mammalian target of rapamycin

NAC - N-acetyl-L-cysteine

NGM - nematode growth media

NRF - NF-E2-related factor

OCR - OSM-9 and capsaicin receptor-related

OE - overexpression

OSM - osmotic avoidance abnormal

P - phosphorylation

PAR - abnormal embryonic partitioning of cytoplasm

PBS - phosphate-buffered saline

PBS-T - phosphate-buffered saline with tween

PCR - polymerase chain reaction

PDK - PDK-class protein kinase

PI3K - phosphoinositide 3-kinase

PIP2 - phosphatidylinositol 4,5-bisphosphate

PIP3 - phosphatidylinositol (3,4,5)-trisphosphate

PKC - protein kinase C

PQM - paraquat (methylviologen) responsive

PRDX - peroxiredoxin

PTEN - phosphatase and tensin homolog

R - reverse

RAF - strain's number in the Ciosk lab collection

REGE - regnase

RLE - regulation of longevity by E3 ubiquitin ligase

RNA - ribonucleic acid

RNAi - RNA interference

RNase - ribonuclease

RNA-seq - RNA sequencing

ROS - reactive oxygen species

RT-qPCR – real-time quantitative PCR

SDS - sodium dodecyl sulfate

sec. - seconds

SEC-ICP-MS - size exclusion chromatography-inductively coupled plasma-mass spectrometry

seq - sequencing

SGK - serum- and glucocorticoid- inducible kinase homolog

sgRNA - single guide RNA

SKN - skinhead

SMF - yeast SMF (divalent cation transporter) homolog

SMK - SMEK (dictyostelium suppressor of MEK null) homolog

SOD - superoxide dismutase

SPDEF - SAM pointed domain containing ETS transcription factor

SVH - suppressor of vhp-1 deletion lethality

T - thymine

T2DM - type 2 diabetes mellitus

TAE - tris-acetate-EDTA

TAX - abnormal chemotaxis

TBB - tubulin, beta

TBS - tris-buffered saline

TEMED - tetramethylethylenediamine

TFEB - transcription factor EB

TfR - transferrin receptor

TRPA - transient receptor potential cation channel subfamily A member

U - ubiquitination

UCP - uncoupling protein

UGT - UDP-glucuronosyltransferase

UNC - uncoordinated

UTR - untranslated region

VHL - von hippel-lindau tumor suppressor

VIT - vitellogenin structural genes (yolk protein genes)

WAT - white adipose tissue

wt - wild type

TABLE OF CONTENTS

Abstract

Hibernation is a strategy developed by some endotherms in order to survive unfavorable environmental conditions. Hibernating animals lower down their core body temperature and reduce their metabolic rate without any negative consequences for their health. The detailed cellular mechanism/mechanisms underlying entrance or exit to the hibernation state has not been fully determined.

To uncover molecular processes involved in hibernation-like response, we employed a simple model organism that enters a hibernation-like state, the nematode *Caenorhabditis elegans*. Our previous research using this model revealed that nematodes lacking ETS-4 transcription factor exhibited improved cold survival via the upregulation of *ftn-1* mRNA. *ftn-1* encodes an ortholog of mammalian ferritin heavy chain (FTH1). Therefore, the main aim of this study was to determine processes underlying the *C. elegans* ferritin-mediated cold protection during hibernation-like response.

In this dissertation, I confirmed that *ftn-1* mRNA was increased in response to the cold treatment of nematodes lacking ETS-4. Additionally, the *ftn-1* overexpression robustly enhanced wild-type *C. elegans* cold resistance, and slightly increased their total lifespan. Moreover, the ferroxidase activity of FTN-1 was crucial for its function in cold survival improvement. Interestingly, my results suggest that FTN-1 acts as an antioxidant in the protection against reactive oxygen species (ROS) generated by cold exposure. Additionally, I characterized the contribution of two other transcription factors, ELT-2 and HIF-1, in the regulation of *ftn-1* expression in the cold. Moreover, I revealed that FTN-1 induction in response to starvation is mediated by different mechanism than the one used in the cold response. Finally, I showed that two RNA-binding proteins cooperating in *ets-4* mRNA regulation upon normal conditions, RLE-1 and REGE-1, are also involved in *ets-4* mRNA silencing during cold response.

Overall, the results obtained within this dissertation revealed a crucial role of ferritin in cold protection. This knowledge may contribute to the improvement of strategies imitating hibernation state with potential use in e.g. treatment of patients with traumatic brain injury.

Streszczenie

Hibernacja to strategia opracowana przez niektóre stałocieplne organizmy w celu przetrwania w niesprzyjających warunkach środowiskowych. Hibernujące zwierzęta obniżają temperaturę ciała oraz zmniejszają tempo przemiany materii bez żadnych negatywnych konsekwencji dla ich zdrowia. Szczegółowy mechanizm/mechanizmy komórkowe leżące u podstaw wejścia lub wyjścia ze stanu hibernacji nie zostały w pełni określone.

Aby zbadać procesy molekularne zaangażowane w reakcję porównywalną do hibernacji zastosowaliśmy prosty organizm modelowy, który potrafi wejść w stan podobny do hibernacji, nicienia *Caenorhabditis elegans.* Nasze wcześniejsze badania, z wykorzystaniem tego organizmu modelowego ujawniły, że brak czynnika transkrypcyjnego ETS-4 przyczynia się do poprawy przeżywalności nicienia w niskiej temperaturze poprzez aktywację ekspresji *ftn-1*. *ftn-1* koduje ortolog ssaczego ciężkiego łańcucha ferrytyny (FTH1). Dlatego też głównym celem poniższych badań było określenie procesów leżących u podstaw ochrony przed zimnem za pośrednictwem ferrytyny u *C. elegans*, podczas stanu podobnego do hibernacji.

W niniejszej rozprawie potwierdziłam, że poziom mRNA *ftn-1* wzrósł podczas odpowiedzi na niską temperaturę u nicienia pozbawionego ETS-4. Ponadto nadekspresja *ftn-1* znacznie poprawiła odporność na zimno u szczepu dzikiego *C. elegans* oraz nieznacznie wydłużyła jego całkowitą długość życia. Co więcej, aktywność ferroksydazy FTN-1 była kluczowa dla jej funkcji w procesie poprawy przeżywalności w zimnie. Co ciekawe, moje wyniki sugerują, że FTN-1 działa jako antyoksydant w ochronie przed reaktywnymi formami tlenu (ROS) generowanymi podczas ekspozycji na niską temperaturę. Dodatkowo scharakteryzowałam udział dwóch innych czynników transkrypcyjnych ELT-2 i HIF-1 w regulacji ekspresji *ftn-1* w zimnie. Ponadto wykazałam, że FTN-1 jest indukowana w odpowiedzi na stres żywieniowy za pomocą mechanizmu innego niż ten obserwowany w odpowiedzi na zimno. Na koniec pokazałam, że dwa białka wiążące RNA, współpracujące w regulacji mRNA *ets-4* w normalnych warunkach, RLE-1 i REGE-1, są zaangażowane w wyciszanie mRNA *ets-4* podczas odpowiedzi na niską temperaturę.

Podsumowując, wyniki uzyskane w ramach niniejszej pracy wykazały kluczową rolę ferrytyny w aspekcie ochrony przed zimnem, co może przyczynić się do polepszenia strategii imitujących stan hibernacji z potencjalnym ich zastosowaniem m.in. w leczeniu pacjentów z urazowym uszkodzeniem mózgu.

1 Introduction

1.1 Hibernation

Living organisms are classified into two groups, based on the ability to adapt their body temperature to the environmental conditions: ectotherms and endotherms (1). Ectotherms adjust their body temperature to the temperature of the surrounding environment, and are represented by plants and a vast group of animals. This strategy does not demand high energy utilization. On the contrary, endothermic organisms, represented by most birds and mammals, keep a constant body temperature, independently of the environmental temperature, what requires much higher energy supply (1,2). Due to the seasonal changes of the year, the environmental conditions are not always favorable. Thus, some endotherms developed a state called torpor that occurs on a daily or seasonal basis helping endotherms to survive harsh environmental conditions (1).

Hibernation is a type of torpor that lasts for days or weeks (1). This process is characterized by the lowered body temperature and metabolic reduction, what is necessary for energy saving, when a hibernator is exposed to the limited food accessibility, wintertime, and/or other inauspicious environmental conditions (3,4). Based on the current knowledge, hibernators are represented by eight groups of mammals: monotremes, rodents, marsupials, shrews, carnivores, insectivores, bats, and primates (5). Certain environmental cues promote changes associated with morphology, physiology, and behavior of hibernating organisms. Nevertheless, these changes are not driven by a unique set of genes specifically assigned for the hibernation state, but by the atypical expression of common mammalian genes (6). However, the detailed mechanism/mechanisms that might activate or inhibit the hibernation process still need a better understanding. Nevertheless, the imitation of hibernation state may have therapeutic potential for example in organ preservation strategies (7), and therapies of various medical conditions like stroke, ischemia/reperfusion injury, or hypoxia (8).

1.1.1 The difference between daily torpor and hibernation

Endotherms use torpor for the adaptation to harsh environmental conditions. Torpor can be divided into two types: daily torpor and hibernation (1,9). The table below describes most of the differences appearing between those two metabolic strategies.

Table 1. Comparison between daily torpor and hibernation.

Daily torpor	Hibernation
Lasts for a short period of time (~3-12 hours per day) (9)	Lasts for days or weeks (1)
Higher minimum metabolic rate (9)	Lower minimum metabolic rate (9)
Higher core body temperature (9)	Lower core body temperature (9)
Lower body mass (9)	Higher body mass (9)
Not necessary to gain weight (10)	Fat storage necessary to survive winter (1)
Often connected with forage during active state (1,10)	Periods of arousals interspacing torpor bouts where animals rewarm to rest usually for less than 1 day (highly energy consuming process) (1)
Independent of ambient temperature (1)	Dependent on ambient temperature (1)
Circadian system used to control torpor time (9)	Torpor time is not controlled by circadian system (9)
Can appear at every time of the year (10)	Mostly seasonal and dedicated to the wintertime (1,10)

Hibernating mammals are represented, inter alia, by bats, ground squirrels (5,7), bears (11,12), and dwarf lemurs (10). According to the way how they save energy, two groups can be distinguished (13): species storing fat (e.g. dwarf lemurs that accumulate fat mainly in their tails (10)), and food-storing species (e.g. European hamster that collect food and eat it during arousal periods (13)). The differences are also observed between hibernators of diverse sizes. Mostly, small hibernators are able to reduce their core body temperature to very lower numbers (oscillating around freezing temperature), whereas bigger animals maintain much higher body temperature e.g., black bear reduces body temperature to around 30°C-33°C (12). Interestingly, black bears do not experience arousal periods observed in small hibernators (12). Moreover, the most spectacular example of hibernation state is manifested by edible dormice, which can hibernate for up to 11 months when the environmental conditions are not encouraging for reproduction (4,14).

1.1.2 Molecular processes involved in cold adaptation

The main goal of the molecular processes involved in cold adaptation is to prepare a hibernating animal to survive the unfavorable environmental conditions under limited food accessibility, thereby a source of energy supply (6,9). In order to adapt to these conditions, hibernating animals go through diverse behavioral, physiological and morphological changes necessary to survive a hypometabolic state (5,6,9). Animals begin to prepare for hibernation

period in late summer by accumulation of their body fat mostly in white adipose tissue (WAT) (1,5). Interestingly, some hibernators are capable of storing fat in the amount equal to their double body mass (5). This stored fat is used by many hibernators as the energy source to survive wintertime, however some animals rely on food caches or utilize both ways simultaneously (1,5,9). A characteristic feature of hibernation is a metabolic change from the utilization of carbohydrates to fatty acid metabolism (6,15,16). This metabolic shift is tightly controlled by transcriptional and translational regulation of crucial genes/proteins leading to the decrease of the carbohydrate metabolism, thereby promoting fatty acid utilization (6). Moreover, an important aspect of the metabolic reprogramming in hibernating animals, is reversible insulin resistance depending on the switch between the active or hibernation state (17-19). Insulin resistance is characterized by incapability of insulin to properly regulate glucose distribution throughout the body (20). In healthy organism, insulin is not only necessary for glucose uptake but also for the regulation of other processes like metabolism of lipids, carbohydrates, and proteins (21). During hibernation, insulin resistance allows animals to save glucose and burn fat (17). Interestingly, natural insulin resistance observed in hibernators makes them an excellent model to study type 2 diabetes mellitus (T2DM), an incurable human disease (19).

In order to hibernate, animals reduce metabolic rate mainly through reversible phosphorylation of certain proteins (5,22,23), repression of global transcription and translation, upregulation of genes necessary for hibernation (e.g. encoding chaperones, unfolded protein response-proteins, and transmembrane transporters) (5,23-26), and activation of the antioxidant defense (5). An excellent example of global transcription repression in hibernating organisms, is the decreased activity of RNA polymerase II detected in muscles of 13-lined ground squirrels during the hibernation state compared with the euthermic values (5,27). Moreover, the switch from polysomes to monosomes, which prevents efficient protein synthesis is characteristic for hibernating animals (5,28). The examples of posttranslational modifications in hibernators are lower levels of phosphorylation and acetylation of amino acid residues of histone H3 (compared with the active state), in the muscles of the 13-lined ground squirrel (5,27). This suggests that transcription inhibition, through posttranslational modification, can also occur at the chromatin level through histone modification during hibernation (5,27).

1.1.2.1 Defense against reactive oxygen species

Small hibernators experience periods of torpor and arousal what resembles a cycle of ischemia and reperfusion (29,30). Therefore, when torpid, hibernating animals radically decrease their blood flow and heart rate leading to the reduction of blood oxygen content (31,32). The negative outcome of reperfusion during arousal is its contribution to the rapid increase of blood flow connected with the promotion of mitochondrial respiration and oxygen consumption. This results in oxidative stress and enhanced production of harmful reactive oxygen species (ROS) (29,30). Moreover, increased levels of polyunsaturated fatty acids (that enable lipid fluidity during hibernation), makes them highly sensitive to oxidation (31). Additionally, brown adipose tissue (BAT) is necessary for non-shivering thermogenesis to generate heat, for the maintenance of proper body temperature during hibernation, when the environmental temperature rapidly drops below the acceptable threshold (6). However, the heating process during arousal, may eventually lead to the increased ROS production (30). Interestingly, some studies suggest that the arousal periods in hibernating organisms lead to the increased oxidative stress (30,33,34). However, other research indicates that the oxidative stress or oxidative injury does not occur in hibernators (30,32). Thus, it is important to determine whether there is a specific mechanism underlying anti-oxidative protection in hibernating organisms, and how does it function.

A few research groups described antioxidant protection in hibernating animals. A first example of the existence of such type of protection is a significant increase of the activities of antioxidant enzymes, such as superoxide dismutase (SOD), and catalase (CAT) in little ground squirrels during period of arousal (35). Another example of the regulation of gene, taking part in cellular defense against oxidative stress, is the forehead box O3 (FoxO3a) that was upregulated in hibernating 13-lined ground squirrels (36). Moreover, plasma ascorbate concentration was reported to be upregulated during hibernation, with the highest consumption during the peak of the oxygen level in rewarming (37). Interestingly, not only antioxidant enzymes, but also heat shock proteins (HSP) like HSP70, HSP90α and HSP60 were upregulated in BAT (first two) and in the liver (the last one) of gray mouse lemurs, during torpor (38). Nevertheless, it is also worth mentioning that the hypometabolic conditions, that occur during hibernation, may impede the mechanism of repairing/replacing macromolecules which were damaged by ROS, leading to their accumulation (23). Thus, the antioxidant defense can also rely on other types of protective proteins like iron-binding proteins (23). Iron is a compound utilized by many proteins, but the excess of free ferrous (Fe^{2+}) ions catalyze the Fenton reaction

resulting in the production of highly toxic hydroxyl and lipid radicals (39). This process might be combated by the ferritin, an iron storage protein upregulated during torpor e.g. in wild hibernating bats (40). All of the above examples suggest that an antioxidant defense in hibernators relies mostly on the antioxidant proteins neutralizing ROS. This process is necessary to protect cells from multiple damages connected with hibernation (23,29). Nevertheless, the antioxidant protection through the upregulation of certain set of genes is not observed in all tissues of hibernating animals and is not common for all hibernators (33,41).

1.1.3 Therapeutic utility of low temperature

Hibernators, due to their unique adaptation to unfavorable environmental conditions, are able to lower their body temperature to near-freezing temperatures, and severely reduce their metabolism. Interestingly, this process does not result in any negative, irreversible consequences for their health and viability (6,8). The approaches imitating hibernation state are gaining attention in the therapeutic strategies for many medical conditions in humans (8). During therapeutic hypothermia the patient's body temperature is under rigorous control (8). Depending on the temperature range hypothermia might be categorized as: mild (33°C~36°C), moderate (28°C~32°C), deep (16°C~27°C), profound (6°C-15°C), and ultra-profound (<5°C) (42). The history of therapeutic hypothermia is very long and the first evidence of its utilization was reported in ancient Egypt (43). Also, in ancient Greece, Hippocrates observed the benefits coming from cooling the parts of the patient's body (44). However, Temple Fay is believed to be a pioneer who introduced therapeutic hypothermia to modern history (44). He revealed a neuroprotective outcomes after application of therapeutic hypothermia, as well as a breast tumor remission in patient treated with local cooling method (44,45). After the World War II, therapeutic hypothermia was widely used (44), especially in humans with cardiac arrest (44,46). Unfortunately, due to a growing number of events with high medical complications appearing in patients treated with prolonged severe hypothermia, the interest in this therapeutic strategy decreased (44). Nevertheless, since 2002 therapeutic hypothermia has regained attention starting from patients after cardiac arrest (47).

Therapeutic hypothermia can be induced using external or internal methods (42). External methods utilize, inter alia, ice packs, cooling blankets, and cold-water immersion (42). Whereas, the internal method can be performed by infusion of cool saline by central venous catheters (42). Nowadays, drug-induced hypothermia is gaining interest due to a lower number of side effects (48). Therapeutic hypothermia is commonly used in many medical conditions

like hemorrhagic shock, ischemia/reperfusion injury (8), sepsis, cardiac arrest (49), and hepatic encephalopathy (50). Since this cooling strategy was shown to be neuroprotective (43,48), it has been used to treat several acute brain insults like ischemic stroke (51,52), spinal cord injury (53), and neonates suffering from hypoxic-ischemic encephalopathy (54).

Even though therapeutic hypothermia has many benefits, it is challenging to maintain proper treatment conditions, such as temperature, time of cooling and the protection against harmful side effects (48,51). The most common side effects are: coagulopathy, cardiac arrhythmias, hypokalemia, infections (mostly pneumonia) (42,55), and shivering induced by thermoregulation (56). Additionally, therapeutic hypothermia is not recommended for some patients after stroke, e.g. elderly patients and those with comorbidities because they may not be able to tolerate cooling procedure (51). Despite the fact that, available methods of therapeutic hypothermia need to be improved, this strategy seems to be beneficial for the enhancement of e.g. neurological patient's treatment (43).

1.2 *Caenorhabditis elegans* as a model organism

Caenorhabditis elegans is a nematode broadly used as a model organism in biological studies (57,58). This animal can be found worldwide, with the highest frequency of occurrence in the temperate climate (57). Usage of *C. elegans*, as a model organism, has many advantages: low cost, ease of maintenance in the laboratory (59), transparent body, small size (~1 mm long), short life cycle, and production of a large number of progeny (58,59). Also, every cell lineage of this organism is mapped (59), and genome is fully sequenced (60). Moreover, this nematode is amenable to genetic manipulations (57,59). In the favorable environmental conditions, *C. elegans* individuals hatch from the egg and increase in size throughout four larval stages (L1, L2, L3 and L4), before reaching adulthood (57). However, stressful factors like heat stress or crowding force larvae to enter the dauer diapause stage that helps them to survive unfavorable conditions even for months (Figure 1) (57,61). The reproduction in *C. elegans* occurs generally through self-fertilization in hermaphrodites (XX), but can also happen by outcrossing with males (X0) (57). Due to the fact that the occurrence of males is extremely low, most of the progeny come from self-fertilization of hermaphrodites (57). Studies using this simple model organism led to breakthrough discoveries like RNA interference or apoptosis (57,62). Additionally, *C. elegans* has one very important feature for the pharmaceutical industry: its usage is not limited by ethical issues that are known limitations in the utility

of vertebrates (63). Moreover, studies conducted in this project took advantage of another feature of *C. elegans* - the fact that it is a poikilothermic organism, which means its body temperature depends on the surrounding temperature (64). Usually, *C. elegans* are cultivated at 15°C-25°C (65), however, they display severely limited survival at temperatures lower than 15° or higher than 25°C. This phenomenon makes *C. elegans* a useful model organism to investigate the adaptive mechanisms induced by changes in environmental temperature.

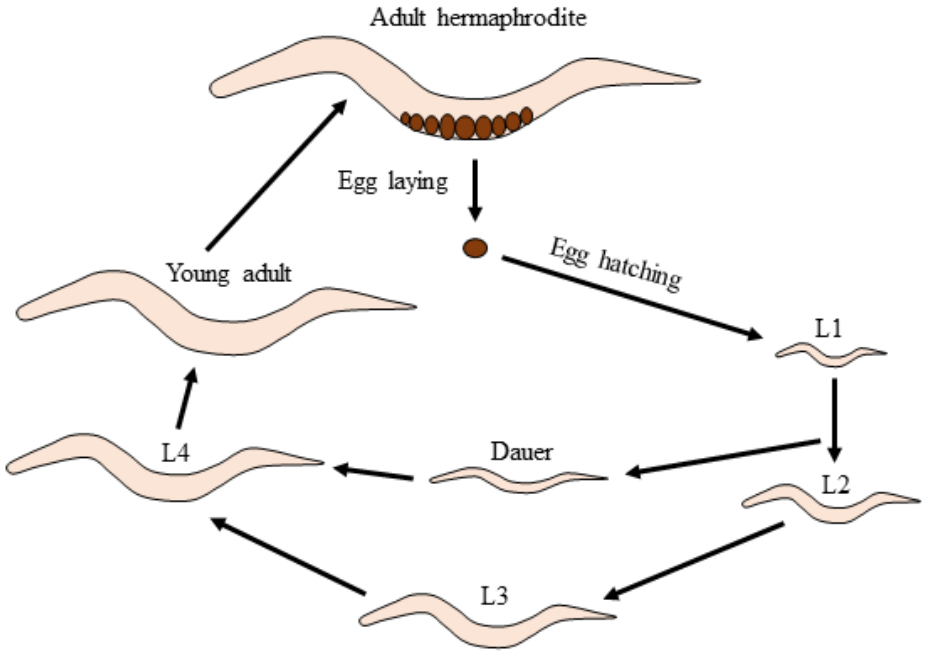

Figure 1. The *C. elegans* life cycle. *C. elegans* hatch from eggs and grow through four larval stages (L1, L2, L3, L4), before reaching adulthood. In order to survive unfavorable environmental conditions, nematodes enter the dauer diapause stage that can last for several months (Adapted from (66)).

1.2.1 Insulin/insulin-like growth factor signaling in *C. elegans*

Insulin is a hormone playing a crucial role in the carbohydrate homeostasis in vertebrates (67). It is produced in the pancreas and subsequently transferred to the bloodstream in order to regulate glucose levels in the body (67,68). Importantly, insulin resistance leads to common metabolic diseases such as T2DM (69). However, an example of exceptions to this rule are hibernating animals. These individuals are characterized by a reversible insulin resistance depending on their metabolic state (active or hibernation), which is a natural adaptation strategy developed by hibernators (17).

The insulin/insulin-like growth factor (IGF)-1 signaling (IIS) pathway is evolutionary conserved from invertebrates to mammals (70), thus, also happens in *C. elegans* (Figure 2)

(70,71). The IIS pathway is regulated by insulin-like peptides (ILPs) that are encoded by 40 genes in *C. elegans* (72,73). Some of the ILPs play a role in activation (agonists), inhibition (antagonists) or activation and inhibition (pleiotropic) of the IIS pathway in *C. elegans* (72-74). ILPs bind to the insulin-like growth factor receptor (DAF-2/IGFR), leading to its activation via autophosphorylation (71-73). This affects the activation of the phosphoinositide 3-kinase (AGE-1/PI3K), that subsequently converts phosphatidylinositol 4, 5-bisphosphate (PIP2) to phosphatidylinositol (3, 4, 5)-trisphosphate (PIP3) (71-73). However, this step can be reversed by phosphatase DAF-18 (homologous to human phosphatase and tensin (PTEN)) that converts PIP3 to PIP2 (72). The generation of PIP3 activates the serine/threonine kinases PDK-1, AKT-1, and AKT-2 (71,72), that phosphorylate the transcription factor DAF-16/FOXO, leading to its inactivation and sequestration in the cytoplasm (70,72). The subcellular localization of DAF-16/FOXO is controlled by 14-3-3 proteins, abnormal embryonic partitioning of cytoplasm (PAR-5), and fourteen-three-three family (FTT-2) (71,73). Interestingly, DAF-16 activity also depends on regulation of longevity by E3 (RLE-1) that ubiquitinates DAF-16 directing it to the proteasomal degradation (75). Moreover, activated PDK-1, when phosphorylating AKT-1 and AKT-2, can also phosphorylate the serum- and glucocorticoid-inducible kinase (SGK-1) (73,76). However, in contrast to mammals, nematodes' SGK-1 regulates DAF-16/FOXO function by interacting with proteins affecting DAF-16/FOXO (73). Although, when the IIS pathway is inhibited, DAF-16/FOXO remains active and translocate into the nucleus leading to the regulation of its target genes (72,73). The phenomenon of the reduced IIS pathway and activation of DAF-16/FOXO in *C. elegans* is associated with the extended lifespan (77), slower aging (70), activated immunity response (78), induced detoxification machinery (79), and regulation of metabolism (80,81). The IIS pathway does not only regulate DAF-16/FOXO, but also other transcription factors like heat shock factor (HSF-1) (82), skinhead /NF-E2-related factor 2 (SKN-1/Nrf2) (83), SMEK (Dictyostelium Suppressor of MEK null) homolog (SMK-1) (84). Relevantly for this thesis, the SKN-1/Nrf2 was proposed to mediate cold stress resistance in *C. elegans* (85).

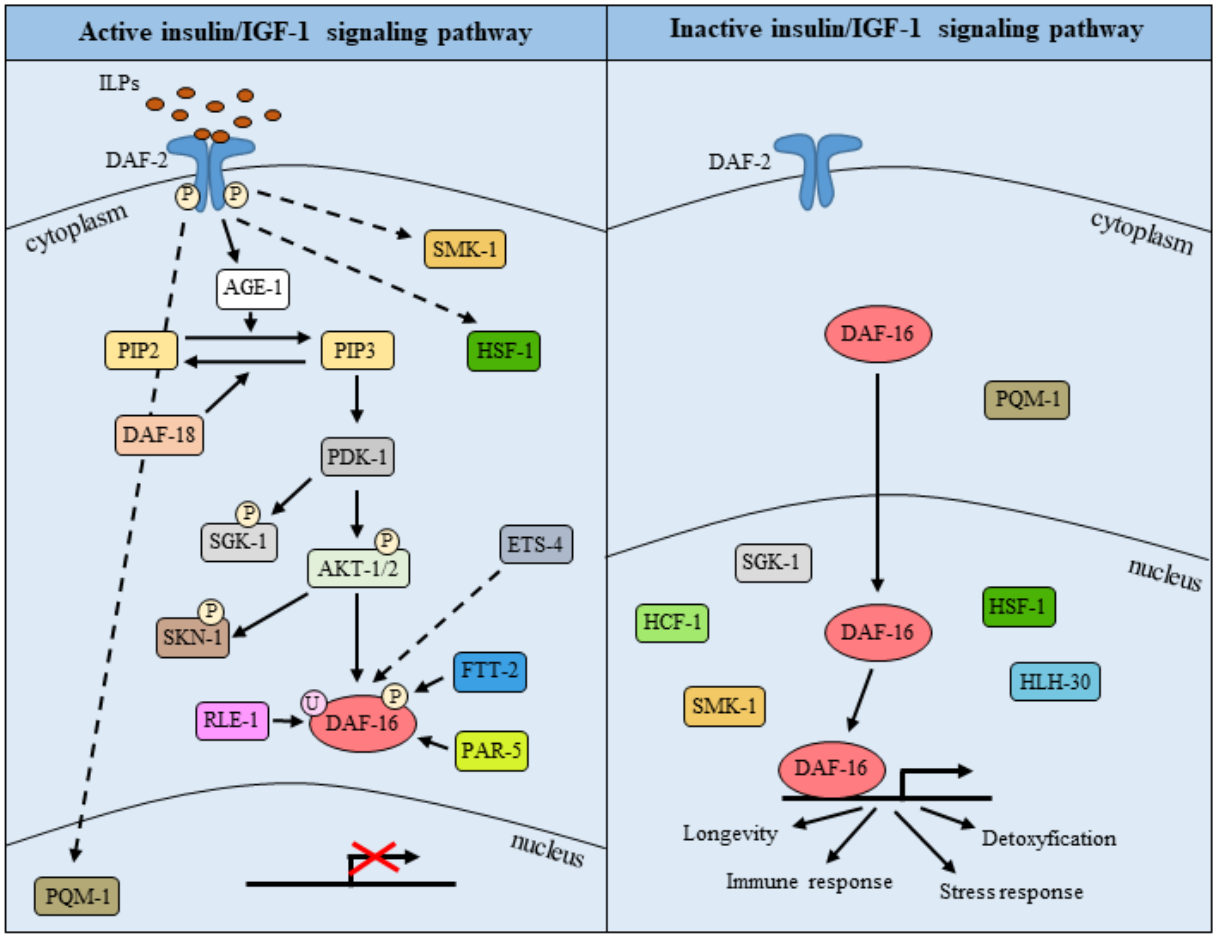

Figure 2. Insulin/IGF-1 signaling pathway in *C. elegans.* The IIS pathway is regulated by insulin-like peptides (ILPs). ILPs bind to the DAF-2 receptor activating it via autophosphorylation (P). This affects the activation of AGE-1 that subsequently converts PIP2 to PIP3. This step can be reversed by phosphatase DAF-18. The generation of PIP3 activates kinases PDK-1, AKT-1, and AKT-2 that phosphorylate (P) the transcription factor DAF-16, leading to its inactivation and sequestration in the cytoplasm. Moreover, the activated PDK-1 phosphorylates (P) SGK-1. SGK-1 has an ability to activate DAF-16 and promote lifespan extension. The subcellular localization of DAF-16 is controlled by the 14-3-3 proteins (PAR-5 and FTT-2), and also depends on RLE-1 which ubiquitinates (U) DAF-16 directing it to proteasomal degradation. The transcription factor ETS-4 acts in parallel to the IIS and antagonizes the DAF-16 function. The IIS pathway also regulates transcription factors like HSF-1, SKN-1, and SMK-1. However, when the IIS pathway is inhibited, DAF-16 translocate into the nucleus subsequently regulating its target genes. PQM-1, HSF-1, SMK-1, HCF-1, and HLH-30/TFEB have been identified as partners of DAF-16 (Adapted from (71,86)).

1.2.1.1 Transcription factors associated with the regulation of lifespan and stress response in *C. elegans*

A transcription factor, essential for stress response and longevity is DAF-16, a *C. elegans* homolog of the forkhead box transcription factors class O (FoxO) (73). DAF-16 promotes longevity when the IIS pathway is inhibited via mutation of *daf-2* or *age-1* (73,87).

As described earlier, under these circumstances DAF-16 remained active and was transferred into the nucleus where it regulated the transcription of numerous genes (87). Importantly for this research, DAF-16 was described to regulate expression of the gene encoding iron storage protein - ferritin (*ftn-1*) in *daf-2* mutant background (88). Nevertheless, DAF-16 has additional roles in the regulation of genes associated with dauer formation, cellular stress, fat storage, and immune response (73). Also, there are known partners for DAF-16 like paraquat (methylviologen) responsive (PQM-1) (89), HSF-1, SMK-1, SKN-1, human host cell factor 1 related (HCF-1) (73,82), helix loop helix/transcription factor EB (HLH-30/TFEB) (90). Moreover, SGK-1 was shown to activate DAF-16 and promote lifespan extension (91).

C. elegans lifespan is not only regulated by the IIS pathway and its downstream target DAF-16 but also by other factors such as E twenty six (ETS) class transcription factor (ETS-4) (92). The *C. elegans* ETS-4 is an ortholog of vertebrate SAM pointed domain containing ETS transcription factor (SPDEF) described to have a role, inter alia, in the lifespan regulation (92). Nevertheless, ETS transcription factor family was established to be essential for many other processes like hematopoietic and vascular development (93), oncogenesis (94), and immunity (95,96). It was shown that ETS transcription factors recognize and bind certain promoters within a 5′-GGAA/T-3′ motif (97,98). ETS-4 was described as a negative regulator of lifespan extension due to the fact that *ets-4*-lacking mutants showed increase of total lifespan compared with the control (92). Interestingly, it was shown that ETS-4 target genes overlapped with DAF-16 targets in the regulation of longevity (92). However, ETS-4 may not function directly through, but in parallel to IIS, and act upstream or in parallel to DAF-16 antagonizing its function in the aspect of lifespan extension. It seems to be true due to the fact that without DAF-16 *ets-4* mutants did not show extended lifespan (92). However, how these two transcription factors cooperate with each other remains unknown.

ETS-4 transcription factor was also shown to be activated by axon injury and subsequently took part in axon regeneration through the induction of the receptor tyrosine kinase - suppressor of vhp-1 deletion lethality (SVH-2) expression (99). Importantly, ETS-4 activity was reported to be tightly regulated. For example, the Mad-like transcription factor (MDL-1) was able to inhibit the *ets-4* transcription what enabled the activation of *svh-2* gene expression when needed (99). Additionally, ETS-4 did not act alone in the activation of the *shv-2* gene, but in a complex with transcription factor CEBP-1 (99). Another example of ETS-4 regulation is an auto-regulatory loop in which the *ets-4* messenger RNA (mRNA) is a target of *C. elegans* ortholog of conserved ribonuclease Regnase-1/ MCPIP1 (REGE-1) in the

regulation of the body fat content (100). It was shown that REGE-1 degraded *ets-4* mRNA within its 3′ untranslated region (UTR) resulting in fat accumulation. However, mutants lacking *rege-1* were characterized by the overexpression of *ets-4* mRNA that was translated into ETS-4 protein leading to the reduced body fat content, developmental delay, and decreased cold resistance (100). Subsequently, further study revealed enhanced resistance to low environmental temperature ("cold") in mutants lacking *ets-4* (101). Additionally, a unique joint role of DAF-16 and PQM-1 was identified upon analyzing regulation of cold survival in the absence of ETS-4 (101). Furthermore, mutants lacking *ets-4* exhibited an increased expression of a conserved iron-binding protein ferritin (FTN-1/FTH1) suggesting its crucial role in lifespan extension (101). The detailed information about FTN-1 role in the aspect of cold survival is described in the Results chapter.

Another transcription factor known to be involved in the lifespan regulation is a conserved zinc finger transcription factor PQM-1 (89). It was established that the PQM-1 nuclear translocation depended on the IIS pathway, and was negatively associated with DAF-16 presence in the nucleus (89). In reference to DAF-16-dependent *ftn-1* regulation, the *ftn-1* upregulation was observed upon activation of innate immune response controlled by the PQM-1 transcription factor (102). Besides the role of PQM-1 in lifespan and immune response, this transcription factor is also an important component for proteostasis maintenance (103), regulation of development, and stress response (89,104).

An erythroid-like transcription factor family (ELT-2) is a conserved GATA-type transcription factor crucial for the proper function of the intestine in *C. elegans* (105). Importantly, the loss of *elt-2* gene is lethal to nematodes indicating its important role in regulating cellular homeostasis (105,106). This factor is active in embryonic stages, all larval stages and in adult nematodes (107). Moreover, ELT-2 was suggested to take part in the transcriptional regulation of almost all genes expressed in the *C. elegans* intestine independently of developmental stage through the binding of TGATAA motifs present in the promoter regions of those genes (107). It was established that ELT-2 bound the GATA sites in the promoter of *ftn-1* gene leading to its regulation (108). Interestingly, it was shown that animals lacking *elt-2* were not able to deal with bacterial infection. This results point out an essential role of ELT-2 in the defense against pathogenic bacterial infection (105).

A hypoxia-inducible factor (HIF-1) is another transcription factor important for the *C. elegans* lifespan regulation and stress response, especially in response to the changeable

oxygen concentration in the environment (109-111). *C. elegans* encodes one *hif-1* gene and nematodes deprived of this gene are not able to survive hypoxia (112,113). Upon high concentration of oxygen, the enzyme egg laying defective (EGL-9) hydroxylates HIF-1. This leads to its recognition by von hippel-lindau tumor suppressor (VHL-1) which directs HIF-1 for the degradation in proteasome. However, low oxygen content, makes HIF-1 protein stable, and enables HIF-1-mediated activation of its target genes expression (113). Importantly, HIF-1 was shown to be incorporated into the iron metabolism and ferritin regulation in *C. elegans* which is described more broadly in chapter 1.2.3.1.

1.2.2 *C. elegans* cold adaptation

Standard conditions for *C. elegans* cultivation are 15°C-25°C (65,114). Additionally, it was shown that lower temperatures (15°C) increased the *C. elegans* lifespan, whereas higher temperatures (25°C) shortened it (115). Importantly, studies investigating how the temperature change affects the *C. elegans* behavior showed that the egg production, growth rate, and the lifespan were all influenced by ambient temperature (115). These observations suggest that, depending on the temperature, *C. elegans* developed different strategies to resist and respond to these environmental changes (116-119). Even though, heat stress has been more broadly studied in *C. elegans* (116,120,121), research focusing on the impact of low temperature on *C. elegans* behavior and metabolism has also been carried out (85,118,122). Thus, it was shown that the exposure to near-freezing temperatures (0°C-4°C) harmed or even killed nematodes, but only when "cold shock" (direct transfer from standard cultivation temperature to extremely low temperature) was applied (85,100,118,119). However, the cold-mediated death can be suppressed by the addition of a pre-incubation step at intermediate temperature (10°C-15°C) before the cold shock. This strategy allows nematode to acclimate to the low temperature resulting in improved survival in the cold (100,101,118,123,124). Moreover, it was shown that cold shock response to moderately or severely low temperatures (~15°C, and 2°C-4°C, respectively), or followed by the return to standard cultivation temperatures, was strictly controlled via specific genetic programs (117-119). Interestingly, *C. elegans* seems to stop aging while exposed to the cold, which may suggest an entrance to a hibernation-like state (100,101).

1.2.2.1 Adaptation to mild temperatures

The thermosensitive TRPA cation channel homolog (TRPA-1) promotes lifespan extension in adult nematodes upon exposure to cold stress generated by mildly low ambient temperature (15°C) (114,117). The response starts when TRPA-1 channels, located in neurons and intestine, sense the temperature decrease which promotes calcium release and subsequently activates a calcium-sensitive kinase PKC (PKC-2) (117). Afterwards, the induction of SGK-1 occurs that is responsible for the activation of DAF-16 leading to the enhanced animal survival (117). Interestingly, it was observed that TRPA-1 channel expression from the intestine could prolong the lifespan of nematodes more efficiently than its expression from neurons (117). Surprisingly, the mechanism described above was shown to extend the lifespan only in adult nematodes while *C. elegans* larvae were characterized by shortened lifespan (114). Nevertheless, the process mediating the response to mild temperature seems to be more complex than the mechanism utilizing TRPA-1 channel and DAF-16. There are some pieces of evidence indicating other factors involved in the survival regulation after mild cold stress like *C. elegans* homolog of co-chaperone p23, DAF-41 (125), fatty acids (65), and germ cells (126).

1.2.2.2 Adaptation to low temperatures

The response induced by the exposure to extremely low temperatures as 2°C (named as “cold shock”) is mediated by a different molecular mechanism than the one observed at 15°C and is lethal to nematodes transferred directly from 20°C-25°C to 0°C-4°C (85,118,119). Severe cold shock at 2°C activates the response in ASJ sensory neurons through the cGMP-gated channel TAX-4, which is known to be involved in temperature sensation (85,118). These neurons release insulin-like molecules responsible for the activation of DAF-2 receptor what subsequently inhibits DAF-16 activity and leads to the reduction of cold tolerance in *C. elegans* exposed to the cold shock (118). Two insulin-like molecules: DAF-28 and insulin related (INS-6) expressed in ASJ neurons were described to activate the IIS pathway. Interestingly, the INS-1 was shown to abolish the DAF-2 activation via inhibition of INS-6 (118). These results suggested that the IIS pathway was crucial for the cold tolerance regulation in cold-shocked nematodes (118).

The Ca^{2+}-dependent endoribonuclease (ENDU-2) was also shown to be important for the regulation of the response to cold shock at 2°C, since the *endu-2(-)* mutants showed an

enhanced cold survival (127). This regulation seems to be mediated in a cell autonomous and non-autonomous manner (127). Furthermore, it was revealed that reduced cold survival was mediated by the activity of ENDU-2 in thermal-sensing ADL neurons and muscles (124,127). What is important, ADL neurons have two TRP channels (osmotic avoidance abnormal (OSM-9), and OSM-9 and capsaicin receptor-related (OCR-2)), that have an impact on the regulation of cold resistance (124,127). Interestingly, cold tolerance mediated by TAX-4 in ASJ neurons acts independently of cold response regulated by ENDU-2 in ADL neurons (127). Additionally, another group of neurons, ASG, was described to sense the cold through mechanoreceptor degeneration of certain neurons (DEG-1), and then interact with the AIN and AVJ interneurons that led to cold tolerance regulation (124,128).

Another phenomenon connected with response to the cold shock is the lipids transfer between the soma and the germline. It was observed that during the rewarming periods at 20°C after the cold shock nematodes were losing their pigmentation in the intestine whereas pigmentation in the gonad was increasing (85,119). The intestinal pigmentation derive mainly from the lipid droplets (85). Thus, the movement of pigmentation may be caused by the lipid translocation from the somatic tissues to the germline in order to improve cold survival outcomes of the progeny (85). This phenomenon was suggested to be regulated by the TAX-2/TAX-4 channel subunits, SKN-1/Nrf2 and vitellogenesis activity (85). Moreover, the auto-regulatory module of REGE-1 and ETS-4 (described in chapter 1.2.1.1.), was also proposed to play an important role in the lipid metabolism regulation in nematodes exposed to the cold (100).

Another example of the receptor involved in the regulation of the cold survival is the G-protein coupled receptor, mammalian follicle stimulating hormone receptor homolog (FSHR-1), identified to be important for the resistance to stresses generated by ROS, heavy metals, and pathogen infection (119,129). The *fshr-1(-)* mutants showed reduced survival while exposed to oxidative stress, indicating that the FSHR-1 receptor was crucial for the activation of ROS defense (129). Surprisingly, in addition to the FSHR-1 role in oxidative stress response, the depletion of the gene encoding this receptor (*fshr-1(-)* mutants) lead to the resistance to the cold shock at 2°C (119). However, it may be possible that this receptor is involved in the recovery after the cold shock through regulation of other processes e.g. energy homeostasis (119).

1.2.3 Iron as an essential factor for organism and cell function

Iron is an important element implicated in many biological reactions crucial for proper functioning of the cell (130). Therefore, iron cofactors (e.g. heme, iron-sulfur clusters) are part of proteins involved in, inter alia, cellular respiration, synthesis of nuclei acids, and oxygen transport (130-133). Iron is at the 4th place of the most abundant metals on the Earth (130,133), and functions in two forms: the reduced Fe^{2+} (ferrous) and the oxidized Fe^{3+} (ferric) (134). Since the iron overload results in generation of ROS through the activation of the Fenton reaction, iron homeostasis should be tightly regulated (133). Moreover, the iron imbalance, driven by iron deficiency or iron overload, is connected with many human diseases like metabolic (e.g. diabetes), hematological (e.g. iron deficiency anemia, thalassemia), and neurodegenerative diseases (e.g. Friedrich's ataxia, and Alzheimer's disease) (131,135). Additionally, excess iron introduced by the exposure to high concentration of ferric ammonium citrate (FAC) in *C. elegans* resulted in protein oxidation, upregulated ROS generation, and shortened lifespan (136). Thus, it is crucial to maintain iron homeostasis to avoid negative consequences of the disruption of iron metabolism and its distribution (131,132).

1.2.3.1 Iron metabolism in *C. elegans*

Proteins essential for iron metabolism are evolutionarily conserved between mammals and *C. elegans* (137). Therefore, *C. elegans* encodes orthologs for divalent metal transporter 1 (SMF-3), iron-storage protein ferritin (FTN-1, FTN-2), mitochondrial iron importer protein mitoferrin (MFN-1) (137,138), and ferroportin responsible for iron export from the cell (FPN-1.1, FPN-1.2, FPN-1.3) (131,137).

The comparison of iron metabolism in *C. elegans* and mammals is shown on Figure 3. In mammals, before the iron is transferred to the cell, it is converted from Fe^{3+} to Fe^{2+} (133). Then, Fe^{2+} is transferred by DMT1 (in *C. elegans* SMF-3) to the cytoplasm (133,137). Subsequently, transported iron is released and included into the cytosolic labile iron pool which is intended for iron export, storage or metabolism (137,139). Some of the iron is utilized in cytosol and other cell compartments, but the largest amount of labile iron pool is used in mitochondria for the synthesis of iron-sulfur clusters and heme (137). In vertebrates, the iron is taken up by the mitochondria via mitochondrial iron importer protein – mitoferrin (MFRN) (140). Likewise, *C. elegans* also expresses an ortholog of human mitoferrin, *mfn-1* (other name *W02B12.9*) (138,141). Iron metabolism differs in nematodes, since they do not have an ability

to synthesize heme *de novo* and need to acquire it from the environment (142). Referring to other methods of iron utility, it can also be exported from the cell by ferroportin that has three orthologs in *C. elegans*: FPN-1.1, FPN-1.2, and FPN-1.3 (137). The rest of unused intracellular iron might be toxic to the cell thus, the excess amount is safely stored via an iron-storing protein called ferritin (137,143). *C. elegans* expresses two ferritin proteins, FTN-1 and FTN-2 encoded by two genes, *ftn-1* and *ftn-2* (144).

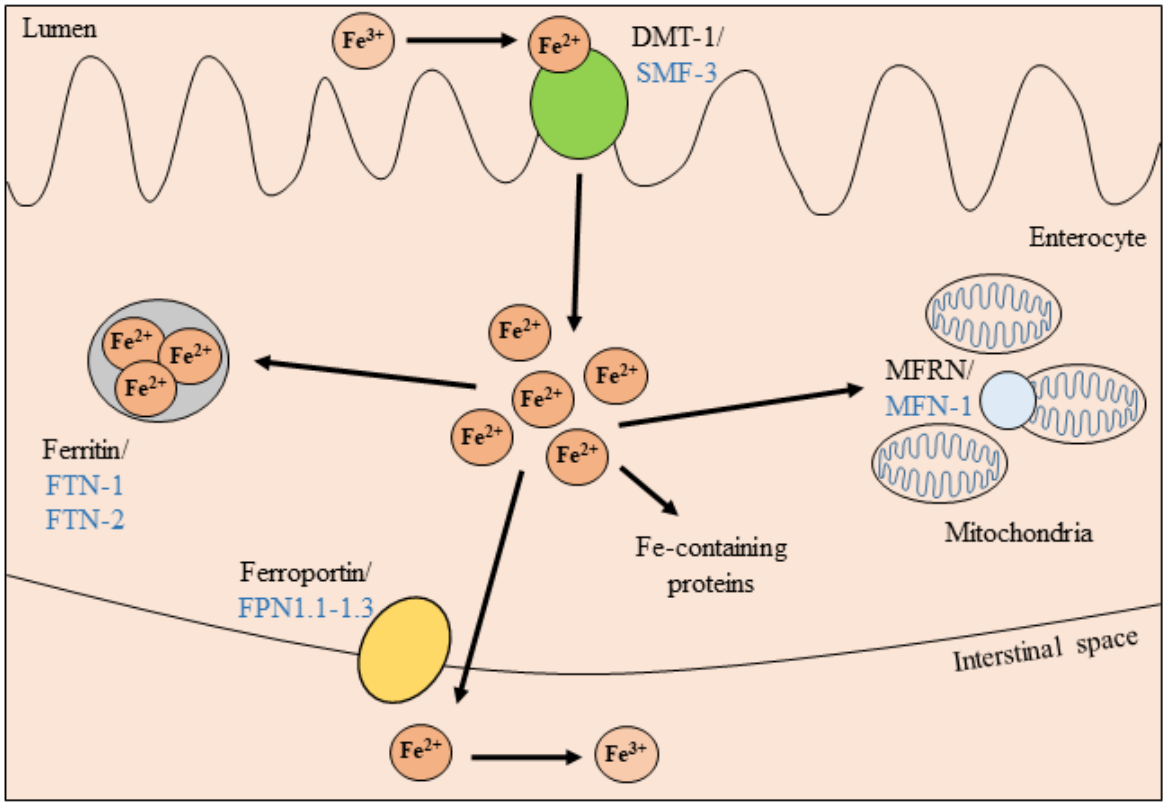

Figure 3. Proteins involved in intestinal iron metabolism are conserved between *C. elegans* and mammals. Proteins from mammals are marked in black whereas from *C. elegans* are labeled in blue. The Fe^{2+} is transferred by DMT1/SMF-3 to the cytoplasm. Then, included in the cytosolic labile iron pool, which can be used in metabolism, exported or stored. Some of the iron is utilized in cytosol and other cell compartments. Mitochondrial MFRN/MFN-1 is responsible for the iron transport to the mitochondria. Iron export from the cell is mediated by ferroportin/FPN-1.1-1.3, and the excess amount of iron is stored in ferritin/ FTN-1, FTN-2 (Adapted from (137)).

Mammalian iron metabolism is tightly regulated by the iron-responsive element (IRE)/iron-regulatory protein (IRP) system (134). IRP1 and IRP2 represent RNA-binding proteins that play a role in iron regulation in the cytoplasm through binding to IREs (133). IRE/IRP system regulates expression of proteins like ferritin, ferroportin and transferrin receptor 1 (TfR1) depending on the iron concentration within the cell (133). In case of ferritin, mRNAs of both subunits possess one IRE localized in their 5´UTRs (133,134). The inhibition

of ferritin translation in iron-deficient cell blocks iron binding (Figure 4) (133,134). However, when the cells are filled with iron, the IRE/IRP system is not activated, resulting in translation of ferritin mRNAs (133). Unlike in vertebrates, *C. elegans* does not utilize IRP1 and IRP2 proteins for iron regulation due to the lack of IRE/IPR system (144,145). Although, *C. elegans* encodes an IRP1 ortholog aconitase (ACO-1) that is sensitive to iron regulation, it does not have an ability to bind RNA (144). Nevertheless, FTN-1 and FTN-2 are regulated by changes in iron concentration at the transcriptional level. It was revealed that ELT-2 transcription factor, responsible for the regulation of basal expression of *C. elegans* ferritins, bound to a conserved 63 bp iron-dependent element (IDE) identified in the promoter regions of *ftn-1* and *ftn-2* (Figure 4) (108,131). This IDE is composed of three direct repeats interspaced by two GATA motifs. The GATA motifs are specifically bound by ELT-2 (108,131). Not only ELT-2 is able to regulate *ftn-1* and *ftn-2* expression, also HIF-1 was shown to regulate ferritins' transcription via binding to hypoxia-response elements (HREs) (131). HREs were identified within the IDE of *ftn-1* and *ftn-2* promoters (131). In the conditions where iron concentration is too low, HIF-1 inhibits *ftn-1* and *ftn-2* expression to prevent iron storage, whereas it stimulates expression of iron uptake gene *smf-3* that also possesses HREs (131). Interestingly for this research, it was reported that ferritin can be regulated in a DAF-16-dependent way resulting in the significantly increased *ftn-1* expression levels in *daf-2* mutants (88). Additionally, the *hif-1* and *daf-16* were observed to regulate *ftn-1* expression utilizing parallel pathways (88). Thanks to all of the similarities but also differences between mammals and *C. elegans* in the iron metabolism regulation, *C. elegans* might serve as a model organism to study mechanisms underlying the control of iron homeostasis under different conditions.

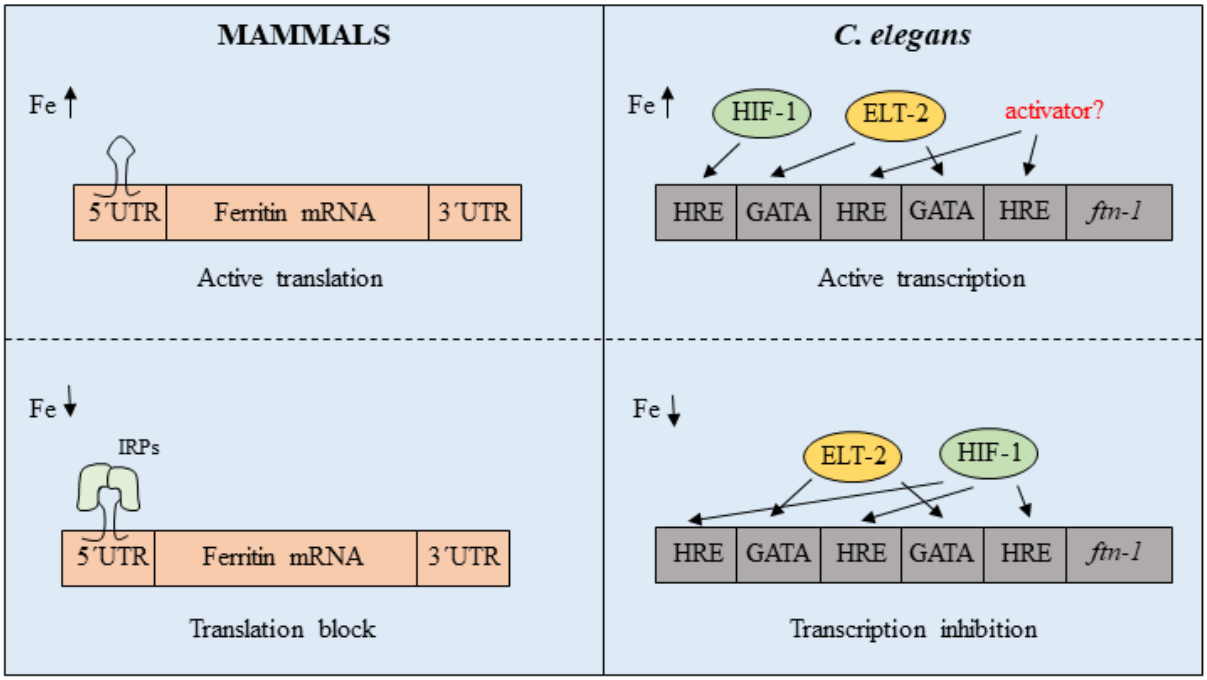

Figure 4. Mechanism regulating ferritin expression in mammals and *C. elegans*. In mammals ferritin is regulated at the post-transcriptional level by iron regulatory proteins (IRPs). During iron deficiency, IRPs bind to the iron responsive elements (IRE) located at the 5´UTR region of ferritin mRNA leading to its translation inhibition. Upon high iron concentration, IRPs do not bind IRE, allowing for the translation of ferritin mRNA. In *C. elegans*, ferritin is regulated at the transcriptional level. The mechanism of iron overload conditions is not fully uncovered. However, during iron homeostasis, ELT-2 binds to GATA motifs located at the promoter region of *ftn-1* allowing for its basal expression. An unidentified transcriptional activator could be responsible for *ftn-1* transcription through the binding to hypoxia-responsible elements (HREs). Also, some undiscovered transcriptional activator could be involved in the promotion of *ftn-1* transcription during iron overload as well. In iron deficient conditions, HIF-1 binds to (HREs) located in the *ftn-1* promoter region inhibiting *ftn-1* transcription. (Inspired by (131,146)).

1.3 Ferritin

Ferritin proteins are ubiquitously expressed, and highly conserved among species (Figure 5A) (147,148). Mammalian ferritins function as heteropolymers building molecular cages made up of iron core and protein shell (149,150). The ferritin protein is usually composed of 24 subunits. However, there are also ferritins built of 36 or 12 subunits. The subunits are divided into two types: heavy (FTH), and light (FTL) (149,150). The spherical structure of those subunits is highly similar and composed of four long α-helices connected to each other via two loops and one short terminal helix (Figure 5C) (149). FTH and FTL subunits exhibit distinct functions depending on the presence of ferroxidase activity (143). FTH binds Fe^{2+} ions and rapidly transfers them to the ferroxidase center where ferric ions are oxidized to ferrous cations (151). Afterwards, the Fe^{3+} ions are directed to the protein cavity of FTL subunit (which

does not possess ferroxidase activity) where they are bound by nucleation sites. This results in the formation of the iron minerals (143,151). Importantly, one ferritin molecule is able to bind and store up to 4500 Fe^{3+} ions (149). Overall, ferritin is not only able to store iron, but also to detoxify it (133,151).

1.3.1 Ferritin in *C. elegans*

C. elegans encodes two ferritin genes, *ftn-1* and *ftn-2,* and the sequences of the resulting nascent proteins FTN-1 and FTN-2 (Figure 5B) are highly conserved to the human FTH (Figure 5A, C) rather than human FTL (137,144). Both *C. elegans* ferritins share common features like the presence of ferroxidase center (137,144), and intestinal expression (108). However, there are also differences between FTN-1 and FTN-2. For example, the abundance of *ftn-2* mRNA is higher than the *ftn-1* mRNA at standard cultivation conditions (144,145,152). Additionally, FTN-2 is expressed also in other tissues like pharynx, hypodermis, and body wall muscle that might suggest separate functions of nematode ferritins (137,145). Even though the expression of *ftn-1* and *ftn-2* is reduced by iron chelation, and upregulated by high iron content suggesting that both ferritins might be regulated by iron (144), only mutants lacking *ftn-1* exhibited shortened lifespan when subjected to high iron concentration (136,137,145). Thus, FTN-1 and FTN-2 seem to play diverse functions in iron metabolism that is also supported by the fact that FTN-2 was shown to be responsible for iron storage what was not observed for FTN-1 (153). Functions of *C. elegans* ferritins were described in diverse conditions like cold response or innate immune defense, will be more discussed in the chapter 6.3., especially in the aspect of FTN-1.

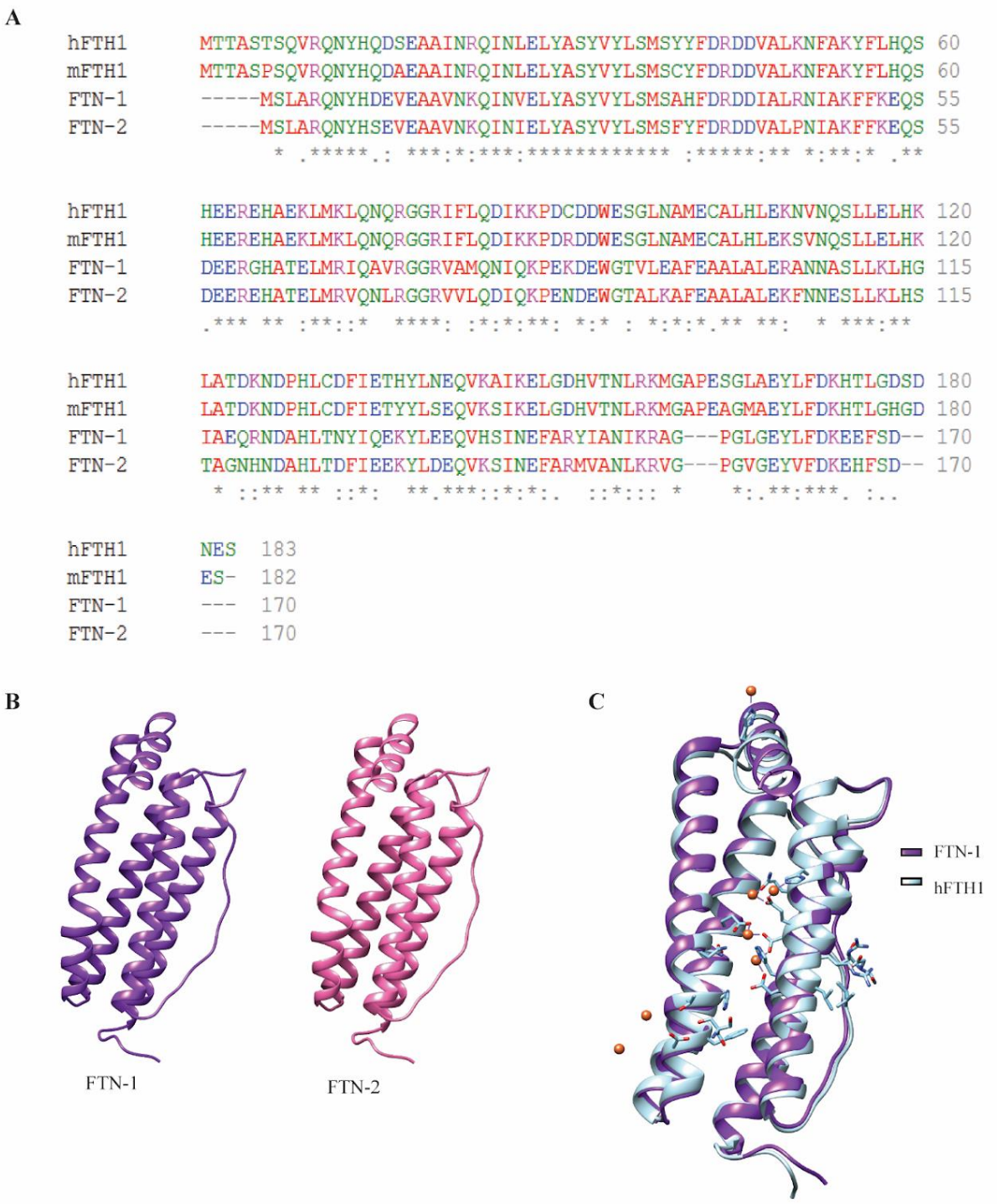

Figure 5. ***C. elegans*** **ferritins are conserved between humans and mice. A.** The alignment of amino acid sequences representing *H. sapiens* ferritin heavy chain 1 (hFTH1), *M. musculus* ferritin heavy chain (mFTH1), *C. elegans* ferritin (FTN-1), *C. elegans* ferritin (FTN-2). The NCBI accession numbers of the amino acid sequences are: NP_002023.2, NP_034369.1, NP_504944.2, NP_491198.1, respectively. The alignment was performed using the multiple sequence alignment Clustal Omega tool (http://www.ebi.ac.uk/Tools/msa/clustalo/) (154,155). The present symbols show residues which are: fully conserved (*), with strongly similar properties (:), and with weakly similar properties (.). **B.** 3D models of *C. elegans* FTN-1 and FTN-2. The prediction of *C. elegans* FTN-1 and FTN-2 structures was achieved by the Phyre2 tool (156). **C.** 3D model showing a structural alignment of amino acid sequences representing *H. sapiens* ferritin heavy chain 1 (hFTH1) (light blue, PDB code 4OYN), and

C. elegans ferritin FTN-1 (purple). The predicted structure of FTN-1 was the same as in 5B. The sticks are marking amino acid residues representing ferroxidase centers. The subsequent colors indicate: carbon atoms - light blue in hFTH1 and purple in FTN-1; nitrogen atom belonging to histidine – violet; oxygen atom belonging to glutamic acid – red; iron atoms – orange balls; coordination bonds – purple dotted lines.

1.3.2 Ferritin in the cold

As mentioned above, proper homeostasis of iron metabolism is essential for living organisms. Interestingly, this process is not only necessary at standard temperature conditions, but also during exposure to low ambient temperatures (157). Ferritin is a main iron storage protein (149), whose increased expression levels were detected during daily torpor (in gray mouse lemur), as well as throughout a hibernation state (in free-ranging dwarf lemurs) (158,159). Those examples suggest that ferritin upregulation is a characteristic phenomenon of some hibernating organisms essential for the cold survival (158,159). The importance of ferritin in those organisms can be exemplified by the fact that antioxidant protection (possible mediated via ferritin) is crucial for hibernating organisms to enter and exit a hibernation state. Moreover, it has been observed that the exposure to cold resulted in iron release, leading to the generation of ROS that damaged a vast group of cells (160-162). Thus, utilizing knowledge about ferritin properties, and using iron chelating molecules (like deferoxamine) or antioxidants enabled the reduction of cellular damages generated by cold exposure in diverse cell culture models and kidney transplant model (160-163). Therefore, it is highly important to investigate iron metabolism during low temperature exposure, since it might help to improve tissue/organ preservation procedures and therapeutic hypothermia strategies. In my PhD dissertation I took advantage of the fact that *C. elegans* has been widely used to study many biological processes, including response to low temperature exposure (57,124). Thus, I decided to investigate the role of ferritin in the aspect of nematodes' cold exposure.

1.3.3 Ferritin in health and disease

Serum ferritin has gained attention in medicine as a relevant marker indicating its iron storage ability (164). Therefore, serum ferritin levels serve as a biomarker for, inter alia, inflammatory diseases (165), infection, neurodegeneration, autoimmune disorders, and malignancy (166). Interestingly, the recent COVID-19 pandemic revealed elevated serum ferritin as an important marker of disease severity (167,168). Moreover, the measurement of serum ferritin levels allows to verify whether the patient suffers from iron deficiency or anemia (164). Additionally, hereditary hemochromatosis is an iron overload disease caused

by disrupted iron absorption that might be diagnosed and monitored by the amount of serum ferritin (164). Nevertheless, it is worth remembering that serum ferritin levels often need to be measured together with other iron metabolism biomarkers allowing for more precise diagnosis of pathological conditions (164,167).

The change in serum ferritin levels is not always an indirect outcome of pathological processes, but it can also be a direct result of mutations within the ferritin gene or its regulatory sites (148,169). Due to this fact, there are diseases characterized by severe health consequences caused by diverse mutations associated with the disruption of ferritin functions e.g. hereditary hyperferritinemia-cataract syndrome. This disease is caused by the mutations localized in the *FTL* gene, specifically, in the 5′UTR within IRE. These mutations result in the abolished interaction of IRE with IRPs leading to the massive production of ferritin, and subsequent increase in the serum (169). Another example of a human disease associated with *FTL* gene mutations is a neurodegenerative disease hereditary ferritinopathy, also called neuroferritinopathy (170). Identified mutations in this disease contribute to the frameshift within the C-terminus of the FTL chain causing a disruption of the proper iron storage (148,170). This disorder is characterized by, inter alia, elevated levels of stored iron and inclusion bodies holding ferritin localized e.g. in neurons (170,171). Interestingly, other neurodegenerative diseases like Parkinson's disease, Alzheimer's disease, restless legs syndrome, and amyotrophic lateral sclerosis are also characterized by disrupted iron homeostasis and iron-related undesirable effects (148,172). Moreover, altered levels of ferritin in the brain are believed to be an outcome of iron metabolism imbalance observed in some neurodegenerative diseases (173). Therefore, ferritin levels in the brain can be used to assess outcomes for, inter alia, Alzheimer's disease (174). All of the above examples highlight an essential role of ferritin in disease diagnosis, prediction and monitoring of the treatment outcomes. Thus, therapeutic drugs imitating ferritin function have gained attention in the medical applications.

Additionally, the specific structure of ferritin which allows for efficient iron storage, has been utilized in biomedical applications (148). Ferritin has been used in nanotechnology due to the fact that it is also able to store and deliver molecules other than iron (148). As a delivery molecule, ferritin possesses many advantages: small size, cell selectivity, self-assembly, ability to attach diverse conjugates to the surface, high stability, and possibility of cage disassembly under specific pH. The latter is highly important for encapsulating a molecule of interest (148,175). All of above advantages allowed ferritin to be successfully

used as a nanocage carrying e.g. chemotherapeutics for cancer treatment, small interfering RNAs for gene expression silencing, as well as molecules for vaccines (148,175,176). Moreover, ferritin nanocages might be used as tumor imaging agents in optical and magnetic resonance imaging (175). To summarize, ferritin is not only an important biomarker in diagnosis but also it exhibits a huge potential for multiple biomedical applications.

2 The aims of the project

The main aim of this study was to determine processes underlying *C. elegans* ferritin-mediated cold protection during hibernation-like state.

Specified aims of the research:

1. To establish the cold survival of *ets-4(-)* or *ftn-1(-)* mutants;
2. To analyze the influence of *ets-4* mutation on the expression of *C. elegans* ferritin protein levels during exposure to cold;
3. To analyze the influence of ferritin overexpression on cold survival and longevity by generating *ftn-1* overexpressing strains;
4. To establish whether the ferroxidase activity of FTN-1 is crucial for cold survival of *ets-4(-)* mutants;
5. To define the change in global ROS and expression levels of ROS-associated genes after cold exposure of *C. elegans* strains;
6. To determine whether transcription factors responsible for FTN-1 regulation: ELT-2 and HIF-1 are involved in response to cold;
7. To analyze the effect of starvation and cold on FTN-1 protein abundance;
8. To establish whether the presence of *ets-4*-regulating proteins, RLE-1 and REGE-1, affects the cold survival.

3 Materials

3.1 Chemicals and reagents

Table 2. Chemicals and reagents used in the research.

CHEMICAL/REAGENT	COMPANY	PURPOSE
40 % ACRYLAMIDE/BIS-ACRYLAMIDE Solutions, UltraPure	BioShop Canada Inc.	Western blot
Agar, Bacteriological Grade	BioShop Canada Inc.	nematode growth media (NGM) plates, NGM plates with 1 mM IPTG and 50 µg/ml ampicillin, LB plates with kanamycin, LB plates with ampicillin
Agarose	BioShop Canada Inc.	Agarose gel electrophoresis, Agar pads
Ammonium Persulfate (APS)	BioShop Canada Inc.	Western blot
Bovine Serum Albumin (BSA)	Sigma-Aldrich	Bradford assay
Bradford Reagent	Sigma-Aldrich	Bradford assay
Calcium chloride dihydrate	BioShop Canada Inc.	NGM plates, NGM plates with 1 mM IPTG and 50 µg/ml ampicillin
Cell Lysis Solution	Qiagen	Genomic DNA isolation from *C. elegans*
Chloroform	POCH	RNA isolation
Cholesterol	Sigma-Aldrich	NGM plates, NGM plates with 1 mM IPTG and 50 µg/ml ampicillin
cOmplete™, Mini, EDTA-free Protease Inhibitor Cocktail	ROCH	Western blot
CutSmart® Buffer	New England Biolabs, Inc.	Restriction enzyme digestion
Dimethyl sulfoxide (DMSO)	BioShop Canada Inc.	Trehalose-DMSO worm freezing solution, ROS assay after cold treatment
D-(+)-TREHALOSE, Dihydrate	BioShop Canada Inc.	Trehalose-DMSO worm freezing solution
DITHIOTHREITOL (DTT), Electrophoresis Grade	BioShop Canada Inc.	Western blot
DNase I	Zymo Research	RNA isolation
Ethanol absolute ≥ 99.8 %	POCH	RNA isolation
Gelatin	BioShop Canada Inc.	Worm lysis buffer
Glycine	BioShop Canada Inc.	Western transfer buffer
Immersol™ 518F	Zeiss	Microscope observation
Invitrogen™ CM-H2DCFDA (General Oxidative Stress Indicator)	ThermoFisher Scientific	Reactive Oxygen Species assay
IPTG (izopropylo-β-D-tiogalaktopiranozyd)	Blirt	NGM plates with 1 mM IPTG and 50 µg/ml ampicillin
1 kb Plus DNA Ladder	New England Biolabs, Inc.	Agarose gel electrophoresis

LB Broth Lennox	BioShop Canada Inc.	Bacteria culture for plasmid cloning
Levamisole hydrochloride, Alkaline phosphatase inhibitor	Abcam	Microscope observation
Liquid nitrogen		RNA isolation
Magnesium chloride hexahydrate	BioShop Canada Inc.	Worm lysis buffer
Magnesium sulfate anhydrous	BioShop Canada Inc.	NGM plates, NGM plates with 1 mM IPTG and 50 µg/ml ampicillin, 10x M9 buffer
Methanol	Chempur	Western transfer buffer
N-acetyl-L-Cysteine (NAC)	Sigma Aldrich	Cold survival assay with antioxidant treatment
NONIDET® P-40 SUBSTITUTE	BioShop Canada Inc.	Worm lysis buffer
Peptone, Bacteriological Grade	BioShop Canada Inc.	NGM plates, NGM plates with 1 mM IPTG and 50 µg/ml ampicillin, LB plates with kanamycin, LB plates with ampicillin
Pharmacy gasoline Benzinum FP	Amara	Microscope observation
Phosphate Buffered Saline tablets (PBS)	BioShop Canada Inc.	Western blot, Reactive Oxygen Species assay after cold treatment
Precision Plus Protein™ All Blue Prestained Protein Standards	Bio-Rad	Western blot
Protein Precipitation Solution	Qiagen	Genomic DNA isolation from *C. elegans*
2-Propanol (Isopropanol)	POCH	Genomic DNA isolation from *C. elegans*
Potassium Chloride	BioShop Canada Inc.	Worm lysis buffer
Potassium hydroxide Pure P.A	POCH	Worm bleaching solution
Potassium phosphate monobasic	BioShop Canada Inc.	10x M9 buffer
Radiance Plus	Azure Biosystems	Western blot
SimplySafe	EURx	Agarose gel electrophoresis
Skim Milk (non-fat powder)	BioShop Canada Inc.	Western blot
Sodium chloride	BioShop Canada Inc.	NGM plates, NGM plates with 1 mM IPTG and 50 µg/ml ampicillin, LB plates with kanamycin, LB plates with ampicillin, 10x M9 buffer
SODIUM DODECYL SULFATE, SDS, 20 % Solution	BioShop Canada Inc.	5x SDS Sample Buffer without bromophenol blue (BPB), 10x running buffer
Sodium hypochlorite 5 %	Chempur	Worm bleaching solution
Sodium phosphate dibasic	BioShop	10x M9 buffer
Sucrose	BioShop Canada Inc.	5x SDS Sample Buffer without BPB
SYBR™ Safe DNA Gel Stain	Sigma-Aldrich	Agarose gel electrophoresis
TAE BUFFER, 50X Liquid Concentrate	BioShop Canada Inc.	Agarose gel electrophoresis
TEMED, Electrophoresis Grade	BioShop Canada Inc.	Western blot
TRI Reagent®	Molecular Research Center, Inc.	RNA isolation

Tricine buffer	VWR Life Science	10x running buffer
TRIS	BioShop Canada Inc.	Worm lysis buffer, 5x SDS Sample Buffer without BPB, 10x running buffer, western transfer buffer
TWEEN® -20, Biotechnology Grade	BioShop Canada Inc.	Worm lysis buffer, 1x PBS-T buffer
WATER, Sterile-filtered, Dnase/Rnase/Protease free	BioShop Canada Inc.	Cold survival assay with antioxidant treatment
Yeast extract	BioShop Canada Inc.	LB plates with kanamycin, LB plates with ampicillin

3.1.1 Materials

Table 3. Materials used in the study.

NAME	COMPANY
Amersham™ Hybond® P Western blotting membranes, PVDF, pore size 0.2 µm	GE Healthcare Life Sciences
Direct-zol RNA MiniPrep Kit	Zymo Research
Gel Blotting Papers Whatman ® GB 005	GE Healthcare Life Sciences
Monarch® PCR & DNA Cleanup Kit (5 µg)	New England Biolabs, Inc.
Plasmid Mini	A&A Biotechnology
Protein LoBind Tubes	Eppendorf

3.1.2 Enzymes

Table 4. Enzymes used in the study.

ENZYME	COMPANY
*Afl*II	New England Biolabs, Inc.
AMPLIFY ME SG Universal Mix	Blirt
Gateway™ BP Clonase™ II Enzyme mix	ThermoFisher Scientific
Gateway™ LR Clonase™ II Enzyme mix	ThermoFisher Scientific
GoTaq®G2 Green Master Mix	Promega
High-Capacity cDNA Reverse Transcription Kit	Applied Biosystems
Phusion HF DNA polymerase	New England Biolabs, Inc.
Proteinase K, Biotechnology Grade	BioShop Canada Inc.
Proteinase K solution	ThermoFisher Scientific
*Xba*I	New England Biolabs, Inc.
*Xho*I	New England Biolabs, Inc.

3.1.3 Antibodies

Table 5. Antibodies used in the research.

ANTIBODY	COMPANY
Anti-Actin Antibody, clone C4 (Cat. No. MAB1501)	EMD Millipore Corp.
Anti-mouse IgG, HRP-linked Antibody (Cat. No. 7076S)	Cell Signaling Technology
Anti-rat IgG, HRP-linked Antibody (Cat. No. 7077S)	Cell Signaling Technology

Myc-tag antibody [9E1], rat monoclonal (Cat. No. 9e1-20)	ChromoTek

3.1.4 Antibiotics

Table 6. Antibiotics used in the research.

ANTIBIOTIC	COMPANY
Ampicillin, sodium salt	BioShop Canada Inc.
Kanamycin Monosulfate	BioShop Canada Inc.
Tetracycline HCL	BioShop Canada Inc.

3.1.5 Buffers and media

3.1.5.1 Buffers used in common experiments made on *C. elegans* culture

Table 7. Buffers necessary for experiments made on *C. elegans* culture.

BUFFER NAME	COMPOUNDS [FINAL CONCENTRATION]
10x M9 buffer	220 mM KH_2PO_4 485 mM $Na_2HPO_4*2H_2O$ 850 mM NaCl 2 mM $MgSO_4*7H_2O$
Trehalose-DMSO worm freezing solution	80 mM Trehalose dihydrate 3.5 % DMSO 1x M9 buffer
Worm bleaching solution	1.5 % Sodium hypochlorite 0.75 mM KOH ddH_2O
Worm lysis buffer	52 mM KCl 10 mM Tris pH 8.3 2.5 mM $MgCl_2$ 0.45 % NP40 0.45 % Tween 20 0.05 % Gelatin ddH_2O

3.1.5.2 Buffers used in western blot

Table 8. Buffers necessary for western blot.

BUFFER NAME	COMPOUNDS [FINAL CONCENTRATION]
1x PBS buffer	PBS tablets ddH_2O
1x PBS-T buffer	1x PBS buffer 0.05 % Tween-20
5x SDS Sample Buffer without BPB	312.5 mM Tris-HCl pH 6.8 25 mM DTT 10 % SDS 25 % sucrose
10x running buffer	250 mM Tris 250 mM Tricine 0.5 % SDS ddH_2O

5 % skim milk	50 g/l skim milk powder 1x PBS-T buffer
Western transfer buffer	25 mM Tris base 192 mM glycine 20 % methanol
4 % stacking gel	4 % acrylamide/bis-acrylamide solutions 380 mM Tris pH 8.8 0.6 %TEMED 0.09 % APS ddH_2O
16.5 % resolving gel	16.5 % acrylamide/bis-acrylamide solutions 1.15 M Tris pH 8.8 0.3 % TEMED 0.045 % APS ddH_2O

3.1.5.3 Buffers used in the ROS assay after cold treatment

Table 9. Buffers necessary for the ROS assay after cold treatment.

BUFFER NAME	COMPOUNDS [FINAL CONCENTRATION]
1x tris-buffered saline (TBS) buffer, pH 7.5	50 mM Tris-HCl 150 mM NaCl ddH_2O

3.1.5.4 Compounds used in agarose gel electrophoresis and for agar pads

Table 10. Compounds used in agarose gel electrophoresis and for agar pads.

NAME	COMPOUNDS [FINAL CONCENTRATION]
1x TAE buffer	1x TAE buffer, liquid concentrate ddH_2O
1 % agarose gel	1 % agarose 1x TAE buffer 1000x SimplySafe
3 % agar pads	3 % agarose 1x TAE buffer

3.1.5.5 Liquid and solid media

Table 11. Liquid and solid media used in the research.

MEDIUM NAME	COMPOUNDS [FINAL CONCENTRATION]
LB medium	20 g/l LB Broth ddH_2O
LB plates with ampicillin, pH 7.2	0.5 % yeast extract 171 mM NaCl 1 % peptone 1.5 % agar 100 µg/ml ampicillin (added when the solution was cooled down to ~50°C) ddH_2O
LB plates with kanamycin, pH 7.2	0.5 % yeast extract 171 mM NaCl 1 % peptone

	1.5 % agar 25 µg/ml kanamycin (added when the solution was cooled down to ~50°C) ddH_2O
NGM plates	2 % agar 0.25 % peptone 0.51 mM NaCl ddH_2O (cool down the solution to ~50°C, then add the rest of the compounds) 5 µg/ml cholesterol in ethanol 1 mM $CaCl_2$ 1 mM $MgSO_4$ 25 mM potassium phosphate, pH 6.0
NGM plates with 1 mM IPTG and 50 µg/ml ampicillin	2 % agar 0.25 % peptone 0.51 mM NaCl 5 µg/ml cholesterol in ethanol 1 mM $CaCl_2$ 1 mM $MgSO_4$ 25 mM potassium phosphate, pH 6.0 1 mM IPTG 50 µg/ml ampicillin

3.2 Primers used in the study

Primers used in this project designed for Sanger sequencing, standard PCR, colony PCR, and RT-qPCR were ordered from Merck. The table below lists all of the primers used in the research.

Table 12. Primers used in the research.

PRIMER NAME	PRIMER SEQUENCE	PURPOSE
ftn-1 RT_Fw1 235	CGGCCGTCAATAAACAGATTAACG	RT-qPCR
ftn-1 RT_Rv1 236	CACGCTCCTCATCCGATTGC	
qPCR *ftn-2* F	TGAAGCTGCCGTTAACAAGC	
qPCR *ftn-2* R	TGTTTGGAAGGGCAACATCG	
act-1 qPCR F1	GTTGCCCAGAGGCTATGTTC	
act-1 qPCR R1	CAAGAGCGGTGATTTCCTTC	
ctl-1 qPCR F	TTTTTCAACGGTCGCTGGAG	
ctl-1 qPCR R	AGTGGATTGCGTCACGAATG	
tbb-2 qPCR R	TGGTGAGGGATACAAGATGG	
tbb-2 qPCR F	GCTCATTCTCGGTTGTACCA	
ctl-2 qPCR F	TTTGGCCACACGGTGATTAC	
ctl-2 qPCR R	AAGGCGGATTGTTCAACCTC	
ctl-3 qPCR F	TTTTTCAACGGTCGCTGGAG	
ctl-3 qPCR R	AGTGGATTGCGTCACGAATG	

gcs-1 qPCR F	AATGCGATGCTTGGAACTGC	
gcs-1 qPCR R	TGCCTCGACAATGTTGAAGC	
gst-1 qPCR F	TGCGGATTATGTGCTGTTCG	
gst-1 qPCR R	TTGATGTTTGGACGCTCAGC	
gst-4 qPCR F	TTTGATGCTCGTGCTCTTGC	
gst-4 qPCR R	AATGGGAAGCTGGCCAAATG	
gst-5 qPCR F	AGGAACAATGGCCAGCATTG	
gst-5 qPCR R	AGCCAAGAAACGAGCAATCG	
gst-38 qPCR F	TTCAAAGCGGCCGGAAAAAC	
gst-38 qPCR R	TTCCGTTGAACCCGAATTCC	
ugt-8 qPCR F	AAAGAAATGGGTGCCGCAAC	
ugt-8 qPCR R	TCCTCCATGGGTCACAAATAGC	
ugt-25 qPCR F	TCGTGCAACAACTTCATGCG	
ugt-25 qPCR R	AAGACCGCAGACAGAAAGTG	
ugt-58 qPCR F	TGACATGGCTGGAAATTGGC	
ugt-58 qPCR R	ATTGTGCAGGCCAGAATTCG	
prdx-2 qPCR F	TTCACTTTCGTGTGCCCAAC	
prdx-2 qPCR R	AGCACAACGGTGTTGATAGC	
prdx-3 qPCR F	AGATCGTGCAAACGAGTTCC	
prdx-3 qPCR R	TGAAATCAGCGAGCAAAGGG	
prdx-6 qPCR F	CGTGCTGTGATGCTTTTTGG	
prdx-6 qPCR R	TTTGTGCCGAGTTGAACACC	
gpx-6 qPCR F	GCGTGGCTCATCATTATCAGC	
gpx-6 qPCR R	AACCGGCTGATCTCTTCTTCC	
gpx-4 qPCR F	AAACAAGGCCTAGTCATCGC	
gpx-4 qPCR R	TTCCAGGACGAACATGAGTCAG	
sod-1 qPCR F	TCTCCAACGCGATTTTTCCG	
sod-1 qPCR R	AACTGCCTGGTCATTTTCGG	
sod-2 qPCR F	TGAGGCAACAACTGGACTTG	
sod-2 qPCR R	TTTGCAAAACGCTCGCTGAC	
sod-3 qPCR F	AAAGCATCATGCCACCTACG	
sod-3 qPCR R	TGAATTTCAGCGCTGGTTGG	
sod-4 qPCR F	AATCATTGGCCGAAGTGTGG	
sod-4 qPCR R	AAGTCGGCTTCCAGCATTTC	
sod-5 qPCR F	ATTGCCAATGCCGTTCTTCC	
sod-5 qPCR R	AGCCAAACAGTTCCGAAGAC	
qPCR_*ets-4*_fw	CTGAGAACCCGAATCATCCA	
qPCR_*ets-4*_rv	TCATTCATGTCTTGACTGCTCC	
C30F12.1_2_fw	CGGCAAATGAATGTTTATCCAG	

C30F12.1_2_rv	ATCAGATCCAGTATTCACAGGTC	
RLE-1 seq 1	CCGATGCCGATGCTCATTG	
RLE-1 internal R	CACCACACGTTGAGGTGTTC	
gt *vit-5* F	CGGAAATGGTGACCGTCGA	Genotyping of *sybSi72*[*Pvit-5*::*ftn-1*::*unc-54* 3′UTR]; *unc-119(ed3)* and *sybSi67*[*Pdpy-30*::*ftn-1*::*unc-54* 3′UTR]; *unc-119(ed3)*
gt *vit-5* R	CAACGTGCATATCGTGGTCG	
gt *vit-5+ftn-1* F	TCGACCACGATATGCACGTT	
gt *vit-5+ftn-1* R	GTTCGGCGATTCCATGAAGC	
gt *ftn-1+unc-54* F1	ATCATGGCAGCGTCGATGAT	
gt *ftn-1+unc-54* R1	TTTGACGTCATGAGAGGCCC	
gt *ftn-1+unc-54* F2	ATCATGGCAGCGTCGATGAT	
gt *ftn-1+unc-54* R2	TTTGACGTCATGAGAGGCCC	
gt *dpy-30* F	TGCACCGTTCGGATTCTGAA	
gt *dpy-30* R	CTTGCGCACCGTACTCTAGT	
gt *dpy-30+ftn-1* F	GCAAACTTGCGTAACGGTGT	
gt *dpy-30+ftn-1* R	GTTCGGCGATTCCATGAAGC	
GS *vit-5* F	GGGGACAACTTTGTATAGAAAAGTTGTGCAAAATCTACGGGAGCGA	Generation of *sybSi72*[*Pvit-5*::*ftn-1*::*unc-54* 3′UTR]; *unc-119(ed3)*
GS *vit-5* R	GGGGACTGCTTTTTTGTACAAACTTGTGCGAGAGTGACTATGGCTTCTCC	
MosSCI ChrII fwd	CAGAATGTGAACAAGACTCGAGC	Genotyping of [*Plips-11*::MYC::*ftn-1*::*ftn-1* 3′UTR; *unc-119(+)*]
Cb P*unc-119* rev	CCCTAACTTTGAGCCAATTCATCC	
ftn-1 genotyp F	TGTTCGACAAAGAGGAATTTTCTG	
MosSCI ChrII rev	ATCGGGAGGCGAACCTAACTG	
Mos1_fwd	CAACCTTGACTGTCGAACCACCATAG	
Mos1_rev	TCTGCGAGTTGTTTTTGCGTTTGAG	
pCFJ150 L-RecArm fwd	GTCCTCCTGATTCCATGATGGTAGC	
FW *lips-11* promoter	GGAGCCGAATCAAGAGTTTT	
RV *ftn-1* gene body	TCAAGGACAGTTCCCCACTC	
M13 F	GTAAAACGACGGCCAG	Plasmid sequencing
M13 R	GTCATAGCTGTTTCCTG	
seq *vit-5* F1	TCAACAAGACTTCCAGCATCGA	
seq *vit-5* F2	CCGTTTTCCAATGATTTCTTTCACG	
seq *vit-5* F3	GGAAGTTGTCCTTTTTGTGAATGA	
pL4440 F	AACCTGGCTTATCGAAATTAATAC	
gt *ftn-1* dysfun. F	AGCTCGTCAAAACTATCACGA	Strain genotyping
gt *ftn-1* dysfun. R	TCAGAAAATTCCTCTTTGTCGAACA	
ftn-1(ok3625) out L	ATGTGTCTCAGATTTCCGCC	

ftn-1(ok3625) out R	GAACCCTTTCGTTGCCAATA	
ftn-1(ok3625) inner L	GGTTGAACCTTTTTAGGAACTGC	
ftn-1(ok3625) inner R	ACAGTCCCGGACACGTAATC	
ets-4 inside F	GCTCAGTCGGTCACAGATGG	
ets-4 inside R	GCATATCCATCGGATGTGG	
glo-1 genot F	CTGAATCATACTGCAGTAATACTTG	
glo-1 genot R	CAAAGCGATGAAATCCCTCTC	
ftn-1 end mCherry F2	GCTTCATGGAATCGCCGAAC	
ftn-1 end mCherry R2	AACATTGTACGCTCCTGGCA	
ftn-1 endogenous F2	AGGCGGCAGTAGATAGACGA	
ftn-1 endogenous R2	CGTAGAATTCCACATGGCGC	
RLE deletion F	GGCACAATTCAGAAAAATTGG	
RLE deletion R	GCATGATTAAGAGCATGCTGAC	
hif-1 outer F	CTCCACTGGCTCCTCCTACT	
hif-1 outer R	CGCAAGTGTGACGAGTTGTG	
hif-1 inner F	TGGACTGAAGACACCATCGC	
hif-1 inner R	AAGAAGCGGAAAGGAGGAGC	
PRC07-seq-s1	ACAAGGGCAGGCAGACAGTA	*ftn-1(syb2550)* sequencing

3.3 Plasmids and bacterial strains

In this project, specific bacteria strains and plasmids were used for RNA interference (RNAi) experiment and to obtain plasmids needed for generation of *C. elegans ftn-1* overexpressing strains (*sybSi72*[*Pvit-5*::*ftn-1*::*unc-54* 3´UTR]; *unc-119*(*ed3*), and *sybSi67*[*Pdpy-30*::*ftn-1*::*unc-54* 3´UTR]; *unc-119*(*ed3*)). All of the used plasmids and bacteria strains are listed in the table below. Plasmids used for RNAi were sequenced using pL4440 F primer, and plasmids obtained from Gateway System Technology were sequenced (*vit-5* promoter in pDONR P4-P1r using primers listed in the table 12) or digested with restriction enzymes (table 14), and analyzed on 1 % agarose gel.

Table 13. Plasmids and bacteria strains used in the study.

PLASMID NAME	**BACTERIA STRAIN**	**ANTIBIOTIC RESISTANCE PLASMIDS**	**PURPOSE**
P*dpy-30*-pENTR P4-P1r	One Shot™ TOP10 Chemically Competent	kanamycin	Generation of *sybSi72*[*Pvit-5*::*ftn-*

	E. coli [Thermo Fisher Scientific]		*1*::*unc-54* 3´UTR]; *unc-119(ed3)* and *sybSi67*[*Pdpy-30*::*ftn-1*::*unc-54* 3´UTR]; *unc-119(ed3)* strains
ftn-1 gene body in p221	*E. coli* DH5α	kanamycin	
unc-54 3´UTR-pENTRP2r-P3	One Shot™ TOP10 Chemically Competent *E. coli* [Thermo Fisher Scientific]	kanamycin	
pCFJ150	*E. coli* DH5α	ampicillin	
vit-5 promoter in pDONR P4-P1r	One Shot™ TOP10 Chemically Competent *E. coli* [Thermo Fisher Scientific]	kanamycin	
pDONR P4-P1r	*E. coli* DH5α	kanamycin	
P*dpy-30*+*ftn-1*GB+*unc-54* 3´UTR	One Shot™ TOP10 Chemically Competent *E. coli* [Thermo Fisher Scientific]	ampicillin	
P*vit-5*+*ftn-1*GB+*unc-54* 3´UTR	One Shot™ TOP10 Chemically Competent *E. coli* [Thermo Fisher Scientific]	ampicillin	
empty vector RNAi	HT115	ampicillin/tetracycline	RNA interference
C33D3.1 (clone in Vidal library – *elt-2* RNAi)	HT115	ampicillin/tetracycline	
-	OP50 *E. coli*	-	Food source

3.4 Restriction enzymes

In this project some restriction enzymes were used to analyze the plasmids generated in the BP and LR reactions from Gateway System Technology. The list of used restriction enzymes is available below in table 14. Around 1 µg of plasmid DNA was incubated with restriction enzymes mix at 37°C for 15 minutes. Then, the heat shock inactivation was carried out at 65°C for 20 minutes. All of the samples were analyzed in 1 % agarose gel to validate the presence of linear products representing the desired size.

Table 14. Restriction enzymes used in the study.

NAME OF THE RESTRICTION ENZYME	PLASMID NAME
*Afl*II	P*dpy-30+ftn-1*GB+*unc-54* 3´UTR, P*vit-5+ftn-1*GB+*unc-54* 3´UTR, *vit-5* promoter in pDONR P4-P1r
*Xho*I	P*dpy-30+ftn-1*GB+*unc-54* 3´UTR
*Xba*I	P*vit-5+ftn-1*GB+*unc-54* 3´UTR, *vit-5* promoter in pDONR P4-P1r

3.5 Laboratory equipment

- Aspirator Lab Helper LH-930 [Bio Medical Science]
- Axio Imager.Z2 [Carl Zeiss]
- Azure c600 Imager [Azure biosystems]
- Centrifuge 5424 [Eppendorf]
- Centrifuge 5424 R [Eppendorf]
- Centrifuge 5804 R [Eppendorf]
- Digital incubator INCU-Line® [VWR]
- Excella E24 Incubator Shaker Series [New Brunswick Scientific]
- Fisherbrand™ Owl™ Separation HEP-1 Semi Dry Electroblotting System [PEQLAB]
- Fluorescent stereomicroscope Nikon SM2 745 [Nikon]
- Incubator HettCube 600 [Hettich]
- KS 130 Basic Shaker [IKA®]
- Laboratory precise balance PA [OHAUS]
- Laboratory incubator with cooling system ILW 115 STD [POL-EKO Aparatura]
- Laboratory fume hood [LabDud]
- Microwave [Amica]
- NanoDrop OneC Microvolume UV-Vis Spectrophotometer [Thermo Fisher Scientific]
- ProFlex PCR System [Applied Biosystems by life technologies]
- SimpliAmp™ Thermal Cycler [Thermo Fisher Scientific]
- Stereoscopic microscope [Nikon]
- Thermomixer C [Eppendorf]
- ThermoMixer F1.5 [Eppendorf]

- Variable Speed 6 Rollers LCD Digital Tube Roller [Dlab]
- Vortex-Genie 2 [Scientific Industry, Inc.]
- Corning® LSE™ Mini Microcentrifuge [Corning]
- PowerPac Basic & Mini PROTEAN Tetra vertical electrophoresis system [Bio-Rad]
- Revolver Rotator [Labnet International]

3.6 *C. elegans* strains selected for the research

In this project, a model organism *C. elegans* was used to study hibernation-like state. The table below represents all strains used in this study.

Table 15. *C. elegans* strains used in the research.

Genotype	**CGC**/RAF/**Other**
N2 Bristol (wild type)	**N2**/5044
ets-4(rrr16) X.	5045
ftn-1(ok3625) V.	**RB2603**/2162
ftn-1(ok3625) V.; ets-4(rrr16) X.	5063
[*Plips-11*::MYC::*ftn-1*::*ftn-1* 3´UTR; *unc-119*(+)] II.	5023
[*Plips-11*::MYC::*ftn-1*::*ftn-1* 3´UTR;*unc-119*(+)] II.; *ets-4(rrr16) X.*	5119
sybSi67[Pdpy-30::ftn-1::unc-54 3´UTR] II.; unc-119(ed3) III.	5069/**PHX1798**
sybSi72[Pvit-5::ftn-1::unc-54 3´UTR] II.; unc-119(ed3) III.	5071/**PHX1920**
hif-1(ia4) V.	**ZG31**/1948
hif-1(ia4) V.; ets-4(rrr16) X.	5166
ftn-1(syb2550) V.	5118
ftn-1(syb2550) V.; ets-4(rrr16) X.	5112
wuIs57[pPD95.77 sod-5::GFP,rol-6(su1006)]	5106/**GA411**
glo-1(zu391) X.	**JJ1271**/908
ftn-1(syb3517) V.; glo-1 (zu391) X.	5164
pqm-1(syb432) II.	2156
daf-16(syb707) I.	5010
ftn-1(syb3517) V.	5153
rle-1(rrr44) III.	2055
rege-1(rrr13) I.	1657
rle-1(rrr44) III.; ets-4(rrr16) X.	5161

"CGC" signifies numbers of *C. elegans* strains available in the Caenorhabditis Genetics Center; "RAF" indicates numbers of *C. elegans* strains in the Ciosk lab collection; "Other" signifies *C. elegans* strains acquired from other sources.

4 Methods

4.1 *C. elegans* strains care

4.1.1 Maintenance and cultivation conditions

C. elegans is a major model organism with well described methods in the wormbook (http://www.wormbook.org/). All *C. elegans* strains used in this research were maintained and cultured on NGM plates (177) (except RNAi experiment), with OP50 *E. coli* bacteria as the food source (except RNAi experiment). For the purpose of maintenance, animals were kept at 15°C. However, before the experiments, animals were chunked and kept for two generations on NGM plates at 20°C.

4.1.2 Generation of one-day-old adults and bleaching procedure

To obtain one-day-old adults, *C. elegans* were kept on NGM plates, seeded with OP50 *E. coli*, for two generations at 20°C and synchronized by bleaching. The bleaching procedure was as follows: animals of a desired strain were harvested in 1x M9 buffer in 15 ml conical tubes by centrifugation for 1 minute at 1,600 g. Then, the supernatant was aspirated and 7 ml of pre-cooled worm bleaching solution was added to the animals' pellet. Animals were shaken vigorously and observed under the stereoscopic microscope every 30 seconds to estimate whether the eggs were released from animals. When eggs were isolated and the animals' debris dissolved, the samples were then centrifuged for 1 minute at 1,600 g. Next, the bleaching solution was removed and the eggs' pellet was washed three times in 1x M9 buffer. Then, the eggs' pellet was suspended in 10 ml of 1x M9 buffer, placed in the revolver rotator at 20°C and left overnight for eggs to hatch. The next day, L1 larvae were put on plates and kept at 20°C for around 3 days to reach the one-day-old adult stage. In all experiments (except lifespan where the young adult stage was used), this particular stage of development was utilized.

4.1.3 Freezing and thawing

C. elegans strains are easy to store for a long period of time (177). It is possible to freeze and thaw animals. The freezing process is started by strain culturing. The animals from the strain of interest were chunked, synchronized by bleaching (as described in 4.1.2), put on NGM plates with OP50 *E. coli* as the food source, and cultured under standard conditions. When animals (most of them were in L1/L2 stage) were starved for around 2 days, 2 ml of freezing

solution per plate was added to harvest animals into freezing tubs. Next, tubes were incubated on ice for 15 minutes and then transferred to -80°C. Each time one tube containing frozen animals was thawed to check if animals from a particular strain were able to recover. To thaw a strain of interest a certain tube was taken out from -80°C and incubated at 20°C. After ice melted, the animals' pellet was gently transferred with a glass Pasteur pipette onto a fresh NGM plate with OP50 *E. coli*, and animals were examined for recovery.

4.2 *C. elegans* strain design and preparation

In this research, all used *C. elegans* strains were taken from a laboratory collection, ordered from CGC or SunyBiotech (a company producing *C. elegans* strains for a customer order), or obtained from other laboratories. The *C. elegans* SOD-5::GFP strain (GA411), was shared by Prof. David Gems. The SunyBiotech used a CRISPR/Cas9 genome editing method to produce the *ftn-1* ferroxidase-inactive mutant named as *ftn-1*$^{FO\text{-}dead}$ (allele *syb2550*), and *ftn-1*::mCherry strain (allele *syb3517*). To obtain the *ftn-1* overexpressing strains (*sybSi67[Pdpy-30::ftn-1::unc-54 3′UTR] II.; unc-119(ed3)*, and *sybSi72[Pvit-5::ftn-1::unc-54 3′UTR] II.; unc-119(ed3)*: named respectively as *ftn-1* OE (*dpy-30*) and *ftn-1* OE (*vit-5*)), constructs were produced using the MultiSite Gateway Technology. To generate these strains, SunyBiotech used the mos1-mediated single copy insertion (MosSCI) method (with the insertion locus ttTi5605) (178). The detailed information of above strains generation is described below.

4.2.1 MultiSite Gateway Technology cloning of MosSCI vector for *C. elegans* strain preparation

The cloning method MultiSite Gateway Technology was performed with the MultiSite Gateway Three-Fragment Vector Construction Kit and carried out based on the company protocol (Version H). Briefly, The MultiSite Gateway Technology is a commercially available cloning method relying on an integration of bacteriophage lambda into the *E. coli* chromosome using specific recombination sites (179,180). The recombination sites used in this technology are *att*B, *att*P, *att*L, *att*R, and are utilized in two reactions: BP and LR. BP reaction uses *att*B sites flanking PCR products (representing a promoter or gene body or UTR of gene of interest), and *att*P sites present in a donor vector. BP reaction using BP Clonase™ Enzyme Mix allows for an insertion of the PCR product into a donor vector to create an entry clone used later in the LR reaction. In the LR reaction, all donor vectors (in this research three vectors) undergo recombination into a destination vector which is performed by LR Clonase™ II Plus Enzyme

Mix (179,180). When the final vectors of interest were generated, they were sent to SunyBiotech that was responsible for making *ftn-1* overexpressing strains (*ftn-1* OE (*dpy-30*), and *ftn-1* OE (*vit-5*)), using the MosSCI method allowing for a single insertion of the desired transgene into a specific genomic locus (178).

4.2.1.1 Genomic DNA isolation from *C. elegans*

To obtain a fragment of nucleic acid sequence necessary for cloning and deriving from *C. elegans* genome, large-scale genomic DNA extraction from N2 Bristol (wild-type) animals was performed. Four 90 mm NGM plates with OP50 *E. coli* as the food source were seeded with bleach-synchronized L1 larvae from wild-type strain. Plates were kept at 20°C until animals were completely starved. Then, animals were collected into a 15 ml conical tube and washed in 1x M9 buffer three times. The animals' pellet was suspended in 600 µl of Cell Lysis Solution, transferred into a 1.5 ml Eppendorf tube, and 20 µl of 20 mg/ml Proteinase K was added. Samples were mixed by inverting and incubated for around 4 hours at 55°C with inversion every 30 minutes. When the solution became clear, 10 mg/ml of RNase A was added in a sufficient quantity giving a final concentration of 40 µg/ml. Next, the samples were incubated at 37°C for 1 hour (mixed every 15 minutes), and then incubated on ice for 1 minute. Afterwards, 200 µl of Protein Precipitation Solution was added to the samples and mixed on the vortex for 20 seconds. Next, samples were cooled on ice for 5 minutes, centrifuged at 4°C for 10 minutes at 15,000 g. The supernatant was transferred into the new 1.5 ml Eppendorf tubes. The centrifugation step was repeated, supernatant transferred into the new 1,5 Eppendorf tubes, and 600 µl of ~100 % isopropanol was added to the samples, followed by samples' centrifugation at 4°C for 15 minutes at 15,000 g. The supernatant was removed and the pellet was washed with 1 ml of 70 % ethanol. Next, samples were centrifuged at 4°C for 5 minutes at 7,500 g, supernatant was removed and the pellet was left to dry. The clear, dry pellet was subsequently suspended in 50 µl of DNase/RNase-free water, and the concentration was measured with spectrophotometry. The isolated *C. elegans* genomic DNA was used for further experiments.

4.2.1.2 Constructs design – generation of entry and destination vectors

For proper Gateway System Technology, cloning constructs were designed in a specific manner allowing for a destination vector assembly in a desired order. The entry clone containing a promoter region of a gene of interest was composed of pDONR™ 221 P4-P1r and

~1.4 kb or ~2 kb PCR product (for *vit-5* and *dpy-30,* respectively), flanked with *att*B4 and *att*B1r recombination sites. The entry clone with the *ftn-1* genomic sequence was composed of pDONR™ 221 and ~1.1 kb PCR product flanked with *att*B1 and *att*B2 recombination sites. The entry clone for *unc-54* 3´UTR region was composed of pDONR™ 221 P2r-P3 and ~0.7 kb PCR product flanked with *att*B2r and *att*B3 recombination sites. Since almost all of the entry clones were available in the laboratory collection, only the entry clone for the *vit-5* promoter region was entirely designed and cloned in this research. For that purpose, a PCR reaction for the *vit-5* promoter region was performed using a specifically designed primer set, available in table 12. The PCR product was analyzed on 1 % agarose gel and purified using the Monarch® PCR & DNA Cleanup Kit (5 μg) according to the protocol. Then, the BP reaction was set up with a ratio of fmoles of PCR to fmoles of vector calculated using a specific formula (described in the MultiSite Gateway Three-Fragment Vector Construction Kit protocol). The BP reaction mixture was used for One Shot™ TOP10 Chemically Competent *E. coli* transformation (described in detail in paragraph 4.2.1.3). After successful transformation, single colonies were selected for further screening using colony PCR (described in paragraph 4.2.1.4). The entry plasmid was isolated according to the protocol of the Plasmid Mini Kit, analyzed by Sanger sequencing (detailed information for primers in the table 12), and used for LR reaction. The LR reaction was performed to obtain both constructs necessary for the generation *ftn-1* overexpressing strains. The LR reaction mixture was used for the transformation of One Shot™ TOP10 Chemically Competent *E. coli* bacteria. Then, selected colonies were cultured, plasmids isolated as above and analyzed by restriction enzyme digestion with enzymes listed in table 14. The concentration of final vectors was analyzed with spectrophotometry using NanoDrop. Finally, the 2 μg of each construct was sent to SunyBiotech for the generation of *ftn-1* overexpressing strains.

4.2.1.3 Bacteria transformation

To one vial of One Shot™ TOP10 Chemically Competent *E. coli* bacteria, kept on ice, 2 μl of BP or LR reaction mixture was added and mixed gently. The samples were left on ice for 30 minutes, then heat-shocked at 42°C for 45 seconds, and incubated on ice for 1 minute. Then, 450 μl of fresh LB media was added and bacteria were cultured for 1 hour at 37°C with gentle shaking. Next, the bacteria were centrifuged for 3 minutes at 845 g, the supernatant was discarded and the bacteria pellet was suspended in the small amount of remaining LB media.

The whole solution was seeded on LB-kanamycin or LB-ampicillin plates (BP and LR reaction, respectively). Then, the plates were incubated at 37°C overnight.

4.2.1.4 Colony PCR

The bacteria colonies, after transformation with the entry plasmid carrying *vit-5* promoter, were screened by colony PCR. Before the bacteria were added into the reaction mixture, the colony was scratched onto a fresh selective plate and incubated at 37°C overnight for maintenance. A single colony was transferred into 10 µl of reaction mixture using a pipette tip. Then, the PCR reaction was performed and PCR products were analyzed on 1 % agarose gel to detect the product of a desired size. In this method, the M13 primer set was used for the colony PCR of the entry clone. The detailed information about colony PCR mix, colony PCR program, and primers sequence, is presented in table 16, table 17, and table 12, respectively.

Table 16. Colony PCR reaction mix per one sample.

COMPOUND	VOLUME [µl]
GoTaq®G2 Green Master Mix	5
M13 F [10 mM]	0.3
M13 R [10 mM]	0.3
Bacteria colony	-
Water	4.4

Table 17. Colony PCR program.

STEP	TEMPERATURE [°C]	TIME [sec.]	NUMBER OF CYCLES
Bacteria lysis	94	180	1
Denaturation	94	30	30
Annealing	50	30	
Extension	72	30	
Final extension	72	420	1
Hold	4	∞	1

4.2.2 *C. elegans* strain with a point mutation

To generate a *ftn-1* ferroxidase-inactive mutant (allele *syb2550*) an amino acid sequence of *C. elegans* FTN-1 (NP_504944.2), and human FTH1 (NP_002023.2) were downloaded from NCBI database and aligned using the multiple sequence alignment Clustal Omega tool

(https://www.ebi.ac.uk/Tools/msa/clustalo/)(154,155). Based on the literature (181,182), and protein sequence alignment, two amino acids crucial for ferroxidase activity were selected for the point mutations. *C. elegans* FTN-1 58th aa was mutated to generate an E to K substitution, and the 61th aa to generate a H to G substitution (counting a codon for methionine as 1). Next, the nucleic acid sequence of the *C54F6.14.1* transcript was downloaded from the WormBase. Then, the SunyBiotech company designed sgRNA and generated the requested *C. elegans* strain using CRISPR/Cas9 technology. The received strain was sequenced in order to validate the presence of desired mutations using primers listed in table 12.

4.2.3 *C. elegans* strain with a fluorescent tag

To obtain a *C. elegans* strain with a fluorescent tag mCherry inserted into the endogenous *ftn-1* gene (allele *syb3517*), a CRISPR/Cas9 precise sequence knock-in was ordered from SunyBiotech. The strain was designed in a way to incorporate the fluorescent tag coding sequence before the termination codon of *C54F6.14.1* transcript (*ftn-1*). The received strain was analyzed by PCR using primers listed in table 12. The PCR products were run on 1 % agarose gel to validate the presence of the mCherry tag coding sequence. Moreover, the strain was analyzed using cold survival with the introduced *ets-4* mutation to define whether the FTN-1::mCherry protein is functional. Thus, it was established that the mCherry tag added to the endogenous FTN-1 protein abolished its proper function.

4.2.4 *C. elegans* strains crossing

A cross of *C. elegans* strains (each representing a single mutation), enables for a generation of strain composed of two mutations. This method was used to obtain double or triple mutants. At the beginning, males from one *C. elegans* strain were prepared. To do that, L4 larvae were exposed to 37°C for 1 hour then kept at 25°C until males hatched from the progeny of heat-shocked animals. For an efficient cross, around 16-20 males were transferred to a 60 mm NGM plate with OP50 *E. coli* as the food source. Then, 4-5 L4 hermaphrodites from a second strain of interest were transferred to the plate with males, and kept at 25°C. Afterwards, hermaphrodites were singled out 24 and 48 hours after crossing. Singled hermaphrodites were observed under the stereoscopic microscope and plates in which around 50 % of progeny was composed of males were selected for further steps. Then, four L4 larvae from F1 were singled and left to generate progeny. When F2 progeny reached the L4 stage, animals were singled again and left to lay eggs. Subsequently, the F2 adult hermaphrodites were

lysed in a worm lysis buffer with 0.01 mg/ml Proteinase K (19 minutes at 65°C, 11 minutes at 95°C, and 4°C hold), genotyped by PCR (primers are listed in table 12), with electrophoresis in 1 % agarose gel or sent for Sanger sequencing to identify animals possessed mutations of interest. After the successful cross, the new *C. elegans* strain was cultured and frozen for long-term maintenance. The table below shows an example of PCR conditions used for strain genotyping.

Table 18. PCR conditions used for *C. elegans* strain genotyping.

STEP	TEMPERATURE [°C]	TIME [sec.]	NUMBER OF CYCLES
Initial denaturation	94	180	1
Denaturation	94	15	35
Annealing	Depends of primer set	Depends of primer set	
Extension	72	30	
Final extension	72	420	1
Hold	4	∞	1

4.3 Cold survival assay

Particular *C. elegans* strains were prepared as described in paragraph 4.1.2. After reaching one-day-old adult stage, animals were incubated for 2 hours at 10°C, and transferred to 4°C. Plates were taken out from 4°C every few days, moved back to 20°C, and scored for viability after 24 hours of rewarming. The viability was assessed based on the ability of animals to move and respond to touch by a worm pick. The statistics for viability scoring are described in paragraph 4.13, and available in Supplementary Table 1.

4.3.1 Cold survival assay with antioxidant treatment

Cold survival assay with antioxidant treatment was performed identical to the regular cold survival assay described in 4.3 with a difference in experimental plate preparation. The experimental procedure was inspired by protocols from selected papers (183-185). N-acetyl-L-cysteine was diluted in RNase/DNase-free water to obtain a 100 mM stock and filtered to sterilize. The freshly prepared, empty 60 mm NGM plates were supplemented with the antioxidant NAC stock solution to achieve the final concentration of 5 mM NAC. The solution was spread on plates, and left to dry overnight. Next, a freshly made OP50 *E. coli* bacteria

culture was seeded on NAC plates, and again left overnight to dry. Thus, plates prepared as described were used for the cold survival assay described in 4.3. The results from statistical analysis (performed as in 4.13), are in Supplementary Table 1.

4.4 Lifespan assay

The *C. elegans* strains selected for lifespan assay were prepared as described in 4.1.2, except that, in this particular experiment, the young adults were used. After reaching a young adult stage at 20°C, animals were transferred to 10°C for cold adaptation for 2 hours, and then to 4°C for 5 days. After that time, animals were moved back to 20°C, and that day was counted as day 0 in the lifespan assay. The counting of animals' viability was done every second day. Animals were transferred to a fresh plate as long as they were laying eggs. Subsequently, once or twice a week animals were moved to a fresh plate to avoid contamination and/or starvation. The lifespan was counted as follow: a number of all alive animals (from a particular day) was divided by the number of nematodes from day 0. The calculation was made till all animals stopped responding to a touch by a worm pick and were considered as dead. The statistics are described in paragraph 4.13, and available in the Supplementary Table 1.

4.5 Reactive Oxygen Species assay after cold treatment

The total ROS levels were measured using a fluorescent dye-based indicator chloromethyl derivative; CM-H_2DCFDA (ThermoFisher Scientific), with a protocol adapted from (186,187). Briefly, around 1000 of one-day-old adult animals per strain and condition were cultured on NGM plates seeded with OP50 *E.coli* bacteria as the food source. One-day-old adult nematodes were transferred to 4°C for 2 hours (with the adaptation step 2 hours at 10°C). After that, animals were washed twice with pre-cooled 1x M9 buffer, once in pre-cooled 1x TBS buffer pH 8.0, then, suspended in 1x TBS and transferred to a 96-well plate. Subsequently, animals were incubated with 50 μM CM-H_2DCFDA for 1 hour in the cold room with gentle shaking. After the incubation step, animals were washed three times in pre-cooled 1x TBS to remove unbound dye (the steps with washes and incubation with the dye last for 2 hours, therefore it is marked that nematodes spent in total 4 hours at 4°C). The fluorescent intensity was measured using a plate reader (VICTOR Nivo 5S Disoencer, PerkinElmer Inc), with a 480/30 nm excitation filter and a 530/30 nm emission filter. Afterwards, the fluorescence intensity was normalized to the protein levels in protein extracts produced as follows: animals from the experiment were transferred from plate wells into 1.5 ml protein LoBind tubes,

suspended in 500 µl of 1x TBS buffer, and centrifuged for 1 minute at 1,600 g. The buffer was removed with a thin needle and syringe. Then, the animals' pellet was suspended in 50 µl of 1x TBS and lysed in pre-cooled Bioruptor Pico sonicator using 30 cycles with 30 seconds on and 30 seconds off. The lysed animals' pellet was centrifuged for 15 minutes at 4°C using maximum speed of the centrifuge. The protein concentration was measured with an absorbance at 280 nm. After the concentration was calculated, the final results were gained by subtraction of the signal from animals non-treated with the dye from animals treated with the dye within a strain and condition, and then normalized to the ROS levels in the wild type.

4.6 Cold treatment of SOD-5::GFP strain

One-day-old adults, prepared as described in 4.1.2., were exposed to the cold as in 4.3. for 3 days. After that time, animals were imaged using fluorescence microscope Axio Imager.Z2 in a way described in details in the paragraph 4.8. A negative control was composed of one-day-old adults from 20°C before cold exposure.

4.7 Starvation assay

Before the starvation assay, animals were grown on NGM plates (with OP50 *E.coli* bacteria as the food source) for two generations, then synchronized by bleaching as described in 4.1.2. L1 larvae were seeded on plates covered with OP50 *E. coli* and kept at 25°C to reach the late L3/early L4 larval stage. Then, animals were transferred by a worm pick onto fresh, empty 60 mm NGM plates. The transferring process was repeated three times to avoid plate contamination with bacteria leftovers. Next, animals were starved for 3 days at 20°C. The negative control was composed of animals kept on plates with OP50 *E. coli* as the food source, and imaged at the similar developmental stage as starved animals. After the selected time of starvation animals were imaged using fluorescence microscope Axio Imager.Z2 as described below.

4.8 Microscope observation

Fluorescent microscopy was used to visualize animals from starvation assay (paragraph 4.7) and cold treatment of SOD-5::GFP strain (paragraph 4.6). Nematodes were anesthetized in 10 mM levamisole solution added on freshly prepared 3 % agar pads. The differential interference contrast (DIC) channel (for unstained samples in visible light), and GFP

fluorescence were imaged for all of the experiments. Additionally, the mCherry fluorescence was imaged in the starvation assay. The Axio Imager.Z2 microscope equipped with an Axiocam 506 mono digital camera was utilized, and the objective Plan-Apochromat 63x/1.40 Oil DIC M27 was selected. All of the images were taken with the same camera settings using a commercial microscope software ZEN 2.5 (blue edition).

4.9 RNA interference assay

RNA interference assay was used to knock-down gene of interest. In such experiment, 90 mm NGM RNAi plates, supplemented with 1 mM IPTG and 50 μg/ml ampicillin, were used. An RNAi clone packed in a L4440 plasmid carried by the HTT15 bacteria strain was delivered to animals as the food source. RNAi clone used in this research was taken from the Vidal Library (188), and is listed in table 13. An empty L4440 plasmid in HTT15 bacteria was used as a negative control. Bacteria carrying double-stranded RNA clone, and empty plasmid were cultured overnight in LB media with addition of ampicillin and tetracycline (final concentration 50 μg/ml and 12.5 μg/ml, respectively). The next day, 1 ml of overnight bacteria culture was seeded on RNAi plates and left overnight to dry. Subsequently, bleach-synchronized L1s were put onto RNAi plates and transferred to 20°C. After reaching one-day-old adult stage, animals were harvested for gene expression levels analysis as described in 4.10 prior to cold adaptation or after 1 day of cold exposure as described in 4.3.

4.10 Gene expression levels analysis

To analyze expression levels of selected genes, the total RNA was isolated from samples using the Direct-zol RNA MiniPrep Kit according to the company protocol. The detailed procedure is described below.

4.10.1 RNA samples harvesting and RNA isolation

Animals were prepared as described in 4.1.2. Around 1000 of one-day-old adult animals were harvested before the cold adaptation (as in paragraph 4.3), at 20°C, and after 1 and/or 3 days at 4°C. The temperature at which the animals were harvested depended on experimental conditions. Animals were washed three times in 1x M9 buffer (pre-cooled for samples from 4°C), in 15 ml conical tubes, suspended in 700 μl of Trizol, and transferred to 1.5 ml Eppendorf tubes. The tubes were frozen in liquid nitrogen and stored at -80°C. To isolate total RNA

samples were incubated at 42°C. When contents of the tubes started to thaw, they were vortexed for 10 seconds and frozen in liquid nitrogen. This step was repeated five times. Then, 140 µl of chloroform was added, samples were shaken for 20 seconds and left for 5 minutes at room temperature. After this step, tubes were centrifuged at 4°C for 10 minutes at 12,000 g. Then, the aqueous phase was transferred into fresh 1.5 ml Eppendorf tubes and an equal amount of 100 % ethanol was added. In the next step, the Direct-zol RNA MiniPrep Kit was used according to the available protocol with the recommended DNase I treatment. Isolated RNA was diluted in 15 µl of DNase/RNase free water. The RNA concentration was measured by spectrophotometry using NanoDrop.

4.10.2 complementary DNA (cDNA) synthesis

After total RNA isolation, 1000 ng of RNA (in case of *rege-1(rrr13)* and *rle-1(rrr44)* mutants 400 ng of RNA), was used to prepare cDNA with the High-Capacity cDNA Reverse Transcription Kit in line with the protocol. The tables below show components of the master mix and program for reverse transcription. The total volume of one sample was 20 µl composed of 10 µl of master mix and 10 µl of DNase/RNase-free water with 1000 ng or 400 ng of RNA. The obtained cDNA was diluted 1:5 into DNase/RNase-free water and used for RT-qPCR analysis.

Table 19. Components of 2x RT master mix per one sample.

NAME OF COMPONENT	VOLUME [µl]
10x RT Buffer	2
25x dNTP Mix (100 mM)	0.8
10x RT Random Primers	2
MultiScribe™ Reverse Transcriptase	1
DNase/RNase-free water	4.2

Table 20. Program for reverse transcription using High-Capacity cDNA Reverse Transcription Kit.

NUMBER OF STEPS	TEMPERATURE [°C]	TIME [min.]
1	25	10
2	37	120
3	85	5
4	4	∞

4.10.3 Real-time quantitative PCR

Real-time quantitative PCR (RT-qPCR), was performed in order to analyze the expression levels of selected genes. The AMPLIFYME SG Universal Mix was used in this experiment. The tables below describe a list of reaction components and conditions. The LightCycler 480 Software release 1.5.1.62 was used to calculate Ct values. The fold change was estimated by the delta-delta Ct method. Statistical analysis for all RT-qPCR experiments was done using the GraphPad/ Prism 6, and is described in the paragraph 4.13.

Table 21. Components of RT-qPCR mix per one sample.

NAME OF COMPONENTS	VOLUME [µl]
AMPLIFYME SG UNIVERSAL Mix	5
Primer F [5 µM]	0.5
Primer R [5 µM]	0.5
DNase/RNase-free water	2/-
cDNA	2/4

Table 22. Program for RT-qPCR.

STEP	TEMPERATURE [°C]/TIME [sec.]	NUMBER OF CYCLES
Pre-incubation	95/180	1
Denaturation	95/5	45
Annealing	60/30	
Extension/Fluorescence detection	60/1	
Melting	95/5	1
	70/60	
Cooling	40/30	1

4.11 Protein expression levels analysis using western blot

Protein levels in the following *C. elegans* strains: wild type, [*Plips-11*::MYC::*ftn-1*::*ftn-1* 3´UTR; *unc-119(+)*], and [*Plips-11*::MYC::*ftn-1*::*ftn-1* 3´UTR; *unc-119*(+)]; *ets-4(rrr16)*, was analyzed using western blot. The wild type was used as a negative control. The detailed procedure is described below.

4.11.1 Protein sample preparation

Animals were prepared as described in 4.1.2. Around 1000 one-day-old adults were harvested before cold adaptation at 20°C, or after 1 and 3 days at 4°C. The temperature at which the animals were harvested depended on experimental conditions. Animals were washed two times in 1x M9 buffer (pre-cooled for samples from 4°C), in 15 ml conical tubes, and once in 1x TBS buffer pH 8.0 (pre-cooled for samples from 4°C). The animals' pellet was then transferred into a 1.5 ml protein LoBind tube and centrifuged for 1 minute at 1,600 g. Then, the supernatant was removed and the animals' pellet was washed in a 1x TBS buffer with an addition of a protease inhibitors cocktail (1 tablet to 10 ml of 1x TBS buffer). Next, the supernatant was removed with a thin needle and a syringe. The resulting animals' pellet was suspended in a 1x TBS buffer with protease inhibitors to the final volume of ~50 µl, and lysed in pre-cooled Bioruptor Pico sonicator using 30 cycles with 30 seconds on and 30 seconds off. The lysed animals' pellet was centrifuged for 15 minutes at 4°C using maximum speed of the centrifuge. The protein concentration of 25x diluted samples was determined using a Bradford assay (450 µl of Bradford reagent, 48 µl of 150 mM NaCl, 2 µl of a sample), based on a standard curve with a range of BSA concentrations. Then, 50 µg of each protein sample was mixed with a 5x loading buffer and denatured for 6 minutes at 90°C.

4.11.2 Electrophoresis under denaturing conditions (SDS-PAGE)

The electrophoresis of protein samples was carried out under denaturing conditions in 16.5 % resolving gel with 4 % stacking gel. The samples containing 50 µg of protein were loaded onto the gel and ran in the 1x Running Buffer for 15 minutes at 90 V and then at 120 V for around 1.5 hours using an electrophoresis system. In order to estimate the size of proteins, the Precision Plus Protein™ All Blue Prestained Protein Standards were used to estimate the protein size between 10 to 250 kDa.

4.11.3 Electrophoretic protein transfer

Proteins separated by gel electrophoresis were transferred onto 0.2 µm nitrocellulose membrane using a semi-dry protein transfer system in transfer buffer. Before the transfer, the membrane was activated in pre-cooled 100 % methanol for 30 seconds and then washed in a transfer buffer. The transfer sandwich was made by 2 wet blotting papers, the membrane in the middle, and the gel on the top, covered by 2 wet blotting papers. The transfer was carried out for 3.5 hours at 85 mA in the cold room.

4.11.4 Membrane incubation with primary and secondary antibodies

The membrane after transfer was washed three times for 5 minutes in a 1x PBS-T buffer. Then, the membrane was blocked for 1 hour in 5 % skim milk diluted in 1x PBS-T buffer. After that step, the membrane was incubated overnight with primary antibody for anti-actin and anti-myc diluted in 5 % skim milk (1:2000 each). After overnight incubation with primary antibody, the membrane was washed in the 1x PBS-T buffer three times for 5 minutes, and incubated for 1 hour with secondary antibodies: anti-mouse and anti-rat diluted in 5 % skim milk (1:5000 each). Next, the membrane was washed three times for 5 minutes in the 1x PBS-T buffer and visualized using Radiance Plus Chemiluminescent Substrate and Azure c600 Imager.

4.12 3D protein structure

The 3D protein structure prediction of *C. elegans* FTN-1 (NP_504944.2), and FTN-2 (NP_491198.1), was done with the Phyre2 tool (156). Then, the free software Chimera 1.15 was used to prepare pictures of 3D single models of FTN-1, FTN-2, and the alignment of *C. elegans* FTN-1 (from Phyre2 tool), and *H. sapiens* FTH1 (PDB ID 4OYN).

4.13 Statistics

The statistical analyses for cold survival assay, cold survival assay with antioxidant treatment, and lifespan assay were performed according to the method established by Yanwu Guo, who is a bioinformatist in our team. The script in R was utilized for statistical comparison of cold survival curves and lifespan between tested strains, utilizing the Pairwise Wilcoxon signed-rank test. The results form statistical analyses are included in Supplementary Table 1. Statistical analysis for all RT-qPCR experiments was calculated by unpaired two-tailed Student t-test, utilizing the GraphPad/ Prism 6. For the statistics in the ROS assay after cold treatment, the F test, was used comparing variances utilizing GraphPad/ Prism 6. In all figures error bars represent SEM. ns – not significant, *$p \leq 0.05$, ** $p \leq 0.01$, *** $p \leq 0.001$, **** $p \leq 0.0001$. All life curves from cold survival assay, RT-qPCR, and lifespan experiments were carried out in at least three biological replicates. For the microscopy analysis at least two biological replicates were done. For the ROS assay four biological replicates were performed.

5 Results

5.1 FTN-1 is required for the cold survival in *ets-4* mutants

C. elegans can enter a hibernation-like state when first adapted to an intermediate temperature of 10°C for 2 hours (100). We have previously shown that young adult nematodes enter a hibernation-like state without an impact on the total lifespan when kept at 4°C (here named as "cold"), for 6 days before the cultivation in normal conditions (20°C) (Figure 6A) (100). That makes *C. elegans* a suitable model to study molecular mechanisms underlying cold resistance. Therefore, in this study, I analyzed how hibernation-like state affects animals' cold survival using a described assay (Figure 6B)(101). In our previous research, we showed that a conserved ribonuclease REGE-1 regulated cold sensitivity by the degradation of mRNA encoding a conserved transcription factor, ETS-4 (100). Mutants lacking ETS-4 (*ets-4(-)* single mutants) or ETS-4 and REGE-1 (*ets-4(-); rege-1(-)* double mutants) were able to survive cold exposure better than the control, suggesting a beneficial role of ETS-4 inhibition for cold survival. Moreover, this process seems to be independent of REGE-1 (101). Interestingly, ETS-4 was reported to be involved in the regulation of nematode's lifespan in parallel to IIS, and the extended lifespan observed in e*ts-4(-)* mutants was shown to be DAF-16-dependent (92). Additionally, DAF-16 transcription factor was essential for the cold tolerance in IIS mutants (189), what we also confirmed in our research (101). Moreover, another transcription factor PQM-1 was shown to be a DAF-16 partner in the extension of *daf-2(-)* mutants' lifespan (89). Therefore, we tested the involvement of DAF-16 and PQM-1 in the enhanced cold survival of *ets-4(-)* mutants. Indeed, we observed that nematodes lacking above-mentioned transcription factors (*ets-4(-)* mutants) were no longer able to survive cold better than the control (101). Thus, PQM-1 and DAF-16 might be responsible for the regulation of genes essential for enhanced cold survival upon absence of ETS-4. To verify our hypothesis, we carried out functional genomic approach. Analysis of the poly(A) mRNA sequencing and ENCODE database (190), identified seven genes involved in the cold response driven by DAF-16 and PQM-1 in the absence of ETS-4. In RNAi-mediated knockdown of those genes, under cold exposure, we revealed ferritin *ftn-1* as a factor essential for cold protection (101). Interestingly, other group showed that *ftn-1* was regulated in DAF-16-dependent manner, while DAF-2 became inactivated (88). Moreover, PQM-1 was described as a factor essential for transcriptional control of *ftn-1* during innate immunity, whereas such regulation was not observed for *ftn-2* (102). Consistent with these data, I confirmed that *ftn-1* (but not *ftn-2*) gene was upregulated

in both the wild type and *ets-4(-)* mutants while exposed to 4°C for 24 hours (with the adaptation step) (Figure 6C, 6D) (101). However, in *ets-4(-)* mutants, the upregulation of *ftn-1* was significantly more robust when compared to the wild type from one day at 4°C (Figure 6C) (101). This suggest that ETS-4 suppresses expression of *ftn-1*. Moreover, the enhanced cold survival of *ets-4(-)* mutants was diminished upon additional deletion of *ftn-1(-)* (Figure 6E) (101), whereas the cold survival of *ftn-1(-)* single mutants was comparable to the wild-type animals (Figure 6E) (101). These results indicate that the presence of *ftn-1* gene is essential for nematodes' cold survival in the absence of ETS-4.

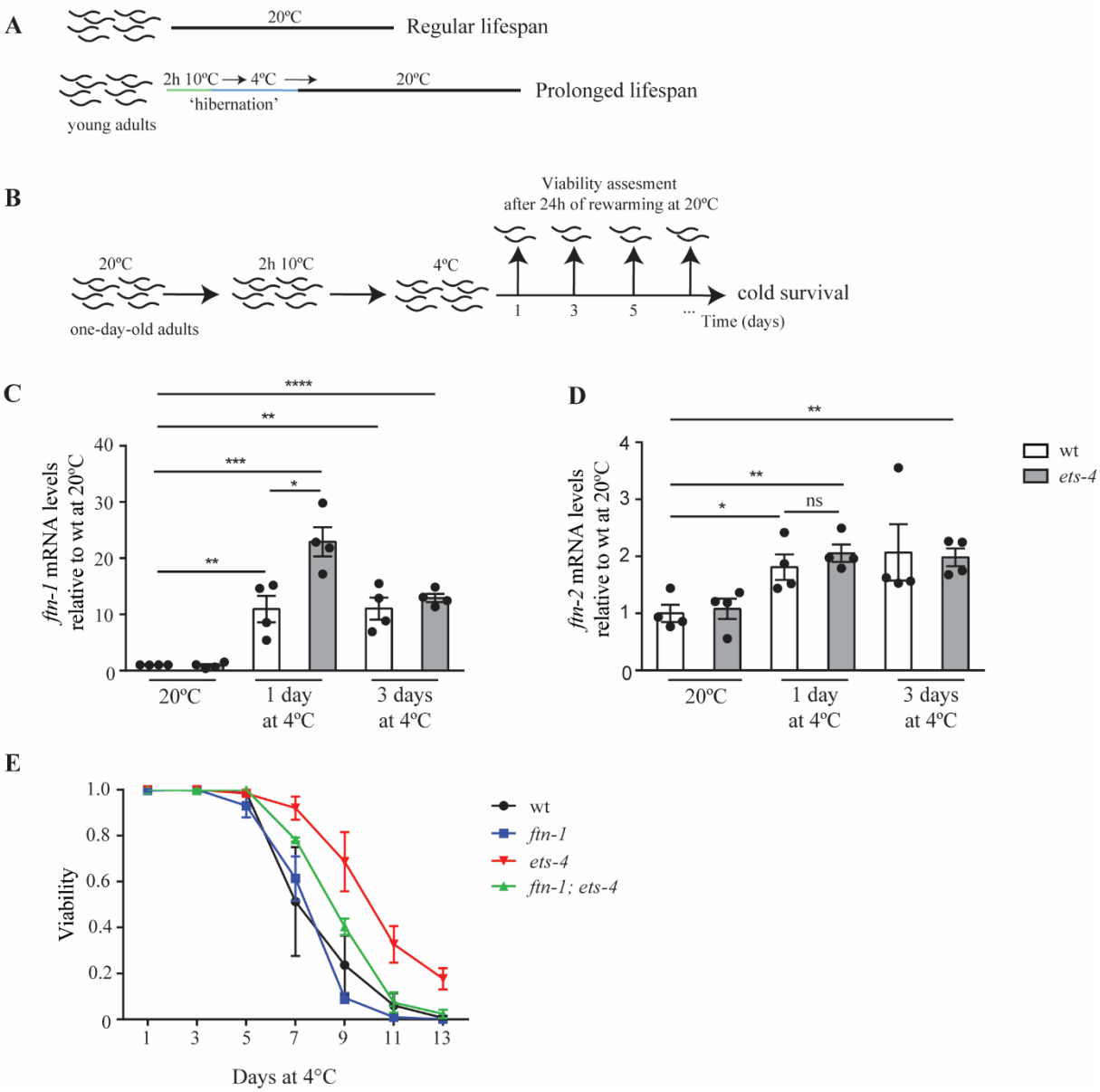

Figure 6. *ets-4* mutants require FTN-1 for enhanced cold survival. A. A Lifespan extension observed in *C. elegans* at the young adult stage, after incubation at 10°C for 2 hours followed by 6 days at 4°C. This phenomenon is considered to imitate the hibernation-like state (100). **B.** A schematic of cold survival assay procedure. Synchronized nematodes kept at 20°C from L1 stage to one-day-old adults. Then, the one-day-old

adults were incubated at intermediate temperature of 10°C for 2 hours, and then transferred to 4°C. Animals were moved from cold to 20°C every few days, and scored for the recovery after 24 hours of rewarming at 20°C. The viability was measured based on the ability to move, and respond to touch by a worm pick. **C.** The *ftn-1* mRNA levels are increased in *ets-4(rrr16)* mutants in the cold. Wild type (wt) and *ets-4(rrr16)* mutants were harvested at 20°C, or after cold exposure for 1 and 3 days. The *ftn-1* mRNA levels were analyzed by RT-qPCR, normalized to actin (*act-1*) mRNA, and compared to the wt from 20°C. Error bars show standard error of mean (SEM), n = 4, * $p \leq 0.05$, ** $p \leq 0.01$, *** $p \leq 0.001$, **** $p \leq 0.0001$, unpaired two-tailed Student t-test. **D.** The *ftn-2* mRNA levels do not differ between the *ets-4(rrr16)* mutants and the wt in the cold. wt and *ets-4(rrr16)* mutants were harvested at 20°C, or after cold exposure for 1 and 3 days. The *ftn-2* mRNA levels were analyzed by RT-qPCR. The levels of *ftn-2* were normalized to *act-1* mRNA, and compared to the wt from 20°C. Error bars show SEM, n = 4, ns - not significant, * $p \leq 0.05$, ** $p \leq 0.01$, unpaired two-tailed Student t-test. **E.** *ets-4(rrr16)* mutants are characterized by the enhanced cold survival. The wt, *ftn-1(ok3625)*, *ets-4(rrr16)*, and *ftn-1(ok3625); ets-4(rrr16)* nematodes were exposed to the cold as in 6B and scored for cold survival. Error bars show SEM, n = 3, Pairwise Wilcoxon signed-rank test.

5.2 Initial attempt to overproduce *ftn-1*: tagging FTN-1 impairs its function

In order to verify the protective effect of FTN-1 in the cold, we decided to prepare a *C. elegans* strain in which *ftn-1* will be overexpressed. Based on RNA-seq data from wild type exposed to cold, *lips-11* appeared as a gene highly upregulated during cold exposure. Thus, we decided to use the promoter of this gene to overexpress *ftn-1*. Additionally, due to the lack of specific antibody recognizing nematode's FTN-1, we added the MYC-tag (Figure 7A). As expected, the obtained strain [*Plips-11*::MYC::*ftn-1*::*ftn-1* 3´UTR; *unc-119(+)*] (*ftn-1* OE (MYC), for short), was characterized by cold-inducible *ftn-1*, but not *ftn-2* overexpression (at least ~1000-fold change) (Figure 7B), after cold treatment carried out for one or three days at 4°C. Subsequently, I analyzed the FTN-1::MYC protein levels in one-day-old nematodes kept at 20°C, or after cold (4°C) for one and three days, using western blot with the wild type as a negative control. The results indicate that the increase in FTN-1::MYC protein levels, after three days of cold exposure, were even more robust in *ets-4(-)* mutants background comparing to the strain expressing ETS-4 (Figure 7C). Above data suggests that the elevated levels of *ftn-1* mRNA in *ets-4(-)* mutants after cold exposure, corresponds to the increased FTN-1 protein levels. Unfortunately, the analysis of the *ftn-1* OE (MYC); *ets-4(-)* double mutants cold survival, and the wild type revealed that MYC-tagged FTN-1 protein lost its functionality (Figure 7D). Nevertheless, the abolished extension of cold survival in the *ftn-1* OE (MYC); *ets-4(-)* double mutants, is puzzling since the endogenous *ftn-1* is present in this mutant. Thus, it seems that it should be sufficient to extend cold survival of *ftn-1* OE (MYC); e*ts-4(-)* mutants, however there is a possibility that endogenous FTN-1 can interfere with the MYC-tagged FTN-

1 and create nonfunctional heteropolymers. Therefore, to analyze the function of *ftn-1* overexpression in the cold, I performed another approach, described the Results, paragraph 5.3.

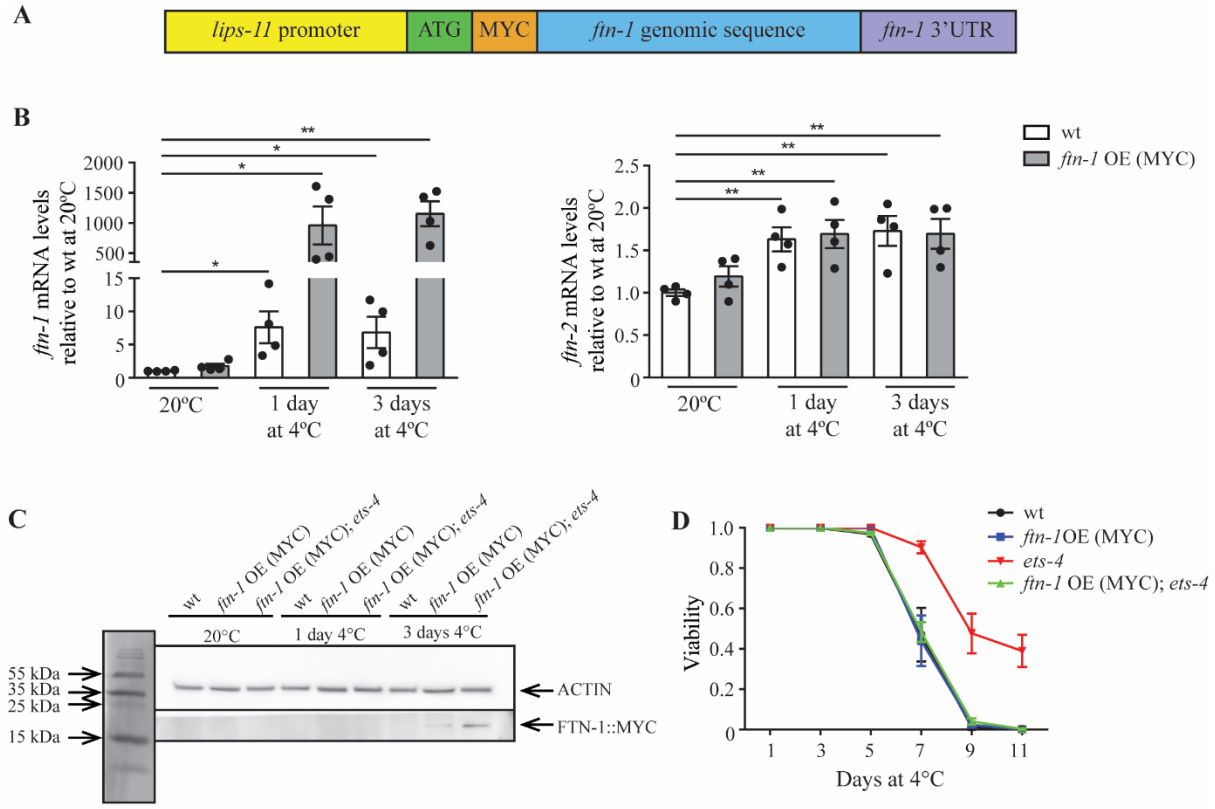

Figure 7. Tagging of FTN-1 diminishes its function. A. A scheme of [*Plips-11*::MYC::*ftn-1*::*ftn-1* 3´UTR; *unc-119(+)*] mutants (simply named as *ftn-1* OE (MYC)). The overexpression of *ftn-1* is driven by *lips-11* promoter and tagged with MYC tag. **B.** Overexpression of *ftn-1* (but not *ftn-2*) mRNA is induced by the cold in the *ftn-1* OE (MYC) mutants. wt and *ftn-1* OE (MYC) mutants were harvested at 20°C, after cold exposure for 1 and 3 days. The *ftn-1* and *ftn-2* mRNA levels were analyzed by RT-qPCR, normalized to *act-1* mRNA, and compared to the wt at 20°C. Error bars show SEM, n = 4, * $p \leq 0.05$, ** $p \leq 0.01$, unpaired two-tailed Student t-test. **C.** The FTN-1 protein levels increases after cold exposure especially in the absence of *ets-4*. wt, *ftn-1* OE (MYC), and *ftn-1* OE (MYC); *ets-4(rrr16)* mutants were harvested at 20°C, or after cold exposure for 1 and 3 days. The samples were analyzed using western blot. The FTN-1::MYC was detected with MYC-tag antibody [9E1]. n = 3. **D.** The *ftn-1* OE (MYC); *ets-4(rrr16)* mutants do not exhibit improved cold survival. The wt, *ftn-1* OE (MYC), *ets-4(rrr16)*, and *ftn-1* OE (MYC); *ets-4(rrr16)* nematodes were exposed to cold as in 6B, and scored for cold survival. Error bars show SEM, n = 3, Pairwise Wilcoxon signed-rank test.

5.3 Ferritin overexpression is sufficient to improve cold survival

Since, the FTN-1 fusion protein turned out to be nonfunctional, I decided to undertake an alternative approach to test the function of *ftn-1* overexpression in the cold. To achieve this, I designed *C. elegans* strains in which the overexpression of non-tagged *ftn-1* was driven from two distinct promoters; *dpy-30* and *vit-5*. The promoter *dpy-30* represents a gene ubiquitously

expressed, whereas *vit-5* is a gene specific for the intestine and not induced by the cold. Moreover, I selected the *unc-54* 3´UTR as an unregulated 3´UTR to avoid any potential, unpredicted regulation of *ftn-1* (Figure 8A). The *ftn-1* overexpressing constructs used to generate *ftn-1* overexpressing strains were not tagged to avoid the inactivation of protein function as I observed for the MYC tag (Figure 7D). For simplicity, I named strains described above as *ftn-1* OE (*dpy-30*) and *ftn-1* OE (*vit-5*), respectively. First, I examined the *ftn-1* mRNA expression levels in both strains by RT-qPCR prior to the cold exposure, or after one and three days at 4°C (without any rewarming time). As expected, the *ftn-1*, but not *ftn-2* mRNA was overexpressed in both strains (at least ~2000 or ~180 fold for *ftn-1* OE (*vit-5*) or *ftn-1* OE (*dpy-30*), respectively) (Figure 8B, 8C). Moreover, the overexpression of *ftn-1* mRNA in *ftn-1* OE (*dpy-30*) and *ftn-1* OE (*vit-5*) strains efficiently enhanced cold survival when compared to the wild type (Figure 8D). Due to the fact that, FTN-1 overexpression exhibited a positive effect on the improvement of nematodes' cold survival, it is possible that this phenomenon might be related to a more general function of ferritin in delaying aging. Therefore, I tested how overexpression of *ftn-1* affects the nematodes' lifespan after cold exposure. To do this, I measured the total lifespan of *ftn-1* OE (*vit-5*) and wild-type nematodes after 5 days of exposure to 4°C (with an incubation step at 10°C for 2 hours) (Figure 8E). Interestingly, the results indicated that the life-spanned *ftn-1* OE (*vit-5*) animals were living only slightly longer than the wild type (Figure 8E). Overall, my data suggest that the FTN-1 is primarily involved in cold survival improvement, but not lifespan extension.

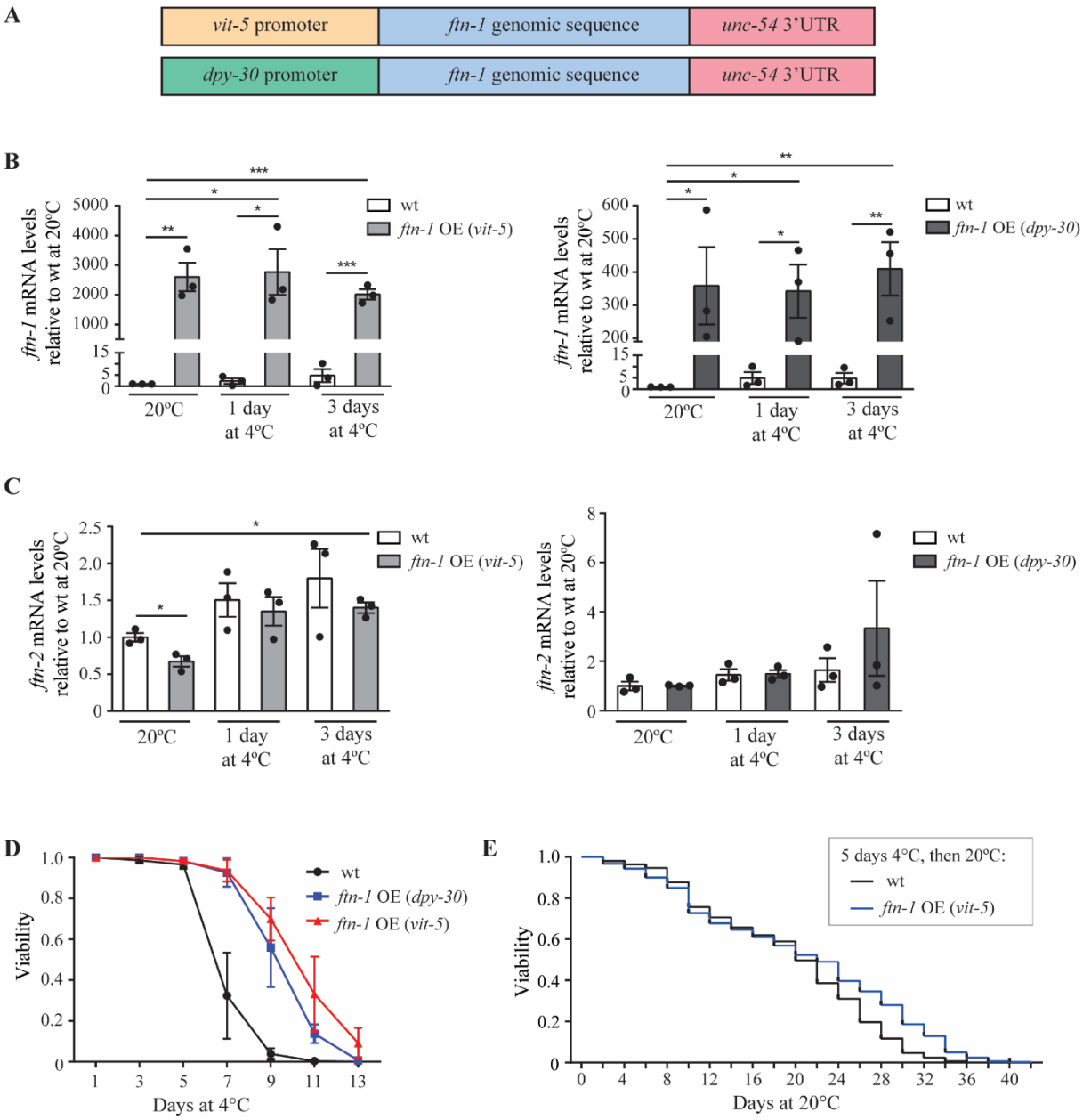

Figure 8. Overexpression of ferritin is sufficient to enhance cold survival. A. A schematic representation of constructs in strains *sybSi67*[*Pdpy-30*::*ftn-1*::*unc-54* 3′UTR]; *unc-119(ed3),* and *sybSi72*[*Pvit-5*::*ftn-1*::*unc-54* 3′UTR]; *unc-119(ed3)* simply named as *ftn-1* OE (*dpy-30*), and *ftn-1* OE (*vit-5*), respectively. The overexpression of *ftn-1* is driven by *dpy-30* or *vit-5* promoter. **B.** *ftn-1* mRNA levels are upregulated in *ftn-1* OE (*vit-5*), and *ftn-1* OE (*dpy-30*) strains after cold exposure. The wt, *ftn-1* OE (*vit-5*), and *ftn-1* OE (*dpy-30*) strains were harvested at 20°C, or after cold exposure for 1 and 3 days. The *ftn-1* mRNA levels were analyzed by RT-qPCR, normalized to *act-1* mRNA, and compared to the wt at 20°C. Error bars show SEM, n = 3, * $p \leq 0.05$, ** $p \leq 0.01$, *** $p \leq 0.001$, unpaired two-tailed Student t-test. **C.** *ftn-2* mRNA levels are not overexpressed in *ftn-1* OE (*vit-5*), and *ftn-1* OE (*dpy-30*) strains after cold exposure. The wt, *ftn-1* OE (*vit-5*), and *ftn-1* OE (*dpy-30*) strains were harvested at 20°C, or after cold exposure for 1 and 3 days. The *ftn-2* mRNA levels were analyzed by RT-qPCR, normalized to *act-1* mRNA, and compared to the wt at 20°C. Error bars show SEM, n = 3, * $p \leq 0.05$, unpaired two-tailed Student t-test. **D.** Overexpression of *ftn-1* results in enhanced cold survival. The wt, *ftn-1* OE (*vit-5*), and *ftn-1* OE (*dpy-30*) strains were exposed to the cold as in 6B, and scored for cold survival. Error bars show SEM, n = 3, Pairwise

Wilcoxon signed-rank test. **E.** The lifespan of *ftn-1* OE (*vit-5*) strain is slightly increased after 5 days of cold exposure. The lifespan measurement of the wt and *ftn-1* OE (*vit-5*) strain at young adult stage was performed as in 6A (but after 5 days at 4°C). n = 3, Pairwise Wilcoxon signed-rank test.

5.4 The ferroxidase activity of FTN-1 is required for cold survival

In mammals, iron detoxification is achieved by the ferroxidase activity of ferritin heavy subunit (ferritin heavy chain – FTH), while ferritin light subunit (ferritin light chain – FTL) does not possess this activity (191). The *C. elegans* ferritin proteins (FTN-1 and FTN-2) share higher sequence conservation with human FTH rather than with human FTL, and both possess conserved residues in ferroxidase centers (137,144,145). In order to verify whether the ferroxidase activity of *C. elegans* FTN-1 is essential for the cold survival of *ets-4(-)* mutants, I ordered (from SunyBiotech company), a *C. elegans* strain harboring ferroxidase-inactivating mutations in the endogenous FTN-1. To design a mutant, I aligned the amino acid sequence of human FTH1, and *C. elegans* FTN-1 using Clustal Omega tool (154,155) (https://www.ebi.ac.uk/Tools/msa/clustalo/). Human FTH1 ferroxidase activity is ensured by some conserved amino acid residues, inter alia, by Glu-63 and His-66 (181,182), thus, for substitution I selected the corresponding amino acid residues in *C. elegans* FTN-1: Glu-58 and His-61 (marked as E58K/H61G) (Figure 9A, 9B). Ferroxidase-inactive FTN-1 (FO-dead) mutant strain *ftn-1(syb2550)* (named as *ftn-1*$^{\text{FO-dead}}$) carrying substitutions described above was created by SunyBiotech company using CRISPR/Cas9 technology in the endogenous allele. I tested the cold survival of the wild type, *ets-4(-)* mutants, *ftn-1*$^{\text{FO-dead}}$ mutants, and *ftn-1*$^{\text{FO-dead}}$; *ets-4(-)* double mutants. I observed that *ets-4* mutants lost their ability to survive cold better than the wild type when they additionally harbored ferroxidase-inactive FTN-1 (Figure 9C). This suggests that the ferroxidase activity of FTN-1 might be crucial for the extended cold survival of *ets-4(-)* mutants. Moreover, since FTN-2 (but not FTN-1) is essential for iron storage (153), the above results implicate the role of FTN-1-mediated iron detoxification in cold survival.

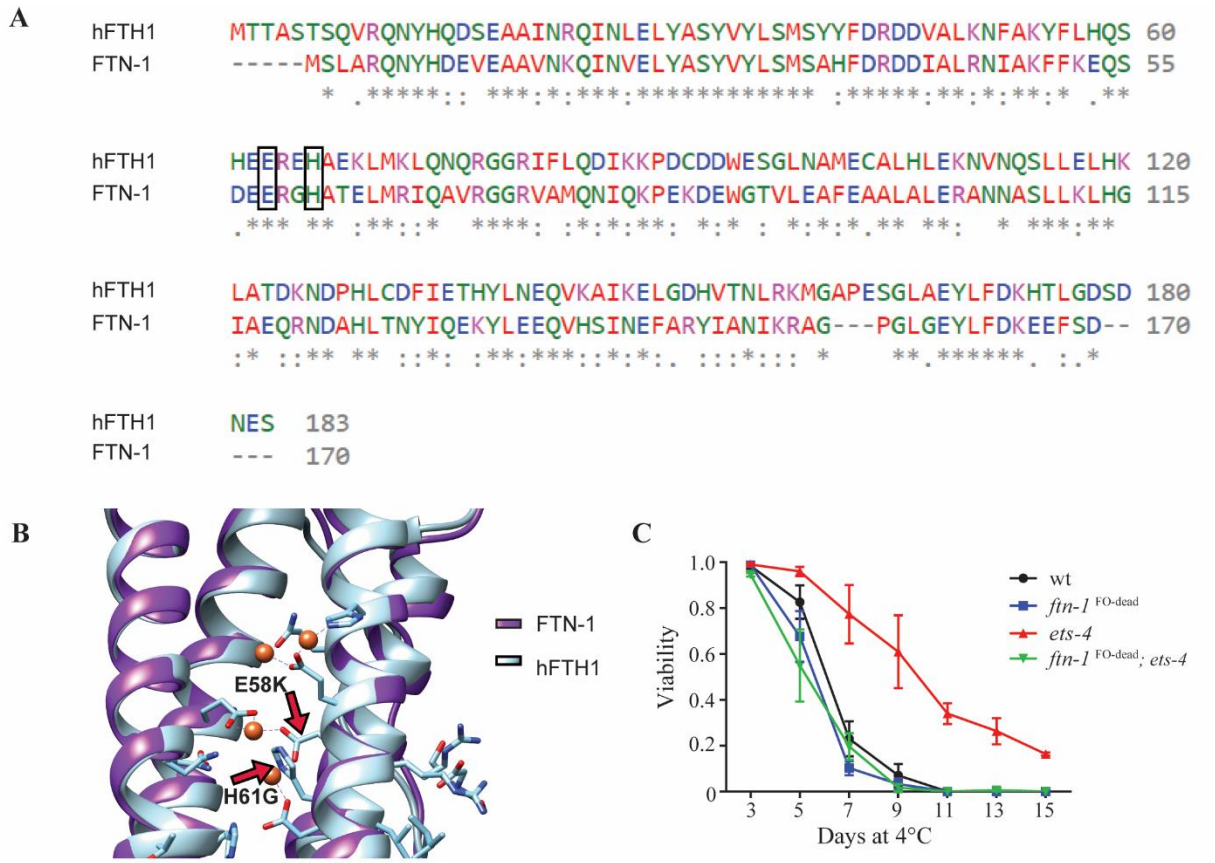

Figure 9. FTN-1 requires functional ferroxidase activity to enhance cold survival. A. Alignment of amino acid sequences representing human (*H. sapiens*) ferritin heavy chain 1 (hFTH1), compared to *C. elegans* ferritin (FTN-1). The NCBI accession numbers are as follows: NP_002023.2, NP_504944.2, respectively. The alignment was performed using the multiple sequence alignment Clustal Omega tool (154,155) (http://www.ebi.ac.uk/Tools/msa/clustalo/). The black boxes indicate amino acid residues representing the ferroxidase active residues in *ftn-1* selected to create a mutant with an inactive ferroxidase activity. The symbols show residues which are: fully conserved (*), with strongly similar properties (:), and with weakly similar properties (.). **B.** 3D model showing selected fragment of the structural alignment of *H. sapiens* ferritin heavy chain 1 (FTH1) (light blue, PDB code 4OYN), and *C. elegans* ferritin (FTN-1, purple). The Phyre2 tool (156), was used to prepare a structural prediction of *C. elegans* FTN-1. The arrows indicate amino acid residues selected for mutations, marked as E58K and H61G (the first methionine is counted as 1). Sticks mark amino acid residues crucial for the ferroxidase activity. The colors represent the following: carbon atoms - light blue in hFTH1 and purple in FTN-1; nitrogen atom belonging to histidine – blue; oxygen atom belonging to glutamic acid – red; iron atoms – orange balls; coordination bonds – purple dotted lines. **C.** Ferroxidase activity in FTN-1 is crucial for *ets-4(rrr16)* mutants cold survival. The wt, *ets-4(rrr16)*, *ftn-1*$^{FO\text{-}dead}$, and *ftn-1*$^{FO\text{-}dead}$*; ets-4(rrr16)* mutants were exposed to the cold as in 6B, and scored for cold survival. Error bars show SEM, n = 3, Pairwise Wilcoxon signed-rank test.

5.5 Ferritin may function as an antioxidant

Antioxidants are essential for the reduction of harmful effects of ROS in living organisms (192). Importantly, ferritin was reported to respond to toxic Fe^{2+} and O_2 ions by exchanging them into less toxic iron form, a mineral, safely stored in ferritin cage avoiding the possibility of ROS production (193). Thus, ferritin's antioxidant activity might help nematodes to cope with ROS generated during cold exposure. Therefore, to imitate the ferritin antioxidant function, and test if nematodes survive cold better in the presence of antioxidant, I performed cold survival assay using culture plates supplemented with an antioxidant, N-acetyl-L-cysteine (NAC). Importantly, the cold survival experiment revealed that the presence of NAC in the culture plates slightly increased cold survival of wild-type nematodes (Figure 10A). Moreover, to test how antioxidant function of FTN-1 affects the ROS levels in animals treated with the cold, I used a probe CM-H_2DCFDA designed to be an indicator of general oxidative stress. When this probe enters the cell, it is cleaved by esterases present inside the cells, which leads to the reaction of a specific chemical groups of this probe with glutathione and other thiols produced inside the cells. Prior the measurement, *C. elegans* strains (wild type, *ftn-1(-), ets-4(-),* and *ftn-1(-); ets-4(-)* mutants) were adapted to the cold for 2 hours at 10°C, and then, kept for 4 hours at 4°C (according to Methods, paragraph 4.5). The ROS measurement with CM-H_2DCFDA was performed after 4 hours at 4°C due to the fact that longer time of cold exposure (e.g. three days at 4°C), made nematodes too sensitive to the treatment with the probe resulting in their death. Despite the low repeatability of the experiment the analysis utilizing CM-H_2DCFDA revealed that mutants devoid of only *ftn-1* or both *ftn-1* and *ets-4* were characterized by elevated ROS levels (~3 fold in *ftn-1(-)* mutants, and ~2,5 fold in *ftn-1(-); ets-4(-)* double mutants), whereas *ets-4(-)* mutants did not differ from the wild type (Figure 10B). Also, I observed higher ROS levels in *ftn-1(-); ets-4(-)* double mutants in comparison to *ets-4(-)* mutants. On the contrary to above results, in our other experiment determining ROS levels using dihydroethidium (DHE) staining of nematodes exposed to the cold for 24 hours (101), we saw that ROS levels in *ftn-1(-)* mutants did not differ from *ftn-1(-); ets-4(-)* double mutants (101). Also, as expected, we noticed lower ROS levels in *ets-4(-)* mutants compared to the wild type (101). The discrepancy between outcomes of those two experiments may result from different cold treatment duration (4 hours at 4°C or 24 hours at 4°C), different developmental stage of nematodes (one-day-old adults or young adults), and the properties of applied ROS indicator (indicator of general oxidative stress or indicator of superoxide radicals). Additionally, it is worth highlighting that ROS measurement on cold-treated nematodes is not

trivial, and brought a lot difficulties associated with high variability between samples, replicates, and types of used probes. The reason why ROS measurement with the probe is so difficult to perform may be due to the fact that cold-treated nematodes are more sensitive than those from standard cultivation conditions. Thus, additional treatment with such a compound may cause their death. Therefore, the obtained results need to be analyzed with a special caution. Nevertheless, despite high variability between the results from the above approaches, one observation was common for both analyzes, the lack of FTN-1 led to the increased ROS levels in cold-treated nematodes. Thus, FTN-1, as an antioxidant, seems to be essential for the protection against cold stress. However, further analysis is required to clarify the mechanism underlying FTN-1 role in the reduction of ROS levels upon cold exposure.

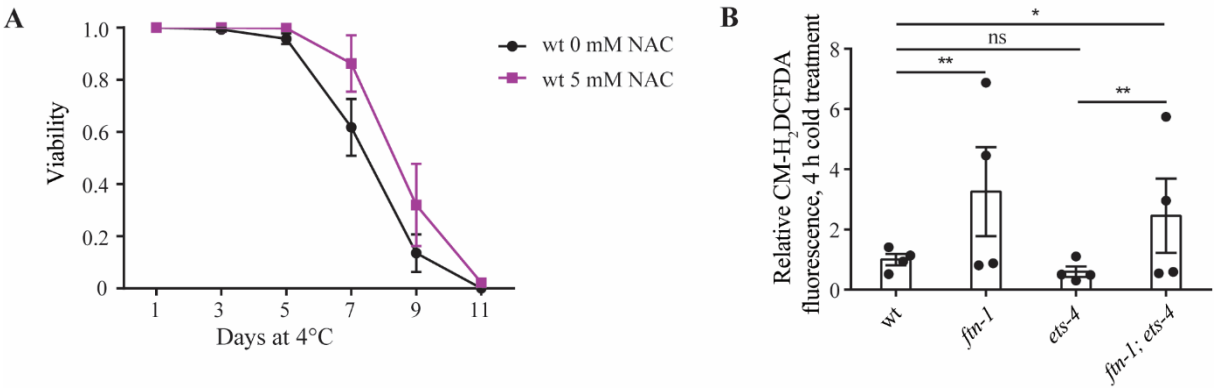

Figure 10. Ferritin may have an antioxidant function. A. The antioxidant treatment improves cold resistance. The wild type incubated with or without the presence of an antioxidant N-acetyl-L-cysteine (NAC, 5 mM), were tested for cold survival as in 6B. Error bars show SEM, n = 4, Pairwise Wilcoxon signed-rank test. **B.** The lack of functional *ftn-1* results in the increased ROS levels. The following *C. elegans* strains: wt, *ftn-1(ok3625)*, *ets-4(rrr16)*, and *ftn-1(ok3625); ets-4(rrr16)* were analyzed for ROS levels after 4 hours at 4°C using fluorescent dye-based indicator CM-H_2DCFDA. Error bars show SEM, n = 4, ns - not significant, * $p \leq 0.05$, ** $p \leq 0.01$, F test to compare variances.

5.6 Genes involved in ROS response change expression in the cold

Ferritin protects cells from the injury and death through the reduction of ROS-generating ferrous ions levels (133). Thus, as described in the previous paragraph, the reduction of cold sensitivity in *ets-4(-)* mutants seems to be mediated by the ROS-lowering function of *ftn-1* overexpression. In order to verify which particular genes are taking part in ROS response in *ets-4(-)* mutants, I decided to analyze the expression levels of a group of selected genes in nematodes exposed to cold. The chosen genes encode ROS-detoxifying enzymes playing important roles in preventing oxidative damages, and mediating the detoxification process, inter alia, against hydrogen peroxide. Thus, their expression levels might serve as indicators of the

state of ROS response (194-196). More specifically, the selected genes encode: catalases (*ctl-1*, *ctl-2*, *ctl-3*), gamma glutamylcysteine synthetase (*gcs-1*), glutathione-S-transferases (*gst-1*, *gst-4*, *gst-5*, *gst-38*), UDP-glucuronosyltransferases (*ugt-8*, *ugt-25*, *ugt-58*), peroxiredoxins (*prdx-2*, *prdx-3*, *prdx-6*), glutathione peroxidases (*gpx-4*, *gpx-6*) and superoxide dismutases (SODs) (*sod-1*, *sod-2*, *sod-3*, *sod-4*, *sod-5*) (187,194-196). First, I measured the mRNA expression levels of these genes by RT-qPCR, in the wild type and *ets-4(-)* mutants at 20°C, or after three days at 4°C (Figure 11A, and B, respectively). The analysis revealed that some of the tested genes were upregulated (e. g. *gst-1*), while others where downregulated (e. g. *ctl-2*, *ugt-8*), or not changed (e. g. *prdx-3*, *prdx-6*), during the cold exposure of the wild type and *ets-4(-)* mutants (Figure 11A and B). Interestingly, I observed a robust increase of *sod-5* mRNA levels, at least ~11 fold, upon cold treatment of both the wild type and *ets-4(-)* mutants (Figure 11A and B). In fact, SOD proteins are described as first factors involved in the defense against reactive oxygen species. Moreover, it is emphasized by the fact that at least one SOD gene is expressed in most organisms living in oxygen-containing environment (197). Interestingly, *C. elegans* encodes five SOD genes (197,198). Therefore, I decided to focus on the *sod-5* gene for further analysis, due to the profound effect of cold exposure on its expression levels. Firstly, I compared the *sod-5* mRNA levels between the wild type and *ets-4(-)* mutants kept at 20°C, or at cold for one or three days. Interestingly, the expression of *sod-5* was slightly downregulated in *ets-4(-)* mutants (~0.3 fold) at 20°C but the levels of *sod-5* mRNA after cold exposure for one or three days did not differ between the wild type and *ets-4(-)* mutants (Figure 11C). These results are surprising, since I expected that the overexpressed *ftn-1* in *ets-4(-)* mutants will significantly reduce the *sod-5* mRNA levels during cold exposure compared to the wild type. This suggests that *ftn-1* and *sod-5* utilize separate pathways during cold exposure, however the analysis focused only on mRNAs levels, but not investigating proteins' levels might lacking the information crucial to make a solid statement (for broader explanation see the Discussion chapter, paragraph 6.4). Subsequently, to define whether SOD-5 protein levels can also be affected by cold exposure, I visualized GFP-tagged SOD-5 protein in a specific *C. elegans* strain (198). The fusion protein, expressed in this mutant has been described to be mainly present in neurons, thus I looked at the SOD-5::GFP protein fluorescence in the head-neurons (198). Interestingly, I detected the increased SOD-5::GFP signal after three days of cold exposure in comparison to the nematodes kept at 20°C (Figure 11D). Thus, the above data suggests that the upregulation of *sod-5* mRNA corresponds to the increase of SOD-5 protein levels during cold exposure. Subsequently, referring to the potential ROS-lowering function of ferritin, I decided to verify whether the robust *ftn-1* overexpression may reduce the

expression of *sod-5* mRNA in the cold. Thus, I analyzed expression levels of the *sod-5* mRNA in *ftn-1* OE (*vit-5*) strain kept at 20°C, or at 4°C for one or three days. The results showed that *ftn-1* overexpression leads to the downregulation of the *sod-5* mRNA at all selected time points of cold exposure, with the highest difference after three days at 4°C reaching ~12 fold (Figure 11E). These results are in contrast to those observed for *ftn-1*-overexpressing *ets-4(-)* mutants. However, it seems like the artificially introduced, robust *ftn-1* overexpression in *ftn-1* OE (*vit-5*) strain can lead to the ectopic expression of *ftn-1* in neurons thereby affecting the *sod-5* mRNA expression levels. On the contrary, in *ets-4(-)* mutants the *ftn-1* overexpression seems to have no impact on *sod-5* expression. Interestingly, it has been proposed that generation of ROS increases with the rewarming time (199). Our results obtained using *C. elegans* and mammalian neurons are in agreement with that hypothesis (101). We saw a transient increase of GFP signal in nematode strain expressing SOD-5::GFP subjected to rewarming time-course after three days at cold, with the highest signal after around 2 hours of rewarming at 20°C (101). Also, similarly to the experiment without rewarming step (Figure 11E), we observed decreased levels of *sod-5* mRNA in *ftn-1* OE (*vit-5*) strain after three days at 4°C with 2 hours of rewarming at 20°C (101). Importantly, both analyzes (with and without rewarming) suggest that ROS is generated by cold exposure, and the overexpression of *ftn-1* induces protection against toxic Fe^{2+}, and thereby against ROS.

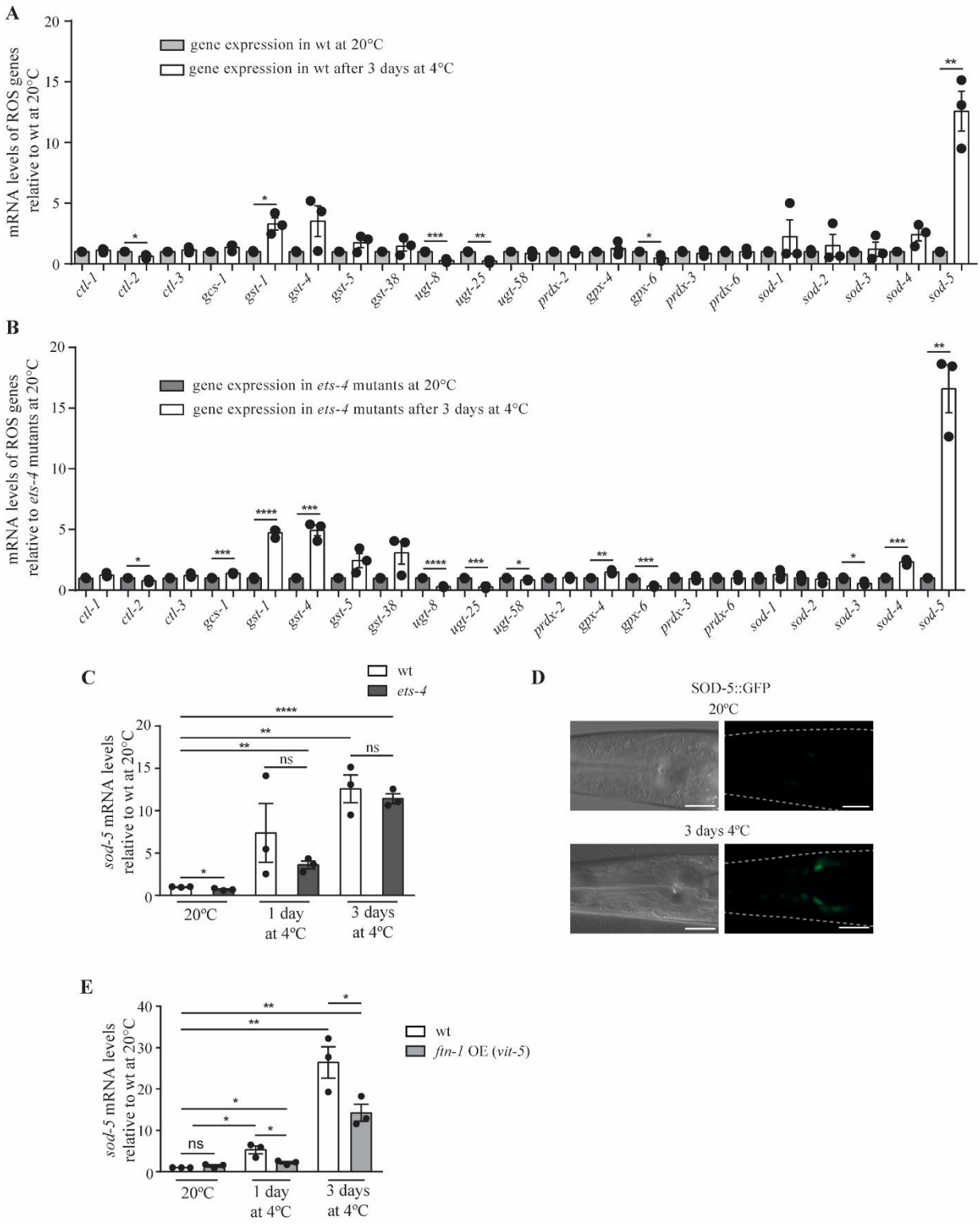

Figure 11. Expression levels of genes involved in ROS response change in the cold. A. Genes described to take part in ROS response change their expression during cold exposure. The wt was harvested at 20°C, or after cold exposure for 3 days. A set of selected genes was analyzed using RT-qPCR. The expression levels of each gene were normalized to *act-1* mRNA, and compared to the wt at 20°C. Error bars show SEM, n = 3, * $p \leq 0.05$, ** $p \leq 0.01$, *** $p \leq 0.001$, unpaired two-tailed Student t-test. **B.** Genes involved in ROS response change expression in the cold in *ets-4(rrr16)* mutants. *ets-4(rrr16)* mutants were harvested at 20°C, or after cold exposure for 3 days. A set of selected genes was analyzed using RT-qPCR. The expression levels of each gene were normalized to *act-*

1 mRNA, and compared to the *ets-4(rrr16)* mutants at 20°C. Error bars show SEM, n = 3, * $p \leq 0.05$, ** $p \leq 0.01$, *** $p \leq 0.001$, **** $p \leq 0.0001$, unpaired two-tailed Student t-test. **C.** mRNA levels of s*od-5* are upregulated in the cold. The wt and *ets-4(rrr16)* mutants were harvested at 20°C, or after cold exposure for 1 and 3 days. The expression levels of the *sod-5* gene were analyzed using RT-qPCR, normalized to *act-1* mRNA, and compared to the wt at 20°C. Error bars show SEM, n = 3, ns – not significant, * $p \leq 0.05$, ** $p \leq 0.01$, **** $p \leq 0.0001$, unpaired two-tailed Student t-test. **D.** SOD-5::GFP protein levels are increased upon cold exposure. Representative images from light (DIC) and fluorescence microscopy showing the expression of SOD-5::GFP fusion protein. The pictures are focused on the head region of one-day-old adult animals prior to the cold incubation at 20°C, and after cold exposure for 3 days. Nematodes are marked with dashed and grey lines. n = 2, scale bar: 20 μm. **E.** mRNA levels of *sod-5* are significantly downregulated upon *ftn-1* overexpression in the cold. The wt and *ftn-1* OE (*vit-5*) strain were harvested at 20°C, or after cold exposure for 1 and 3 days. The expression levels of the *sod-5* gene were analyzed using RT-qPCR, normalized to *act-1* mRNA, and compared to the wt at 20°C. Error bars show SEM, n = 3, ns – not significant, * $p \leq 0.05$, ** $p \leq 0.01$, unpaired two-tailed Student t-test.

5.7 ELT-2 and HIF-1 transcription factors contribute to the regulation of *ftn-1* in the cold

It has been previously described that the increased *ftn-1* mRNA levels in the *daf-2* mutants depend on DAF-16 transcription factor that is involved in the IIS (88). Moreover, *ftn-1* upregulation was also observed in different experimental conditions upon activation of innate immune response controlled by the PQM-1 transcription factor (102). Additionally, our research characterized DAF-16 and PQM-1-dependent regulation of *ftn-1* during cold exposure (101). For the first time, it depicted that DAF-16 and PQM-1 can act together rather than in the opposite manner (89). Nevertheless, the expression of *ftn-1* is not only controlled by DAF-16 and PQM-1 transcription factors, but also by ELT-2 and HIF-1. Therefore, the latter might also be involved in *ftn-1* regulation upon cold exposure. ELT-2 was described to bind to the GATA motifs present in the iron-dependent elements (IDEs) of *ftn-1* and *ftn-2* promoter regions leading to a transcriptional activation of those genes (108). However, HIF-1 was characterized as a suppressor of *ftn-1* expression (131). Therefore, I decided to examine whether the ELT-2 and HIF-1 are also involved in the regulation of *ftn-1* upon cold exposure. Due to the fact that the loss of *elt-2* gene is lethal for nematodes (106), I knock-down *elt-2* using RNAi and quantified the expression levels of *ftn-1* in the wild type or *ets-4(-)* mutants cultured at 20°C, or one day at 4°C. Obtained results showed that the knockdown of *elt-2* led to the downregulation of *ftn-1* mRNA in the wild type (~0.6 fold) as well as in *ets-4(-)* mutants (~3.5 fold), only in cold conditions (Figure 12A). Interestingly, such an effect was not observed upon standard cultivation conditions of 20°C (Figure 12B). However, it can be explained by low, basal expression levels of *ftn-1* in *ets-4(-)* mutants at 20°C, which is upregulated only in the

cold. Overall, the above results suggest that ELT-2 is necessary for the regulation of *ftn-1* mRNA only in the cold, so it may act through a different pathway than the one used in 20°C. Subsequently, to test the influence of HIF-1 transcription factor on the regulation of *ftn-1* mRNA during cold exposure, I created *ets-4(-); hif-1(-)* double mutants strain. Subsequently, I determined the expression levels of *ftn-1* mRNA in the wild type, *ets-4(-)*, and *hif-1(-)* single mutants, or in *hif-1(-); ets-4(-)* double mutants in two temperature conditions: 20°C, and after one day at 4°C. Obtained results indicated that the expression levels of *ftn-1* were highly upregulated in *hif-1(-)* single mutants, and *ets-4(-); hif-1(-)* double mutants in both tested conditions ~120-fold (Figure 12C). However, *ftn-1* mRNA regulation was independent of the presence of ETS-4 in *hif-1(-)* mutants. Therefore, these results clearly show that HIF-1 represses the expression of *ftn-1* mRNA in standard cultivation conditions as well as in the cold, and ETS-4 is not implicated in this mechanism.

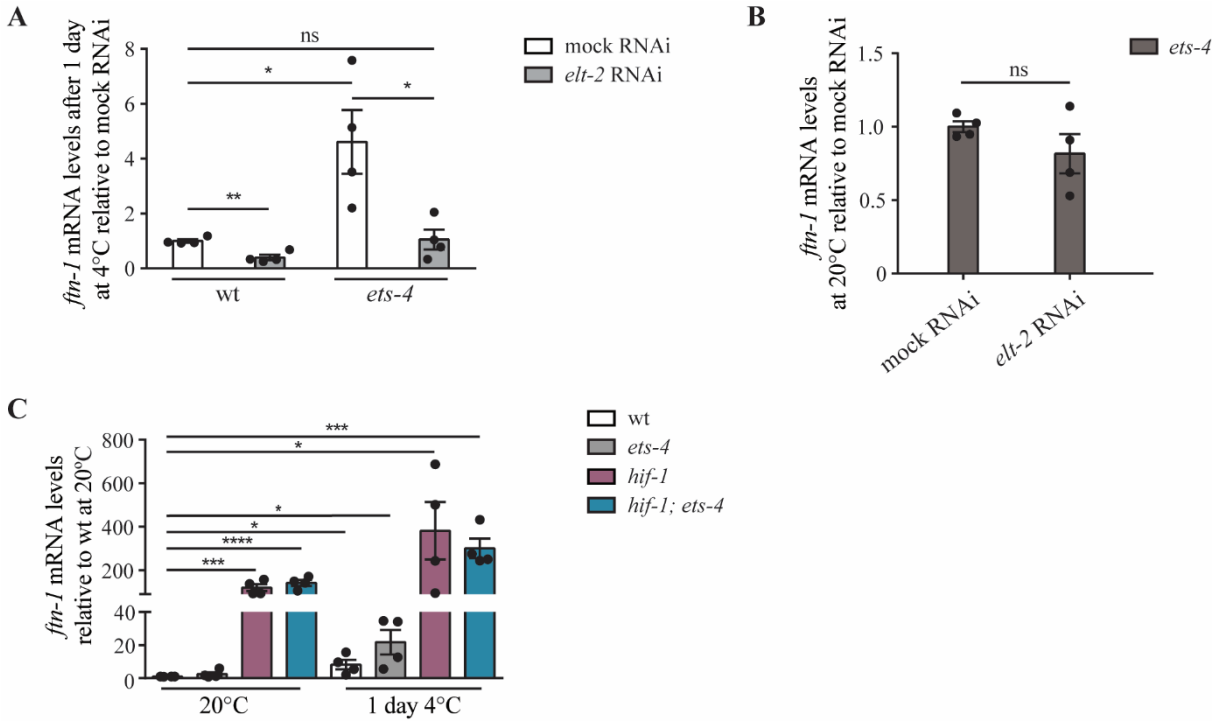

Figure 12. FTN-1 is regulated by ELT-2 and HIF-1 transcription factors in the cold. A. The knockdown of *elt-2* significantly decreases the mRNA levels of *ftn-1* during cold exposure. The wt and *ets-4(rrr16)* mutants were exposed to the empty vector (mock RNAi) or *elt-2* RNAi, and after reaching one-day-old adult stage were exposed to the cold. The samples were collected after 1 day at 4°C. Then, the mRNA levels of *ftn-1 w*ere analyzed using RT-qPCR, normalized to *act-1* mRNA, and compared to the wt from mock RNAi. Error bars show SEM, n = 4, ns – not significant, * $p \leq 0.05$, ** $p \leq 0.01$, unpaired two-tailed Student t-test. **B**. ELT-2 does not regulate the mRNA levels of *ftn-1* in *ets-4(rrr16)* mutants at 20°C. *ets-4(rrr16)* mutants were exposed to the empty vector (mock RNAi) or *elt-2* RNAi. Samples were collected at 20°C. The mRNA levels of *ftn-1* were analyzed using RT-qPCR, normalized to *act-1* mRNA, and compared to the mock RNAi. Error bars show SEM, n = 4, ns – not significant, unpaired two-tailed Student t-test. **C.** HIF-1 is a transcriptional repressor of *ftn-1* at standard and cold

conditions. The wt, *ets-4(rrr16)*, *hif-1(ia4)*, and *ets-4(rrr16); hif-1(ia4)* mutants were analyzed for the expression levels of *ftn-1* using RT-qPCR. The nematodes were harvested at 20°C, or after cold exposure for 1 day. The mRNA levels of *ftn-1* were normalized to *act-1* mRNA, and compared to the wt at 20°C. Error bars show SEM, n = 4, * $p \leq 0.05$, *** $p \leq 0.001$, **** $p \leq 0.0001$, unpaired two-tailed Student t-test.

5.8 FTN-1 induction by starvation is different from its induction by the cold

It was previously described that *daf-2* mutants, characterized by IIS pathway inactivation and extended longevity, exhibited upregulated levels of *ftn-1* mRNA dependently on DAF-16 (88). Additionally, DAF-16 was shown to be activated and localized to the nucleus when nematodes were exposed to starvation (200). Since DAF-16 expression is activated in starved and cold-exposed nematodes alike, there is a possibility that at the initial stage of cold exposure the DAF-16 expression is induced by starvation. Therefore, it was essential to verify whether the regulatory axis composed of transcription factors DAF-16, PQM-1, and ETS-4, described by our group (101), is specific to cold, or is activated by starvation in nematodes exposed to cold. In order to test this, I performed starvation assay. First, I selected specific *C. elegans* strains harboring fluorescent tags *pqm-1(syb432)*, and *daf-16(syb707)* animals (named PQM-1::MCHERRY, and DAF-16::GFP, respectively), and I starved them for three days. I selected this time point due to the fact that the cold exposure of above-mentioned strains led to the translocation into nucleus of fluorescently tagged DAF-16 and PQM-1. Moreover both fusion proteins were strongly expressed after three days of cold exposure (101). Interestingly, my starvation assay revealed, in contrast to the results obtained when studying cold axis, that neither PQM-1 nor DAF-16 were present in the nuclei of PQM-1::MCHERRY, and DAF-16::GFP strains after three days of starvation (Figure 13A). Furthermore, to visualize the FTN-1 protein levels, I used the *ftn-1(syb3517)* strain (named as FTN-1::MCHERRY), in which the endogenous FTN-1 was tagged with mCherry. Despite the fact that the FTN-1::MCHERRY fusion protein was not functional, based on the cold assay (data not shown), it served as an indicator of FTN-1 protein synthesis in the starvation assay. Moreover, to get rid of false positive signal coming from the autofluorescence of gut granules, the above strain was crossed to the *glo-1(zu391)* strain which is devoid of gut granules (201). Interestingly, I observed a strong, intestine-specific mCherry signal after three days of starvation (Figure 13B). This suggests the upregulation of the FTN-1 in the response to starvation through a different pathway than the one used in the cold. More specifically, despite the activation of DAF-16 in starved nematodes observed by others (but for shorter time than three days) (200), and in nematodes exposed to cold (101), the activation of *ftn-1* expression in the cold requires other transcription

factor, PQM-1, which is clearly not expressed in response to starvation (Figure 13A). Therefore, the results obtained here imply that the regulatory axis described for cold differs from regulatory pathway mediating expression of *ftn-1* upon starvation. Importantly, there is no evidence that nematodes exposed to cold are starving, due to the fact that during hibernation (probably also in hibernation-like state in *C. elegans*), metabolism and energy demand are decreased compared to the ambient temperature.

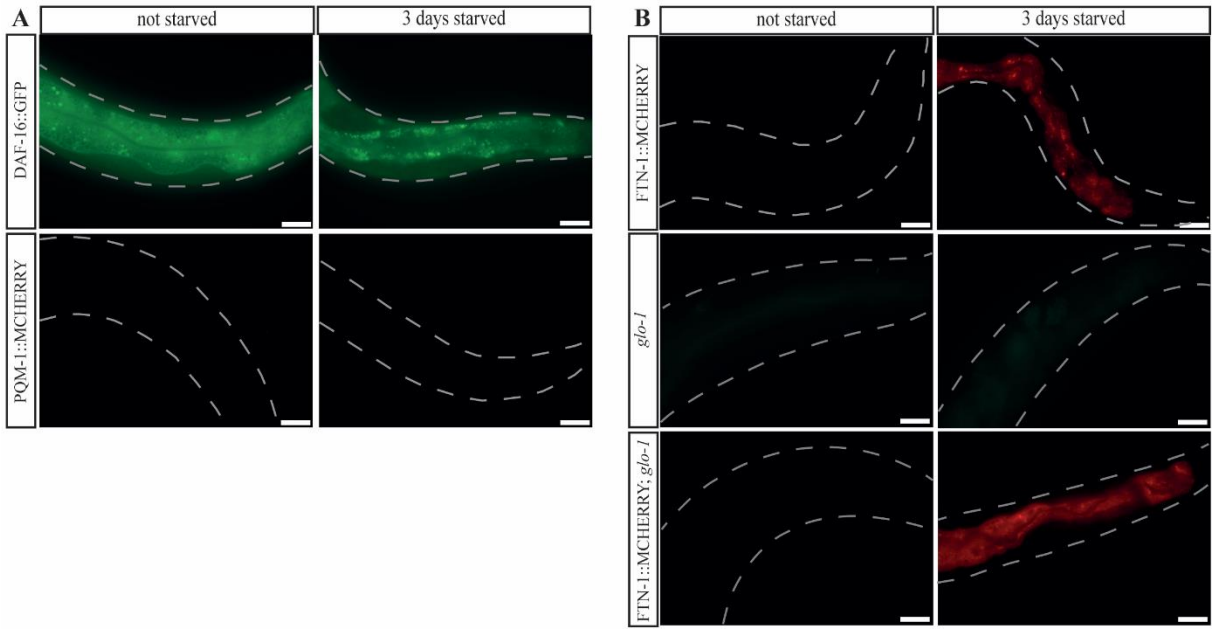

Figure 13. Starvation and response to the cold utilize separate mechanisms for FTN-1 induction. A. DAF-16 and PQM-1 are not involved in the prolonged starvation. A representative images of *daf-16(syb707)*, and *pqm-1(syb432)* strains (named as DAF-16::GFP, and PQM-1::MCHERRY, respectively), used in the starvation assay. Nematodes representing each strain were starved for 3 days at 20°C after reaching the late L3/early L4 larval stage. n = 3, scale bar 20 μm. **B.** FTN-1 is involved in the response to starvation. The representative images of *ftn-1(syb3517)*, *glo-1(zu391)*, and *ftn-1(syb3517); glo-1 (zu391)* strains (named as FTN-1::MCHERRY, *glo-1*, and FTN-1::MCHERRY; *glo-1*, respectively), used in the starvation assay. Nematodes representing each strain were starved for 3 days at 20°C after reaching the late L3/early L4 larval stage. n = 3, scale bar 20 μm.

5.9 RLE-1 and REGE-1 mediated *ets-4* regulation affects cold survival

Our previous study identified ETS-4 as a negative factor of cold resistance (100,101). We showed that endoribonuclease REGE-1 degrades the mRNA of *ets-4* in an auto-regulatory module, leading to the accumulation of body fat (100), and promotion of cold resistance (100,101). Interestingly, we have recently described RLE-1, an ortholog of RNA-binding protein Roquin-1 (75,202), as a partner of REGE-1 in *ets-4* mRNA decay (203). Thus, I decided to examine how cold affects RLE-1-mediated mRNA silencing. First, I analyzed the mRNA

levels of *ets-4* in *rege-1(-)* and *rle-1(-)* mutants after 20°C, or cold exposure for one day. In agreement with our research (101), the mRNA levels of *ets-4* were upregulated ~3 fold in the wild type after one day of cold exposure (Figure 14A). Moreover, *rege-1(-)* and *rle-1(-)* mutants exhibited upregulated *ets-4* mRNA levels for at least ~7 fold not only after cold exposure, but also at standard temperature of 20°C (Figure 14A) (203). These results indicate that REGE-1 and RLE-1 regulate *ets-4* mRNA also in the cold. Subsequently, to verify whether the mRNA levels of *rege-1* and *rle-1* can be affected by the cold in the wild type, I analyzed their expression at 20°C and after cold exposure for one and three days. It turned out that the levels of *rege-1* and *rle-1* mRNA were not affected after one day of cold exposure compared to the 20°C (Figure 14B, 14C), but were slightly downregulated (~0.3 fold) after three days at 4°C (Figure 14B, 14C). Those results may be surprising; however, the mechanism of transcription and translation is not fully examined in nematodes expressing hibernation-like response. Since animals exposed to prolonged cold stress eventually start dying it seems that the reduced expression of *rle-1* and *rege-1* mRNAs is a sign of a transcriptional switch to more important processes essential for the cold survival. However, to prove this hypothesis further analysis is required. Moreover, I tested the RLE-1 influence on the cold survival of *ets-4(-)* mutants. My results suggest that *rle-1(-)* mutants survived cold worse than the wild type, however, *rle-1(-); ets-4(-)* double mutants survived cold similarly to the wild type (Figure 14D), which is in opposite to the cold survival of *rege-1(-); ets-4(-)* double mutants (101,203). These results suggest that besides the contribution of RLE-1 to the regulation of *ets-4* mRNA mediated by REGE-1, RLE-1 may have additional functions that are independent from REGE-1 (203).

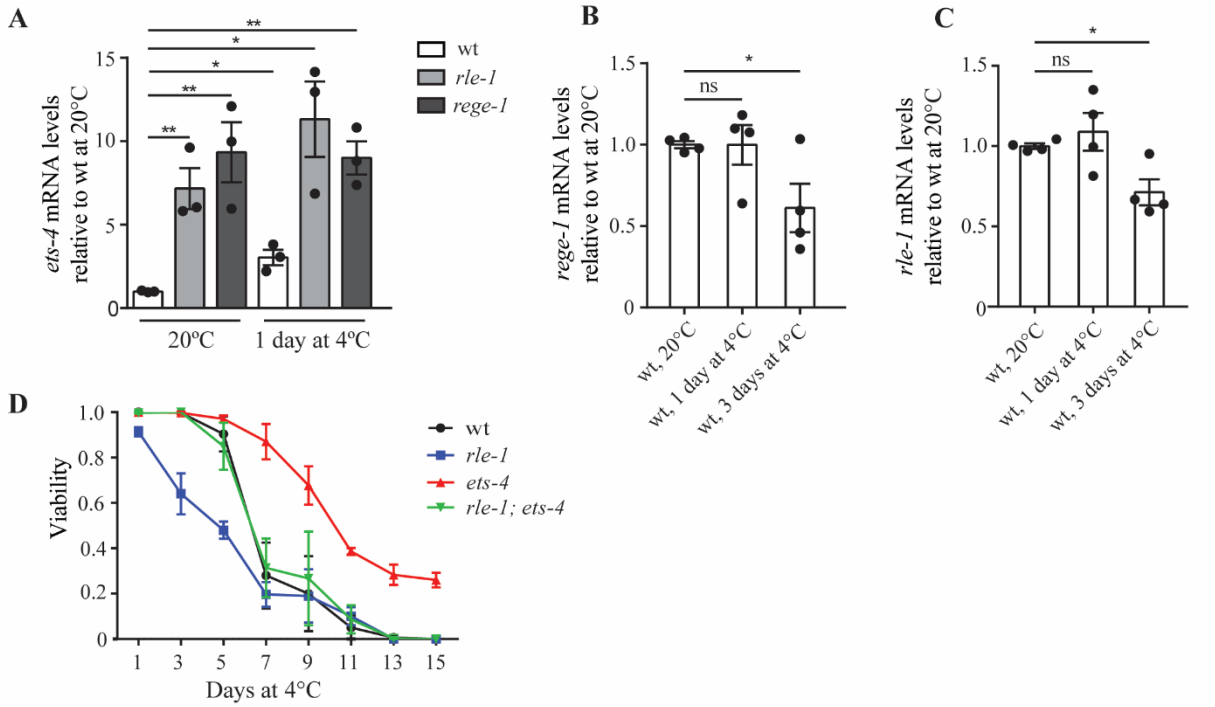

Figure 14. *ets-4* regulation mediated by RLE-1 and REGE-1 affects cold survival. A. mRNA levels of *ets-4* are upregulated upon absence of RLE-1 or REGE-1 in standard, and cold conditions. The wt, *rle-1(rrr44)* and *rege-1(rrr13)* mutants were harvested at 20°C, or after cold exposure for 1 day. The mRNA levels of *ets-4* were analyzed by RT-qPCR, normalized to beta-tubulin (*tbb-2)* mRNA, and compared to the wt at 20°C. Error bars show SEM, n = 3, * $p \leq 0.05$, ** $p \leq 0.01$, unpaired two-tailed Student t-test. **B.** The mRNA levels of *rege-1* are downregulated after 3 days in the cold. The wt animals were harvested at 20°C, or after cold exposure for 1 and 3 days. The mRNA levels of *rege-1* were analyzed by RT-qPCR, normalized to *tbb-2* mRNA, and compared to the wt at 20°C. Error bars show SEM, n = 4, ns – not significant, * $p \leq 0.05$, unpaired two-tailed Student t-test. **C.** The mRNA levels of *rle-1* were downregulated after 3 days in the cold. The wt animals were harvested at 20°C, or after cold exposure for 1 and 3 days. The mRNA levels of *rle-1* were analyzed by RT-qPCR, normalized to *tbb-2* mRNA, and compared to the wt at 20°C. Error bars show SEM, n = 4, ns – not significant, * $p \leq 0.05$, unpaired two-tailed Student t-test. **D.** The absence of *rle-1* abolishes the extended cold survival of *ets-4(rrr16)* mutants. The wt, *ets-4(rrr16)*, *rle-1(rrr44)*, and *ets-4(rrr16); rle-1(rrr44)* mutants were exposed to the cold as in 6B, and scored for cold survival. Error bars show SEM, n = 3, Pairwise Wilcoxon signed-rank test.

6 Discussion

6.1 Evolution of ferritin proteins and their role in iron detoxification

Since a vast group of biological processes is conserved among species *C. elegans* can be used as a model organism to study most of them. However, it is also worth remembering that many mechanisms are unique for some species and their evolutional pathway sometimes remain uncovered. An interesting example describing not only similarities, but also differences between species is shown by the ferritin family (150). *C. elegans* expresses two separate genes encoding two ferritin proteins (144). Although, there is no evidence that nematode's ferritins may form a heteropolymer what might be possible due to their sequence conservation. By contrast, mammals also encode two separate genes for two ferritin subunits (FTH and FTL) that form one cytosolic, heteropolymeric ferritin protein (204,205). Moreover, mammals express not only cytosolic, but also mitochondrial ferritin (206), and ferritin heavy chain like 17 (FTHL17) that is specific for the testis (204). Nevertheless, in this paragraph I will focus on the cytosolic ferritin, due to sequence and functional similarity between *C. elegans* FTN-1 and FTN-2, and the FTH subunit of mammalian cytosolic ferritin (101,145). The above-mentioned presence of two ferritin proteins in nematodes and only one in mammals raise evolutionary questions. Did two cytosolic ferritins acquired specialized function during the evolution to act as subunits within one heteropolymeric complex? Are nematode ferritins also able to form a heteropolymer? The answer to those questions does not seem to be trivial since ferritin proteins are not fully characterized in various organisms (147). Nevertheless, the examples described below may shed some light on the evolution of ferritin proteins. A single-cell organism, *E. coli*, expresses three ferritin-like molecules: bacterioferritin, bacterial ferritin (Ferritin-A), and dodecameric ferritin (207). The first two possess conserved ferroxidase sites similar to those observed in mammalian FTH (207). Additionally, an unique feature for bacterioferritin is the existence of heme groups (207). Although, all of these three proteins are able to bind iron, the bacterial ferritin can also function as an iron source, and the dodecameric ferritin is able to protect against hydrogen peroxide through oxidizing Fe^{2+} with H_2O_2 (207,208). On the contrary to *E. coli*, an eukaryotic model organism *Saccharomyces cerevisiae* does not encode any ferritin-like protein and stores excess iron mainly in the vacuoles (209,210). In contrast to above examples, but similarly to mammals, a multicellular invertebrate organism, *Drosophila melanogaster*, possesses one secretory ferritin encompassed by two subunits encoded by two separate genes: heavy chain (*Fer1HCH*) and light chain (*Fer2LCH*) (211,212). Importantly,

Fer1HCH possess ferroxidase-active center (like FTH subunit), whereas Fer2LCH carries the nucleation sites responsible for iron mineralization (like FTL subunit) (211). Nevertheless, an insect's ferritin localization differs from mammalian ferritins, as it is a secretory protein mainly present in hemolymph rather than in cytoplasm (213). Another interesting example is a fish, Atlantic salmon (*Salmo salar*), whose ferritin is built from two types of ferritin subunits: heavy and middle (M). Moreover, all subunits contain conserved amino acid residues building the ferroxidase sites whereas M chains additionally express nucleation sites similar to those present in mammalian FTL (147). Since, the M chain in *S. salar* possess both ferroxidase and nucleation sites (147), while the L chain is not present, it is possible that M subunit has been lost in mammals during the evolution, and replaced by a more specialized L subunit (214). However, further studies are needed to clarify this. Interestingly, plants also express ferritin-like proteins named phytoferritins, which consist of only H subunits containing both ferroxidase and nucleation sites (215). However, in contrast to mammalian ferritin, phytoferritin is mostly present in plastids rather than in cytoplasm (215). Interestingly, ferritins from diverse organisms share not only amino acid sequence conservation, but also the structure of their genes exhibits common features. It was described that ferritin genes from some vertebrates (human, *Danio rerio*, and *Salmo salar*) are composed of 4 exons and 3 introns (147,182). However, the structure of ferritin genes from *D. melanogaster* and *C. elegans* highly differ from those observed in vertebrates (216). Additionally, the ferritin's gene structure also differs between insects and nematodes, what may suggest that it evolved through separate mechanisms (216). Another difficulty in studying the ferritin evolution are distinct conclusions made by different laboratories. For example, the phylogenetic analysis carried out by one research group suggested that ferritin subunits evolved autonomously in vertebrates and non-vertebrates due to the duplications process specific for these groups (214). By contrast, another research group revealed that ferritins evolved from one ancestral protein similar to prokaryotic rubrerythrin-like proteins (150). Therefore, to clarify why ferritin proteins differ between species further investigation is required. Overall, above examples present various features of ferritin proteins across different species, however it leads to one certain conclusion. In each described organism, at least one ferritin protein exhibits conserved ferroxidase activity. This observation highlights how important is the maintenance of iron homeostasis in most of the living organisms under various circumstances, and how evolutionary conserved is ferroxidase activity. Within this thesis, I revealed that ferroxidase activity of FTN-1 in *C. elegans* is crucial for their cold resistance, however why *C. elegans* has two separate ferritin proteins rather than one composed of two subunits remains to be tested.

6.2 *C. elegans* ferritins

The *C. elegans* expresses two ferritin genes, *ftn-1* located on chromosome V, and *ftn-2* on chromosome I, encoding FTN-1 and FTN-2 proteins, respectively (136,144,216). FTN-1 and FTN-2 share high sequence similarity, are regulated by iron (144,145), and by iron-dependent element (IDE) in their promoter regions (108). Additionally, both ferritins possess ferroxidase activity (145), and are expressed in the intestine (108). Besides above similarities, there are also some differences between *C. elegans* ferritins. Firstly, FTN-2 is not only present in the intestine, but also in other tissues like body wall muscle, hypodermis and pharynx (145). Secondly, *ftn-1* transcription is regulated in DAF-16-dependent manner, which does not apply to the *ftn-2* (88,101). Thirdly, as it has already been mentioned in the introduction, the abundance of *ftn-2* mRNA is higher than the *ftn-1* mRNA under standard cultivation temperature (145,152). All of the above examples rise the question: how is it possible that, despite the high similarity between FTN-1 and FTN-2, these proteins function in diverse processes? James, et al. reported FTN-2 involvement in iron storage (153), whereas our research assigned FTN-1 function in iron detoxification (101). Specifically, we confirmed that the lack of *ftn-1* in the cold does not influence the total as well as ferritin-associated iron content, suggesting FTN-1 role in iron detoxification. However, the deprivation of *ftn-2* led to the reduction of total and ferritin-associated iron, thus confirming the FTN-2 role in iron storage (101). Interestingly, the balance between the protein levels of these two ferritins seems to be tightly controlled, since the mutants lacking *ftn-2* exhibited elevated *ftn-1* expression levels, not only at standard cultivation conditions but also in the cold (our own data). Additionally, similar results were reported by others studying standard culture temperature (145), whereas in nematodes expressing *ftn-1::gfp* construct the elevated GFP signal was observed in the mutants additionally lacking *ftn-2* (145). In contrast, *ftn-2* mRNA was not affected when the *C. elegans* strain was deprived of *ftn-1* (our own data). These observations may imply that the iron-detoxifying FTN-1 can also bind iron at some point, when FTN-2 is not available. This hypothesis is confirmed by our results from the *in vitro* assay which suggested that not only FTN-1 is able to detoxify iron, but it can also bind it. Admittedly, this process was slowed down, but not inhibited when ferritins' ferroxidase center was inactivated (101). However, *in vitro* studies might not always reflect complex mechanisms present in the cell. By contrast, our SEC-ICP-MS data carried out on extracts from nematodes exposed to the cold revealed that there was no ferritin-associated iron in animals lacking *ftn-2*, confirming that FTN-2 (but not FTN-1) is crucial for iron storage. The above results suggest that FTN-1 is mainly devoted

to iron detoxification and probably at a small extent to iron binding. However, to clarify whether FTN-1 is also taking part in iron binding in *C. elegans* it would be important to develop a method allowing the tracking of single iron ions *in vivo* with real-time-analysis. Another unsolved aspect is the putative ability of FTN-1 and FTN-2 to create heteropolymeric structure, similarly to human cytosolic ferritin composed of FTH and FTL subunits. Since there are no available antibodies for *C. elegans* ferritins, it is hard to apply the biological methods to study the presumed heterodimeric structure of FTN-1 and FTN-2. Nevertheless, to verify this hypothesis, computational intelligence approach could be utilized to predict the structure of a potential heteropolymer (217). Additionally, it would be useful to visualize FTN-1 and FTN-2 structures by X-ray crystallography (218), since it has not been done so far. Another issue is the limitation of available and simple techniques for tracking the change of iron binding/detoxification within a multicellular living organism. This analysis is not trivial to perform but hopefully possible in the future. For now, a method used by James et. al., a synchrotron-based X-ray fluorescence microscopy seems to be a suitable method to quantify the distribution of iron in nematodes in the cold (153).

6.3 Biological role of FTN-1

Iron homeostasis is implicated in many different cellular processes. Therefore, it is not surprising, that the role of *C. elegans* FTN-1 was described in the context of longevity (145), aging (136,153), immune response (102), hypoxia (219), cold response (101), and starvation (88). It has been reported that increased expression of *ftn-1* is characteristic of nematodes lacking the DAF-2 insulin receptor (88). As it is widely known, *daf-2* mutants are characterized by extended longevity (220). Interestingly, a group of transcription factors essential for the IIS-dependent lifespan regulation was described to also influences the expression of *ftn-1* (88). Additionally, the disruption of iron homeostasis was reported to shorten the lifespan of *C. elegans* and activate expression of *ftn-1* (145). Thus, it may be possible that elevated *ftn-1* mRNA levels may contribute to the lifespan regulation through the control of iron homeostasis (136). Therefore, a number of reports discussed the impact of ferritin dysfunction or overexpression on the total lifespan of nematodes. Despite the fact that previous reports showed that *ftn-1* overexpression did not extend or shorten the lifespan under standard cultivation conditions (136), my experiment indicated that incubation in the cold for a certain time slightly extended the lifespan of *ftn-1* overexpressing strain. Nevertheless, this lifespan extension seems to be minimal when compared to the robust overexpression of *ftn-1* mRNA

(101). Importantly, I looked at the lifespan of nematodes that were transferred to the standard temperature of 20°C after cold exposure. Thus, my results cannot be directly compared to the results obtained only in standard growth conditions applied in other studies. Therefore, to compare my results with others, a lifespan on the wild type and our *ftn-1* overexpressing strain should be carried out without any cold exposure. Besides examining the lifespan of nematodes with the *ftn-1* overexpression, the influence of *ftn-1* or *ftn-2* mutation on animals' lifespan has also been investigated by several groups. It was shown that neither the *ftn-2(-)* mutants nor animals with RNAi-mediated depletion of *ftn-1* exhibited differences in the lifespan, when compared to the wild type (145). Importantly, the *ftn-1(-)* mutants displayed reduced lifespan, but only when exposed to high iron concentration (145). On the contrary, another group showed a reduced lifespan of the mutants lacking *ftn-2,* compared to the wild type when exposed to high iron concentration (153). Also, nematodes deprived of both ferritins exhibited shorter lifespan than those lacking only *ftn-2* (221). Characterization of ferritin from another point of view, with the focus on its antioxidant function, can shed light on the unsolved questions of aging. One hypothesis of aging indicates that the accumulation of free radicals, or in general oxidative stress, may cause aging due to the accumulation of molecular damages (222). However, ferritin, as an iron chelating protein equipped with ferroxidase activity, possesses antioxidant function necessary for the reduction of toxic iron which then prevents generation of ROS (193,223). The implication of ferritin in preventing the aging process seems to be reasonable since *ftn-1* was shown to be overexpressed in *daf-2* mutants that are characterized by slower aging (136,224). However, the iron-storage function of ferritin was shown to be reduced during aging in *C. elegans* (153). Altogether, above examples point to the possible roles of *C. elegans* ferritins in longevity and aging control (221).

Besides the potential impact of FTN-1 on aging and lifespan, the involvement of FTN-1 was also observed in conditions like hypoxia (219), starvation (88), innate immune defense (102,219,225), and response to the cold (101). Tight regulation of iron and oxygen metabolisms is essential, since any disruption in the balance between these processes can lead to the reaction of free iron with hydrogen peroxide, and hence the production of ROS causing serious damages in the living organism (219). FTN-1 serves as an antioxidant; thus it is not surprising that the intestinal expression of *ftn-1* is affected by the changes in oxygen concentration (21% or 1% O_2) (219). It was shown that at 21% O_2, the *ftn-1* expression in the intestine was inhibited by oxygen-sensing neurons AQR, URX, and PQR (219). Additionally, this process required hydroxylated form of HIF-1 (219). By contrast, the hypoxia conditions (1% O_2) led to the

activation of *ftn-1* expression in HIF-1-independent manner (219). On the contrary to 21% O_2, above-mentioned neurons were not implicated in the *ftn-1* regulation at 1% O_2, which is not surprising, since the low levels of oxygen are inhibiting their activity (219). The comparison of conditions with normal (21% O_2), and low (1% O_2) oxygen concentration suggests separate mechanisms regulating *ftn-1* expression. Although, the specific reason why, and what factor is responsible for the activation of *ftn-1* expression in hypoxia still remains unanswered.

Starvation is another type of stress connected with FTN-1 upregulation. I observed the elevated levels of *ftn-1*::mCherry signal in nematodes starved for three days, which is in agreement with the observation made by another research group that noticed increased GFP signal in starved nematodes carrying the *pftn-1::gfp* construct (88). Based on the results from another scientific group, the starvation process seems to be mediated by DAF-16 (226). However, the translocation of DAF-16 into the nucleus was observed only in the nematodes exposed to short periods of starvation (226). The prolonged starvation was characterized by DAF-16 translocation into the cytoplasm (226), which is in agreement with my results. Additionally, my results indicated that a partner of DAF-16, PQM-1 is not implicated in the response to starvation. Unfortunately, little is known about the iron metabolism in starved nematodes. However, it can be assumed that the elevated levels of FTN-1 during starvation are caused by the disrupted iron homeostasis and increased amount of free iron. This observation might be supported by the fact that increased ferritin levels were observed in patients suffering from anorexia nervosa (227). Nevertheless, conclusions coming from above data should be considered with caution, since protein tagging might affect its function. Unfortunately, antibodies specific for *C. elegans* proteins are not available, thus alternative methods including tagging of a protein of interest need to be utilized to study protein expression levels. Therefore, in this project I employed two *C. elegans* strains in which FTN-1 was tagged with MYC (for cold experiment) or mCherry (for starvation assay) to enable its visualization by western blot and fluorescence microscopy, respectively. However, protein tagging may affect its conformation, expression, and thus its activity. Indeed, I observed the loss of FTN-1 function in both mentioned strains. Nevertheless, *in vivo* FTN-1 tagging by mCherry or GFP that enables fluorescent detection of protein localization and levels has been previously reported (145,219). Therefore, even though the protein tagging makes it biologically inactive, it is still beneficial by enabling its visualization under selected conditions. Despite the fact that FTN-1 fusion proteins were not functional, it enabled me to show that FTN-1 protein levels are upregulated in starvation what is in agreement with previous study (88).

Subsequent examples refer to the role of FTN-1 in innate immune responses. Since pathogens assimilate iron from the infected host (228), hosts developed mechanisms reducing iron availability for pathogens (229). It was shown that *C. elegans* limits iron availability during innate immune defense by activating cellular iron uptake through the metal transporter SMF-3 (102). Additionally, in the above conditions the increased expression levels of *ftn-1* were observed what authors explained as FTN-1 role in iron binding (102). However, our research indicated FTN-1 main role in iron detoxification. Therefore, it is possible that activation of FTN-1 during the innate immune response is mainly associated with its function in the iron detoxification rather than iron binding. Another example referring to the *ftn-1* role in immune defense is its iron concentration-dependent regulation via the mammalian target of rapamycin (mTOR) pathway and autophagy upon *Salmonella enterica* serovar Typhimurium infection (225). Additionally, the increased levels of FTN-1 turned out to be essential for immune resistance to *Pseudomonas aeruginosa* infection during hypoxia (219). Moreover, the elevated levels of serum ferritin have been observed in humans living in environments characterized by high pathogen concentrations (230). Additionally, the increased rate of human deaths caused by pathogen infection was found to be associated with oral iron supplementation (230). All of the above examples highlight the meaningful role of FTN-1 in the innate immune response through the limitation of iron access for pathogens.

Another example describing the role of FTN-1 in *C. elegans* reaction to stressful conditions is response to low environmental temperatures (like 4°C) (101). We revealed that the enhanced cold survival observed in *ets-4(-)* mutants was mediated by *ftn-1* overexpression. Additionally, the *ftn-1* overexpression was sufficient to increase the cold resistance of wild-type animals (101). Also, I showed that the ferroxidase activity of FTN-1 is crucial for cold survival improvement observed in *ets-4(-)* mutants. Furthermore, we showed that FTN-2 is responsible for iron storage, whereas FTN-1 is mostly devoted to iron detoxification during cold response (101). However, we are not able to compare our results with the pathways described upon exposure to cold shock or exposure to 15°C (117-119), because we applied pre-incubation step at intermediate temperature of 10°C for 2 hours before transferring animals to 4°C. Therefore, whether the FTN-1 also takes part in the response to direct cold shock at 2°C-4°C or response to 15°C remains to be determined.

As a part of the response to stressful conditions, *ftn-1* expression is tightly regulated by several transcription factors and proteins, for example DAF-16, PQM-1, ELT-2, and HIF-1 that were described in more details in the introduction (88,102,108,131). In our research

we additionally showed a specific *ftn-1* regulatory axis mediated by DAF-16 and PQM-1 in nematodes lacking ETS-4 exposed to the cold (101). Additionally, within this dissertation, I proposed that ELT-2 and HIF-1 are also involved in the regulation of *ftn-1* expression in the cold. Interestingly, these transcription factors seem to utilize separate pathways, because the *ftn-1* regulation mediated by HIF-1 appears to be ETS-4-independent, whereas ELT-2 utilized ETS-4-dependent pathway, but only in the cold. Therefore, it would be interesting to identify other factors involved in FTN-1 regulation during cold exposure. Nevertheless, there are also many other transcription factors and proteins contributing to the *ftn-1* transcriptional regulation (137). Additionally, the *ftn-1* regulation is not always regulated in iron-dependent manner as in the case of ELT-2 (108), HIF-1 (88), ATPase with AAA domain homolog (ATAD-3) (231), and MEIS-class homeodomain protein (UNC-62) (88,232). There are also other factors and proteins essential for *ftn-1* regulation in iron-independent way like transcription factor MAD-like (MDL-1) (88), HSF-1 (88,233), and the protein helix loop helix (HLH-29) (234). Overall, the *ftn-1* regulation in conditions that depended or not on iron concentrations highlight the essential function of FTN-1 in many different processes essential for living organisms.

6.4 Ferritin as a protectant against ROS in hibernation-like state in *C. elegans*

Our previous studies showed that *C. elegans* is able to enter a hibernation-like state at 4°C, when first adapted to intermediate temperature of 10°C for 2 hours (100). Subsequently, we observed that nematodes exposed to cold showed elevated ROS levels (101). Within this project, I quantified the general ROS levels directly via fluorescent dye-based indicator CM-H_2DCFDA, but also indirectly by the examination of mRNA levels of ROS-detoxifying enzymes (194) present in *C. elegans* (187,194,197,198). I tested their expression levels in the wild type and *ets-4(-)* mutants before and after cold exposure. As expected, I observed significant changes in mRNA levels of some of these genes, suggesting an activation of ROS generation/detoxification pathways by cold. Due to the fact that *ets-4(-)* mutants are able to survive cold much better than the wild type, we assumed that this phenomenon could be associated with lower ROS levels. Unexpectedly, there were no obvious differences in the mRNA levels of ROS genes between *ets-4(-)* mutants and the wild type. However, it is worth remembering that mRNA levels may not always reflect the changes at the protein levels, and also not all genes encoding ROS-detoxifying enzymes were tested. Nevertheless, my analysis revealed strong upregulation of the *sod-5* gene encoding superoxide dismutase enzyme, which is essential for the regulation of ROS levels (197). The SOD enzymes exist as distinct SOD

isoforms specific for cell compartments (cytosolic, extracellular and mitochondrial matrix) (198). Within eukaryotic organisms usually one SOD isoform is present per one cell compartment whereas *C. elegans* contains two SOD isoforms for one cell compartment (198). To further test SOD-5 protein levels, I used the *C. elegans* strain expressing GFP-tagged SOD-5 (198). Previous research using this strain carried out by R. Doonan revealed that *sod-5* is expressed in nematodes mostly at dauer stage, and function as an auxiliary isoform (198). Moreover, they showed that *sod-5::gfp* expression is in general observed in ASK, ASI, and ASG neurons (198). Interestingly, the ASG neurons were described to sense the cold through the mechanoreceptor DEG-1, and then regulate cold tolerance in *C. elegans* through the interaction with the interneurons (AIN and AVJ) (124,128). Another interesting issue is the fact that the FTN-1 is specifically expressed in the intestine whereas SOD-5 is mainly present in neurons. However, *ftn-1* overexpression was able to significantly reduce *sod-5* mRNA levels in the cold. It could be possible that an additional factor is involved in this process. Therefore, it would be important to investigate the relationship between intestinal FTN-1 and neuronal SOD-5 in low temperature conditions. Interestingly, it was observed that *sod-5* expression levels are increased in *daf-2* mutants (198). Also, *sod-5* was shown to be upregulated by IIS pathway through DAF-16 binding to the putative DAF-16 binding element (DBE) identified in the promoter region of *sod-5* gene (235). Similarly to *sod-5*, *ftn-1* was shown to be overexpressed in *daf-2* mutants, and regulated in DAF-16-dependent manner at standard cultivation temperatures (88), and in the cold (101). Therefore, the above data indicated that both *sod-5* and *ftn-1* might be regulated in DAF-16-dependent manner in the cold conditions. Additionally, the promoter region of *sod-5* has a putative binding site for SKN-1 (235), which was proposed to mediate resistance to cold stress in *C. elegans* (85). Also, SKN-1 was shown to be a transcription factor crucial for reestablishment of homeostasis after different types of stresses, inter alia, oxidative stress (85). However, it remains unknown whether the activation of *sod-5* expression might be mediated by SKN-1 in cold conditions studied by our group. Moreover, whether DAF-16 and SKN-1 function in parallel during cold response remains to be clarified. Nevertheless, the above data may explain the upregulated levels of *sod-5* and *ftn-1* mRNA after cold exposure. However, how *ftn-1* overexpression was able to reduce *sod-5* expression? Due to the fact that both of these genes are expressed in separate tissues there is a possibility that an unidentified factor mediates the interaction between them. Moreover, this undefined factor probably is able to adjust the levels of response to the levels of oxidative stress generated within the organism. Due to the fact that FTN-1 function as antioxidant, its overexpression is able to reduce ROS levels in *ets-4(-)* mutants (101), thereby the protection

against oxidative stress generated by other ROS-detoxifying factors might be less severe. Therefore, the ROS-lowering *ftn-1* overexpression in the intestine could be sensed via the unidentified factor that transmitted the signal to the neurons. Subsequently, neurons could adjust their response to oxidative stress by ROS-detoxifying SOD-5 according to the ROS levels within the organism. If such a phenomenon exists, it could serve as an explanation of the reduced *sod-5* expression levels in *ftn-1* overexpressing strain in the cold. By contrast, there is also a possibility that the *ftn-1* overexpression in used *C. elegans* strain led to the ectopic expression of *ftn-1* in neurons which had an impact on the *sod-5* expression. Nevertheless, to verify how intestinal expression of *ftn-1* influences neuronal expression of *sod-5* further analysis is required.

6.5 Ferritin in hibernation and hypothermia

The presence of mechanisms involved in antioxidant protection against excess ROS levels is a characteristic feature of some hibernating animals (33,35,37). Small hibernators experience cycles imitating ischemia/reperfusion during hibernation, appearing as periods of torpor and arousal (29,30). However, this phenomenon might cause damages in tissues and organs sensitive to changes in oxygen concentration e.g. the brain. Therefore, it was necessary for hibernators to generate pathways leading to specific antioxidant protection to survive harmful conditions. Interestingly, oxidative damage of the brain was not observed in hibernating animals suggesting the presence of an unique, efficient antioxidant protection (33). Therefore, it is essential to determine the molecular mechanism underlying protection against oxidative stress in tissues and organs of hibernating animals. Interestingly, such antioxidant protection might be achieved by proteins possessing antioxidant function e.g. ferritins (193). It is supported by the fact that the expression levels of genes encoding ferritin subunits were highly elevated in the dwarf lemurs during torpor (159). This suggests a putative role of ferritin in response to increased oxidative stress in hibernating mammals during torpor (159). Additionally, research investigating the ischemia-reperfusion injury on renal tubular epithelial cells showed that hibernating mammals do not experience lipid peroxidation and ferroptotic cell death during anoxia and subsequent reoxygenation in contrast to mouse (236). The specific feature present in hibernating animals was the increased levels of ferritin H subunit during reoxygenation conditions in cells isolated from Syrian hamster (236). These observations prove an essential role of ferritin in the protection against oxidative stress (236). Therapeutic hypothermia is a type of treatment reported to give neuroprotective outcomes (43). Such

neuroprotective effects can be additionally induced by a drug imitating ferritin function, deferoxamine (DFO) (237). It is in agreement with our research showing that DFO allowed neurons to survive cold better than neurons without any treatment. In our research, we examined the function of ferritin in murine neurons exposed to the cold (101). Also, we noticed that the rewarming time after cold exposure resulted in increased levels of Fe^{2+}, which were successfully reduced by the addition of DFO. In agreement with the ferritin role as an antioxidant, we showed that cold treatment of neurons overexpressing *Fth1* led to improved cold survival, reduced levels of ROS, and reduced amount of Fe^{2+} (101). Those results strongly highlight an essential role of ferritin in neuronal protection during cold exposure. Moreover, our results are consistent with other studies also pointing out DFO as a potential drug in therapeutic hypothermia especially in promotion of neuronal survival after hypoxia/ischemia (238). Importantly, research conducted by our group on murine neurons confirmed iron-detoxifying and antioxidant functions of *C. elegans* FTN-1. Above conclusion highlights how powerful simple model organisms are in studying complex processes, especially when the underlying mechanism exhibits high conservation. Moreover, outcomes of our studies might help to improve therapeutic hypothermia applications to cure e.g. several acute brain insults.

6.6 Future perspectives

We found that FTN-1 contributes to the enhanced cold survival observed in *ets-4(-)* mutants. More specifically, FTN-1 protects nematodes against elevated ROS levels resulting from the exposure to cold, through its iron-detoxifying function mediated by ferroxidase activity. Nevertheless, there are still unanswered questions. Importantly, our research revealing the *ftn-1* role in nematodes exposed to cold was performed in the artificial background, where the *C. elegans* strain was lacking ETS-4. In those conditions only *ftn-1* (but not *ftn-2*) was overexpressed relative to the wild type. Even though, the role of FTN-2 in cold protection is not clear, it seems to be relevant because not only iron detoxification, but also iron storage is crucial to prevent the generation of highly toxic hydroxyl radicals via the Fenton reaction (151). It might be possible that another signaling pathway mediates *ftn-2* expression in response to cold. Here, we showed that the *ftn-2* expression levels were elevated (only ~0.8 fold) in cold exposure when compared to standard cultivation conditions, but the effect was not so strong as for *ftn-1* (~10 fold). However, this change was not dependent on the described axis involving transcription factors DAF-16 and PQM-1 (101). By contrast, the HIF signaling pathway was shown to repress the transcription of *ftn-1* and *ftn-2* during low iron concentration through the

binding to HREs in their promoter regions (131). In this study, I revealed that *ftn-1* expression depends on *hif-1* during cold exposure, but this process seems to be independent of ETS-4. However, whether the *ftn-2* expression is influenced by HIF-1 in cold conditions remains to be tested. Interestingly, the ELT-2 transcription factor was shown to be involved in the regulation of *ftn-1* (and probably *ftn-2*) transcription in an iron-dependent manner (108). Moreover, I showed that ELT-2 is also necessary for the induction of the *ftn-1* expression in the cold in an ETS-4-dependent pathway. Due to the fact that all players of the regulatory pathway involved in cold response are not fully established in *C. elegans* yet, further research is needed to identify other factors involved in that process. I would start by investigating the role of *ftn-2* in cold protection. In addition to this, there was no significant difference in the cold survival of the *ftn-2(-)* mutants in comparison to the wild type. Interestingly, in mutants lacking both ferritin genes (*ftn-1* and *ftn-2*) cold survival was indistinguishable from the wild type. However, triple mutants deprived of *ftn-1, ftn-2* and also *ets-4* survived cold even worse than the control suggesting an additional role of *ftn-2* in *ets-4(-)* mutants cold protection (our own data). Nevertheless, to obtain a broader picture, the cold survival utilizing mutants expressing *ftn-1* but deprived of *ftn-2* and *ets-4* should be tested. Due to the fact that amino acid sequences of FTN-1 and FTN-2 are highly conserved and both ferritins possess ferroxidase activity, I would examine if inactivation of the ferroxidase activity in FTN-2 can have an impact on cold survival of nematodes. This approach would help me to verify whether FTN-2 is also involved in cold protection. Subsequently, the strain overexpressing *ftn-2* under strong, cold-resistant promoter should be used to clarify if the increase of *ftn-2* expression levels is able to extend cold survival like I observed for *ftn-1* overexpression. In the following steps, the role of HIF-1 and ELT-2 transcription factors in *ftn-1* and *ftn-2* regulation in response to cold should be examined. In a subsequent step, I would verify whether transcription factor SKN-1, described in previous paragraph, is also involved in the regulation of *ftn-1* expression in response to cold since it was suggested to mediate cold stress resistance in *C. elegans* (85). Additionally, it was shown that certain types of neurons were responsible for cold sensation in cold-shocked nematodes or animals exposed to 15°C (85,114,117,118). Therefore, the analysis whether and/or which neurons are involved in the cold sensation in hibernation-like response might shed light on this mechanism. Furthermore, the iron distribution within the *C. elegans* tissues treated with cold has not been tested in this research. However, as mentioned earlier, a synchrotron-based X-ray fluorescence microscopy used by James et. al. seems to be a powerful method to quantify the spatial distribution of iron in nematodes treated or not with the cold (153). All of the described

examples of future research directions may improve the knowledge about molecular mechanisms involved in the *C. elegans* hibernation-like response.

7 Conclusions

In this research, I investigated the role of *C. elegans* ferritin FTN-1 in cold protection. Based on my results, the main conclusions from this dissertation are as follows:

- *ftn-1* (not *ftn-2*) overexpression significantly contributes to the enhanced cold survival of *ets-4* mutants;
- Tagging of FTN-1 impairs its function, however, the elevated levels of *ftn-1* mRNA seems to correspond with the increased FTN-1 protein levels after three days of cold exposure, especially in the absence of *ets-4* gene;
- The *ftn-1* overexpression significantly enhances cold survival but marginally contributes to the lifespan extension after 5 days of cold treatment;
- The ferroxidase activity of FTN-1 is crucial for the enhancement of cold survival in *ets-4* mutants;
- The presence of antioxidant in the culturing plates improves cold resistance of nematodes;
- The global levels of ROS are elevated in nematodes lacking *ftn-1* and exposed to the cold;
- The levels of *sod-5* mRNA and protein are significantly elevated in nematodes exposed to the cold, suggesting an important role of ROS-detoxifying enzymes in the response to low environmental temperature;
- The levels of *sod-5* mRNA in the cold significantly decrease upon *ftn-1* overexpression;
- ELT-2 and HIF-1 transcription factors are both involved in the *ftn-1* regulation in response to the cold but utilize separate pathways;
- *ftn-1* regulation mediated by HIF-1 seems to be ETS-4-independent, whereas regulation driven by ELT-2 is ETS-4-dependent in the cold;
- FTN-1 is implicated in the response to starvation that is regulated independently of DAF-16/PQM-1 pathway utilized in cold;
- RLE-1 and REGE-1 are involved in cold response by *ets-4* regulation.

8 Attachment

Supplementary Table 1. Statistics for cold survival assay, cold survival assay with antioxidant treatment, and lifespan assay.

FIGURE NUMBER	NAME OF THE COMPARED STRAINS	WILCOXON SIGNED RANK TEST
Figure 6E	*ftn-1(ok3625)* vs *ets-4(rrr16)*	0.00086
	ftn-1(ok3625); ets-4(rrr16) vs *ets-4(rrr16)*	0.00129
	wt vs *ets-4(rrr16)*	0.00089
	ftn-1(ok3625); ets-4(rrr16) vs *ftn-1(ok3625)*	0.00089
	wt vs *ftn-1(ok3625)*	0.25516
	wt vs *ftn-1(ok3625);ets-4(rrr16)*	0.02369
Figure 7D	[P*lips-11*::MYC::*ftn-1*::*ftn-1* 3'UTR; *unc-119(+)*] vs *ets-4(rrr16)*	0.0118
	[P*lips-11*::MYC::*ftn-1*::*ftn-1* 3'UTR; *unc-119(+)*]; *ets-4(rrr16)* vs *ets-4(rrr16)*	0.0076
	wt vs *ets-4(rrr16)*	0.0076
	[P*lips-11*::MYC::*ftn-1*::*ftn-1* 3'UTR; *unc-119(+)*]; *ets-4(rrr16)* vs [P*lips-11*::MYC::*ftn-1*::*ftn-1* 3'UTR; *unc-119(+)*]	1
	wt vs [P*lips-11*::MYC::*ftn-1*::*ftn-1* 3'UTR; *unc-119(+)*]	0.6167
	wt vs [P*lips-11*::MYC::*ftn-1*::*ftn-1* 3'UTR; *unc-119(+)*]; *ets-4(rrr16)*	0.3509
Figure 8D	*sybSi72*[P*vit-5::ftn-1::unc-54* 3'UTR];*unc-119(ed3)* vs *sybSi67*[*Pdpy-30::ftn-1::unc-54* 3'UTR];*unc-119(ed3)*	0.1175
	wt vs *sybSi67*[*Pdpy-30::ftn-1::unc-54* 3'UTR];*unc-119(ed3)*	0.0025
	wt vs *sybSi72*[*Pvit-5::ftn-1::unc-54* 3'UTR];*unc-119(ed3)*	0.0025
Figure 8E	wt vs *sybSi72*[*Pvit-5::ftn-1::unc-54* 3'UTR];*unc-119(ed3)*	0.0067
Figure 9C	*ftn-1(syb2550)* vs *ets-4(rrr16)*	0.00029
	ftn-1(syb2550); ets-4(rrr16) vs *ets-4(rrr16)*	0.00029
	wt vs *ets-4(rrr16)*	0.00029
	ftn-1(syb2550); ets-4(rrr16) vs *ftn-1(syb2550)*	0.34518
	wt vs *ftn-1(syb2550)*	0.01793
	wt vs *ftn-1(syb2550); ets-4(rrr16)*	0.00856
Figure 10A	wt 0 mM NAC vs wt 5 mM NAC	0.00038
Figure 14D	*rle-1(rrr44)* vs *ets-4(rrr16)*	0.00012
	rle-1(rrr44); ets-4(rrr16) vs *ets-4(rrr16)*	0.00039
	wt vs *ets-4(rrr16)*	0.00039
	rle-1(rrr44); ets-4(rrr16) vs *rle-1(rrr44)*	0.0221
	wt vs *rle-1(rrr44)*	0.02239
	wt vs *rle-1(rrr44); ets-4(rrr16)*	0.2558

9 Literature

1. Geiser, F. (2013) Hibernation. *Curr Biol*, **23**, R188-193.
2. Seebacher, F. and Little, A.G. (2017) Plasticity of Performance Curves Can Buffer Reaction Rates from Body Temperature Variation in Active Endotherms. *Front Physiol*, **8**, 575.
3. Grabek, K.R., Martin, S.L. and Hindle, A.G. (2015) Proteomics approaches shed new light on hibernation physiology. *J Comp Physiol B*, **185**, 607-627.
4. Nowack, J., Stawski, C. and Geiser, F. (2017) More functions of torpor and their roles in a changing world. *J Comp Physiol B*, **187**, 889-897.
5. Storey, K.B. (2010) Out cold: biochemical regulation of mammalian hibernation - a mini-review. *Gerontology*, **56**, 220-230.
6. Carey, H.V., Andrews, M.T. and Martin, S.L. (2003) Mammalian hibernation: cellular and molecular responses to depressed metabolism and low temperature. *Physiol Rev*, **83**, 1153-1181.
7. Ratigan, E.D. and McKay, D.B. (2016) Exploring principles of hibernation for organ preservation. *Transplant Rev (Orlando)*, **30**, 13-19.
8. Wolf, A., Lusczek, E.R. and Beilman, G.J. (2018) Hibernation-Based Approaches in the Treatment of Hemorrhagic Shock. *Shock*, **50**, 14-23.
9. Ruf, T. and Geiser, F. (2015) Daily torpor and hibernation in birds and mammals. *Biol Rev Camb Philos Soc*, **90**, 891-926.
10. Blanco, M.B., Greene, L.K., Schopler, R., Williams, C.V., Lynch, D., Browning, J., Welser, K., Simmons, M., Klopfer, P.H. and Ehmke, E.E. (2021) On the modulation and maintenance of hibernation in captive dwarf lemurs. *Sci Rep*, **11**, 5740.
11. Hogan, H.R.H., Hutzenbiler, B.D.E., Robbins, C.T. and Jansen, H.T. (2022) Changing lanes: seasonal differences in cellular metabolism of adipocytes in grizzly bears (Ursus arctos horribilis). *J Comp Physiol B*, **192**, 397-410.
12. Toien, O., Blake, J., Edgar, D.M., Grahn, D.A., Heller, H.C. and Barnes, B.M. (2011) Hibernation in black bears: independence of metabolic suppression from body temperature. *Science*, **331**, 906-909.
13. Gautier, C., Bothorel, B., Ciocca, D., Valour, D., Gaudeau, A., Dupre, C., Lizzo, G., Brasseur, C., Riest-Fery, I., Stephan, J.P., Nosjean, O., Boutin, J.A., Guenin, S.P. and Simonneaux, V. (2018) Gene expression profiling during hibernation in the European hamster. *Sci Rep*, **8**, 13167.
14. Bieber, C. and Ruf, T. (2009) Summer dormancy in edible dormice (Glis glis) without energetic constraints. *Naturwissenschaften*, **96**, 165-171.
15. Chazarin, B., Storey, K.B., Ziemianin, A., Chanon, S., Plumel, M., Chery, I., Durand, C., Evans, A.L., Arnemo, J.M., Zedrosser, A., Swenson, J.E., Gauquelin-Koch, G., Simon, C., Blanc, S., Lefai, E. and Bertile, F. (2019) Metabolic reprogramming involving glycolysis in the hibernating brown bear skeletal muscle. *Front Zool*, **16**, 12.
16. Herinckx, G., Hussain, N., Opperdoes, F.R., Storey, K.B., Rider, M.H. and Vertommen, D. (2017) Changes in the phosphoproteome of brown adipose tissue during hibernation in the ground squirrel, Ictidomys tridecemlineatus. *Physiol Genomics*, **49**, 462-472.
17. Rigano, K.S., Gehring, J.L., Evans Hutzenbiler, B.D., Chen, A.V., Nelson, O.L., Vella, C.A., Robbins, C.T. and Jansen, H.T. (2017) Life in the fat lane: seasonal regulation of insulin sensitivity, food intake, and adipose biology in brown bears. *J Comp Physiol B*, **187**, 649-676.
18. Jansen, H.T., Trojahn, S., Saxton, M.W., Quackenbush, C.R., Evans Hutzenbiler, B.D., Nelson, O.L., Cornejo, O.E., Robbins, C.T. and Kelley, J.L. (2019) Hibernation induces

widespread transcriptional remodeling in metabolic tissues of the grizzly bear. *Commun Biol*, **2**, 336.
19. Wu, C.W., Biggar, K.K. and Storey, K.B. (2013) Biochemical adaptations of mammalian hibernation: exploring squirrels as a perspective model for naturally induced reversible insulin resistance. *Braz J Med Biol Res*, **46**, 1-13.
20. Brown, A.E. and Walker, M. (2016) Genetics of Insulin Resistance and the Metabolic Syndrome. *Curr Cardiol Rep*, **18**, 75.
21. Wilcox, G. (2005) Insulin and insulin resistance. *Clin Biochem Rev*, **26**, 19-39.
22. Chen, Y., Matsushita, M., Nairn, A.C., Damuni, Z., Cai, D., Frerichs, K.U. and Hallenbeck, J.M. (2001) Mechanisms for increased levels of phosphorylation of elongation factor-2 during hibernation in ground squirrels. *Biochemistry*, **40**, 11565-11570.
23. Storey, K.B. and Storey, J.M. (2007) Tribute to P. L. Lutz: putting life on 'pause'--molecular regulation of hypometabolism. *J Exp Biol*, **210**, 1700-1714.
24. Andrews, M.T. (2019) Molecular interactions underpinning the phenotype of hibernation in mammals. *J Exp Biol*, **222**.
25. Mamady, H. and Storey, K.B. (2006) Up-regulation of the endoplasmic reticulum molecular chaperone GRP78 during hibernation in thirteen-lined ground squirrels. *Mol Cell Biochem*, **292**, 89-98.
26. Zhang, J., Wei, Y., Qu, T., Wang, Z., Xu, S., Peng, X., Yan, X., Chang, H., Wang, H. and Gao, Y. (2019) Prosurvival roles mediated by the PERK signaling pathway effectively prevent excessive endoplasmic reticulum stress-induced skeletal muscle loss during high-stress conditions of hibernation. *J Cell Physiol*, **234**, 19728-19739.
27. Morin, P., Jr. and Storey, K.B. (2006) Evidence for a reduced transcriptional state during hibernation in ground squirrels. *Cryobiology*, **53**, 310-318.
28. Knight, J.E., Narus, E.N., Martin, S.L., Jacobson, A., Barnes, B.M. and Boyer, B.B. (2000) mRNA stability and polysome loss in hibernating Arctic ground squirrels (Spermophilus parryii). *Mol Cell Biol*, **20**, 6374-6379.
29. Yin, Q., Ge, H., Liao, C.C., Liu, D., Zhang, S. and Pan, Y.H. (2016) Antioxidant Defenses in the Brains of Bats during Hibernation. *PLoS One*, **11**, e0152135.
30. Orr, A.L., Lohse, L.A., Drew, K.L. and Hermes-Lima, M. (2009) Physiological oxidative stress after arousal from hibernation in Arctic ground squirrel. *Comp Biochem Physiol A Mol Integr Physiol*, **153**, 213-221.
31. Morin, P., Jr., Ni, Z., McMullen, D.C. and Storey, K.B. (2008) Expression of Nrf2 and its downstream gene targets in hibernating 13-lined ground squirrels, Spermophilus tridecemlineatus. *Mol Cell Biochem*, **312**, 121-129.
32. Ma, Y.L., Zhu, X., Rivera, P.M., Toien, O., Barnes, B.M., LaManna, J.C., Smith, M.A. and Drew, K.L. (2005) Absence of cellular stress in brain after hypoxia induced by arousal from hibernation in Arctic ground squirrels. *Am J Physiol Regul Integr Comp Physiol*, **289**, R1297-1306.
33. Wei, Y., Zhang, J., Xu, S., Peng, X., Yan, X., Li, X., Wang, H., Chang, H. and Gao, Y. (2018) Controllable oxidative stress and tissue specificity in major tissues during the torpor-arousal cycle in hibernating Daurian ground squirrels. *Open Biol*, **8**.
34. Carey, H.V., Frank, C.L. and Seifert, J.P. (2000) Hibernation induces oxidative stress and activation of NK-kappaB in ground squirrel intestine. *J Comp Physiol B*, **170**, 551-559.
35. Klichkhanov, N.K., Nikitina, E.R., Shihamirova, Z.M., Astaeva, M.D., Chalabov, S.I. and Krivchenko, A.I. (2021) Erythrocytes of Little Ground Squirrels Undergo Reversible Oxidative Stress During Arousal From Hibernation. *Front Physiol*, **12**, 730657.

36. Wu, C.W. and Storey, K.B. (2014) FoxO3a-mediated activation of stress responsive genes during early torpor in a mammalian hibernator. *Mol Cell Biochem*, **390**, 185-195.
37. Drew, K.L., Toien, O., Rivera, P.M., Smith, M.A., Perry, G. and Rice, M.E. (2002) Role of the antioxidant ascorbate in hibernation and warming from hibernation. *Comp Biochem Physiol C Toxicol Pharmacol*, **133**, 483-492.
38. Wu, C.W., Biggar, K.K., Zhang, J., Tessier, S.N., Pifferi, F., Perret, M. and Storey, K.B. (2015) Induction of Antioxidant and Heat Shock Protein Responses During Torpor in the Gray Mouse Lemur, Microcebus murinus. *Genomics Proteomics Bioinformatics*, **13**, 119-126.
39. Hentze, M.W., Muckenthaler, M.U. and Andrews, N.C. (2004) Balancing acts: molecular control of mammalian iron metabolism. *Cell*, **117**, 285-297.
40. Sun, H., Wang, J., Xing, Y., Pan, Y.H. and Mao, X. (2020) Gut transcriptomic changes during hibernation in the greater horseshoe bat (Rhinolophus ferrumequinum). *Front Zool*, **17**, 21.
41. Chazarin, B., Ziemianin, A., Evans, A.L., Meugnier, E., Loizon, E., Chery, I., Arnemo, J.M., Swenson, J.E., Gauquelin-Koch, G., Simon, C., Blanc, S., Lefai, E. and Bertile, F. (2019) Limited Oxidative Stress Favors Resistance to Skeletal Muscle Atrophy in Hibernating Brown Bears (Ursus Arctos). *Antioxidants (Basel)*, **8**.
42. Andresen, M., Gazmuri, J.T., Marin, A., Regueira, T. and Rovegno, M. (2015) Therapeutic hypothermia for acute brain injuries. *Scand J Trauma Resusc Emerg Med*, **23**, 42.
43. Sun, Y.J., Zhang, Z.Y., Fan, B. and Li, G.Y. (2019) Neuroprotection by Therapeutic Hypothermia. *Front Neurosci*, **13**, 586.
44. Bohl, M.A., Martirosyan, N.L., Killeen, Z.W., Belykh, E., Zabramski, J.M., Spetzler, R.F. and Preul, M.C. (2018) The history of therapeutic hypothermia and its use in neurosurgery. *J Neurosurg*, 1-15.
45. Fay, T. (1959) Early experiences with local and generalized refrigeration of the human brain. *J Neurosurg*, **16**, 239-259; discussion 259-260.
46. Benson, D.W., Williams, G.R., Jr., Spencer, F.C. and Yates, A.J. (1959) The use of hypothermia after cardiac arrest. *Anesth Analg*, **38**, 423-428.
47. Karnatovskaia, L.V., Wartenberg, K.E. and Freeman, W.D. (2014) Therapeutic hypothermia for neuroprotection: history, mechanisms, risks, and clinical applications. *Neurohospitalist*, **4**, 153-163.
48. Kurisu, K., Kim, J.Y., You, J. and Yenari, M.A. (2019) Therapeutic Hypothermia and Neuroprotection in Acute Neurological Disease. *Curr Med Chem*, **26**, 5430-5455.
49. Hypothermia after Cardiac Arrest Study, G. (2002) Mild therapeutic hypothermia to improve the neurologic outcome after cardiac arrest. *N Engl J Med*, **346**, 549-556.
50. Karvellas, C.J., Todd Stravitz, R., Battenhouse, H., Lee, W.M., Schilsky, M.L. and Group, U.S.A.L.F.S. (2015) Therapeutic hypothermia in acute liver failure: a multicenter retrospective cohort analysis. *Liver Transpl*, **21**, 4-12.
51. Kurisu, K. and Yenari, M.A. (2018) Therapeutic hypothermia for ischemic stroke; pathophysiology and future promise. *Neuropharmacology*, **134**, 302-309.
52. Hong, J.M., Lee, J.S., Song, H.J., Jeong, H.S., Choi, H.A. and Lee, K. (2014) Therapeutic hypothermia after recanalization in patients with acute ischemic stroke. *Stroke*, **45**, 134-140.
53. Martirosyan, N.L., Patel, A.A., Carotenuto, A., Kalani, M.Y., Bohl, M.A., Preul, M.C. and Theodore, N. (2017) The role of therapeutic hypothermia in the management of acute spinal cord injury. *Clin Neurol Neurosurg*, **154**, 79-88.
54. Shankaran, S., Laptook, A.R., Ehrenkranz, R.A., Tyson, J.E., McDonald, S.A., Donovan, E.F., Fanaroff, A.A., Poole, W.K., Wright, L.L., Higgins, R.D., Finer, N.N.,

Carlo, W.A., Duara, S., Oh, W., Cotten, C.M., Stevenson, D.K., Stoll, B.J., Lemons, J.A., Guillet, R., Jobe, A.H., National Institute of Child, H. and Human Development Neonatal Research, N. (2005) Whole-body hypothermia for neonates with hypoxic-ischemic encephalopathy. *N Engl J Med*, **353**, 1574-1584.
55. Sadaka, F. and Veremakis, C. (2012) Therapeutic hypothermia for the management of intracranial hypertension in severe traumatic brain injury: a systematic review. *Brain Inj*, **26**, 899-908.
56. Jinka, T.R., Combs, V.M. and Drew, K.L. (2015) Translating drug-induced hibernation to therapeutic hypothermia. *ACS Chem Neurosci*, **6**, 899-904.
57. Frezal, L. and Felix, M.A. (2015) C. elegans outside the Petri dish. *Elife*, **4**.
58. Hunt, P.R. (2017) The C. elegans model in toxicity testing. *J Appl Toxicol*, **37**, 50-59.
59. Leung, M.C., Williams, P.L., Benedetto, A., Au, C., Helmcke, K.J., Aschner, M. and Meyer, J.N. (2008) Caenorhabditis elegans: an emerging model in biomedical and environmental toxicology. *Toxicol Sci*, **106**, 5-28.
60. Consortium, C.e.S. (1998) Genome sequence of the nematode C. elegans: a platform for investigating biology. *Science*, **282**, 2012-2018.
61. Fielenbach, N. and Antebi, A. (2008) C. elegans dauer formation and the molecular basis of plasticity. *Genes Dev*, **22**, 2149-2165.
62. Grishok, A. (2013) Biology and Mechanisms of Short RNAs in Caenorhabditis elegans. *Adv Genet*, **83**, 1-69.
63. Giunti, S., Andersen, N., Rayes, D. and De Rosa, M.J. (2021) Drug discovery: Insights from the invertebrate Caenorhabditis elegans. *Pharmacol Res Perspect*, **9**, e00721.
64. Mendenhall, A., Crane, M.M., Leiser, S., Sutphin, G., Tedesco, P.M., Kaeberlein, M., Johnson, T.E. and Brent, R. (2017) Environmental Canalization of Life Span and Gene Expression in Caenorhabditis elegans. *J Gerontol A Biol Sci Med Sci*, **72**, 1033-1037.
65. Chen, Y.L., Tao, J., Zhao, P.J., Tang, W., Xu, J.P., Zhang, K.Q. and Zou, C.G. (2019) Adiponectin receptor PAQR-2 signaling senses low temperature to promote C. elegans longevity by regulating autophagy. *Nat Commun*, **10**, 2602.
66. Dhakal, R., Yosofvand, M., Yavari, M., Abdulrahman, R., Schurr, R., Moustaid-Moussa, N. and Moussa, H. (2021) Review of Biological Effects of Acute and Chronic Radiation Exposure on Caenorhabditis elegans. *Cells*, **10**.
67. Islam, M.M., Aktaruzzaman, M. and Mohamed, Z. (2015) Comparative sequence-structure analysis of Aves insulin. *Bioinformation*, **11**, 67-72.
68. Kolb, H., Kempf, K., Rohling, M. and Martin, S. (2020) Insulin: too much of a good thing is bad. *BMC Med*, **18**, 224.
69. Galicia-Garcia, U., Benito-Vicente, A., Jebari, S., Larrea-Sebal, A., Siddiqi, H., Uribe, K.B., Ostolaza, H. and Martin, C. (2020) Pathophysiology of Type 2 Diabetes Mellitus. *Int J Mol Sci*, **21**.
70. Sun, X., Chen, W.D. and Wang, Y.D. (2017) DAF-16/FOXO Transcription Factor in Aging and Longevity. *Front Pharmacol*, **8**, 548.
71. Murphy, C.T. and Hu, P.J. (2013) Insulin/insulin-like growth factor signaling in C. elegans. *WormBook*, 1-43.
72. Biglou, S.G., Bendena, W.G. and Chin-Sang, I. (2021) An overview of the insulin signaling pathway in model organisms Drosophila melanogaster and Caenorhabditis elegans. *Peptides*, **145**, 170640.
73. Zecic, A. and Braeckman, B.P. (2020) DAF-16/FoxO in Caenorhabditis elegans and Its Role in Metabolic Remodeling. *Cells*, **9**.
74. Zheng, S., Chiu, H., Boudreau, J., Papanicolaou, T., Bendena, W. and Chin-Sang, I. (2018) A functional study of all 40 Caenorhabditis elegans insulin-like peptides. *J Biol Chem*, **293**, 16912-16922.

75. Li, W., Gao, B., Lee, S.M., Bennett, K. and Fang, D. (2007) RLE-1, an E3 ubiquitin ligase, regulates C. elegans aging by catalyzing DAF-16 polyubiquitination. *Dev Cell*, **12**, 235-246.
76. Hertweck, M., Gobel, C. and Baumeister, R. (2004) C. elegans SGK-1 is the critical component in the Akt/PKB kinase complex to control stress response and life span. *Dev Cell*, **6**, 577-588.
77. Zhao, Y., Zhang, B., Marcu, I., Athar, F., Wang, H., Galimov, E.R., Chapman, H. and Gems, D. (2021) Mutation of daf-2 extends lifespan via tissue-specific effectors that suppress distinct life-limiting pathologies. *Aging Cell*, **20**, e13324.
78. Singh, V. and Aballay, A. (2009) Regulation of DAF-16-mediated Innate Immunity in Caenorhabditis elegans. *J Biol Chem*, **284**, 35580-35587.
79. Kumar, N., Jain, V., Singh, A., Jagtap, U., Verma, S. and Mukhopadhyay, A. (2015) Genome-wide endogenous DAF-16/FOXO recruitment dynamics during lowered insulin signalling in C. elegans. *Oncotarget*, **6**, 41418-41433.
80. Kimura, K.D., Tissenbaum, H.A., Liu, Y. and Ruvkun, G. (1997) daf-2, an insulin receptor-like gene that regulates longevity and diapause in Caenorhabditis elegans. *Science*, **277**, 942-946.
81. Lee, S.S., Kennedy, S., Tolonen, A.C. and Ruvkun, G. (2003) DAF-16 target genes that control C. elegans life-span and metabolism. *Science*, **300**, 644-647.
82. Chiang, W.C., Ching, T.T., Lee, H.C., Mousigian, C. and Hsu, A.L. (2012) HSF-1 regulators DDL-1/2 link insulin-like signaling to heat-shock responses and modulation of longevity. *Cell*, **148**, 322-334.
83. Tullet, J.M., Hertweck, M., An, J.H., Baker, J., Hwang, J.Y., Liu, S., Oliveira, R.P., Baumeister, R. and Blackwell, T.K. (2008) Direct inhibition of the longevity-promoting factor SKN-1 by insulin-like signaling in C. elegans. *Cell*, **132**, 1025-1038.
84. Wolff, S., Ma, H., Burch, D., Maciel, G.A., Hunter, T. and Dillin, A. (2006) SMK-1, an essential regulator of DAF-16-mediated longevity. *Cell*, **124**, 1039-1053.
85. Gulyas, L. and Powell, J.R. (2022) Cold shock induces a terminal investment reproductive response in C. elegans. *Sci Rep*, **12**, 1338.
86. Altintas, O., Park, S. and Lee, S.J. (2016) The role of insulin/IGF-1 signaling in the longevity of model invertebrates, C. elegans and D. melanogaster. *BMB Rep*, **49**, 81-92.
87. Tullet, J.M. (2015) DAF-16 target identification in C. elegans: past, present and future. *Biogerontology*, **16**, 221-234.
88. Ackerman, D. and Gems, D. (2012) Insulin/IGF-1 and hypoxia signaling act in concert to regulate iron homeostasis in Caenorhabditis elegans. *PLoS Genet*, **8**, e1002498.
89. Tepper, R.G., Ashraf, J., Kaletsky, R., Kleemann, G., Murphy, C.T. and Bussemaker, H.J. (2013) PQM-1 complements DAF-16 as a key transcriptional regulator of DAF-2-mediated development and longevity. *Cell*, **154**, 676-690.
90. Lin, X.X., Sen, I., Janssens, G.E., Zhou, X., Fonslow, B.R., Edgar, D., Stroustrup, N., Swoboda, P., Yates, J.R., 3rd, Ruvkun, G. and Riedel, C.G. (2018) DAF-16/FOXO and HLH-30/TFEB function as combinatorial transcription factors to promote stress resistance and longevity. *Nat Commun*, **9**, 4400.
91. Chen, A.T., Guo, C., Dumas, K.J., Ashrafi, K. and Hu, P.J. (2013) Effects of Caenorhabditis elegans sgk-1 mutations on lifespan, stress resistance, and DAF-16/FoxO regulation. *Aging Cell*, **12**, 932-940.
92. Thyagarajan, B., Blaszczak, A.G., Chandler, K.J., Watts, J.L., Johnson, W.E. and Graves, B.J. (2010) ETS-4 is a transcriptional regulator of life span in Caenorhabditis elegans. *PLoS Genet*, **6**, e1001125.

93. Zhao, H., Xu, C., Lee, T.J., Liu, F. and Choi, K. (2017) ETS transcription factor ETV2/ER71/Etsrp in hematopoietic and vascular development, injury, and regeneration. *Dev Dyn*, **246**, 318-327.
94. Sood, A.K., Geradts, J. and Young, J. (2017) Prostate-derived Ets factor, an oncogenic driver in breast cancer. *Tumour Biol*, **39**, 1010428317691688.
95. Luo, C.T., Osmanbeyoglu, H.U., Do, M.H., Bivona, M.R., Toure, A., Kang, D., Xie, Y., Leslie, C.S. and Li, M.O. (2017) Ets transcription factor GABP controls T cell homeostasis and immunity. *Nat Commun*, **8**, 1062.
96. Gallant, S. and Gilkeson, G. (2006) ETS transcription factors and regulation of immunity. *Arch Immunol Ther Exp (Warsz)*, **54**, 149-163.
97. Nye, J.A., Petersen, J.M., Gunther, C.V., Jonsen, M.D. and Graves, B.J. (1992) Interaction of murine ets-1 with GGA-binding sites establishes the ETS domain as a new DNA-binding motif. *Genes Dev*, **6**, 975-990.
98. Oikawa, T. and Yamada, T. (2003) Molecular biology of the Ets family of transcription factors. *Gene*, **303**, 11-34.
99. Shimizu, T., Pastuhov, S.I., Hanafusa, H., Sakai, Y., Todoroki, Y., Hisamoto, N. and Matsumoto, K. (2021) Caenorhabditis elegans F-Box Protein Promotes Axon Regeneration by Inducing Degradation of the Mad Transcription Factor. *J Neurosci*, **41**, 2373-2381.
100. Habacher, C., Guo, Y., Venz, R., Kumari, P., Neagu, A., Gaidatzis, D., Harvald, E.B., Faergeman, N.J., Gut, H. and Ciosk, R. (2016) Ribonuclease-Mediated Control of Body Fat. *Dev Cell*, **39**, 359-369.
101. Pekec, T., Lewandowski, J., Komur, A.A., Sobańska, D., Guo, Y., Świtońska-Kurkowska, K., Małecki, J.M., Dubey, A.A., Pokrzywa, W., Frankowski, M., Figiel, M. and Ciosk, R. (2022) Ferritin-mediated iron detoxification promotes hypothermia survival in Caenorhabditis elegans and murine neurons. *Nat Commun* **13**, 4883.
102. Rajan, M., Anderson, C.P., Rindler, P.M., Romney, S.J., Ferreira Dos Santos, M.C., Gertz, J. and Leibold, E.A. (2019) NHR-14 loss of function couples intestinal iron uptake with innate immunity in C. elegans through PQM-1 signaling. *Elife*, **8**.
103. O'Brien, D., Jones, L.M., Good, S., Miles, J., Vijayabaskar, M.S., Aston, R., Smith, C.E., Westhead, D.R. and van Oosten-Hawle, P. (2018) A PQM-1-Mediated Response Triggers Transcellular Chaperone Signaling and Regulates Organismal Proteostasis. *Cell Rep*, **23**, 3905-3919.
104. Heimbucher, T., Hog, J., Gupta, P. and Murphy, C.T. (2020) PQM-1 controls hypoxic survival via regulation of lipid metabolism. *Nat Commun*, **11**, 4627.
105. Head, B. and Aballay, A. (2014) Recovery from an acute infection in C. elegans requires the GATA transcription factor ELT-2. *PLoS Genet*, **10**, e1004609.
106. Fukushige, T., Hawkins, M.G. and McGhee, J.D. (1998) The GATA-factor elt-2 is essential for formation of the Caenorhabditis elegans intestine. *Dev Biol*, **198**, 286-302.
107. Wiesenfahrt, T., Berg, J.Y., Osborne Nishimura, E., Robinson, A.G., Goszczynski, B., Lieb, J.D. and McGhee, J.D. (2016) The function and regulation of the GATA factor ELT-2 in the C. elegans endoderm. *Development*, **143**, 483-491.
108. Romney, S.J., Thacker, C. and Leibold, E.A. (2008) An iron enhancer element in the FTN-1 gene directs iron-dependent expression in Caenorhabditis elegans intestine. *J Biol Chem*, **283**, 716-725.
109. Mehta, R., Steinkraus, K.A., Sutphin, G.L., Ramos, F.J., Shamieh, L.S., Huh, A., Davis, C., Chandler-Brown, D. and Kaeberlein, M. (2009) Proteasomal regulation of the hypoxic response modulates aging in C. elegans. *Science*, **324**, 1196-1198.
110. Zhang, Y., Shao, Z., Zhai, Z., Shen, C. and Powell-Coffman, J.A. (2009) The HIF-1 hypoxia-inducible factor modulates lifespan in C. elegans. *PLoS One*, **4**, e6348.

111. Pender, C.L. and Horvitz, H.R. (2018) Hypoxia-inducible factor cell non-autonomously regulates C. elegans stress responses and behavior via a nuclear receptor. *Elife*, **7**.
112. Jiang, H., Guo, R. and Powell-Coffman, J.A. (2001) The Caenorhabditis elegans hif-1 gene encodes a bHLH-PAS protein that is required for adaptation to hypoxia. *Proc Natl Acad Sci U S A*, **98**, 7916-7921.
113. Feng, D., Zhai, Z., Shao, Z., Zhang, Y. and Powell-Coffman, J.A. (2021) Crosstalk in oxygen homeostasis networks: SKN-1/NRF inhibits the HIF-1 hypoxia-inducible factor in Caenorhabditis elegans. *PLoS One*, **16**, e0249103.
114. Zhang, B., Xiao, R., Ronan, E.A., He, Y., Hsu, A.L., Liu, J. and Xu, X.Z. (2015) Environmental Temperature Differentially Modulates C. elegans Longevity through a Thermosensitive TRP Channel. *Cell Rep*, **11**, 1414-1424.
115. Klass, M.R. (1977) Aging in the nematode Caenorhabditis elegans: major biological and environmental factors influencing life span. *Mech Ageing Dev*, **6**, 413-429.
116. Morley, J.F. and Morimoto, R.I. (2004) Regulation of longevity in Caenorhabditis elegans by heat shock factor and molecular chaperones. *Mol Biol Cell*, **15**, 657-664.
117. Xiao, R., Zhang, B., Dong, Y., Gong, J., Xu, T., Liu, J. and Xu, X.Z. (2013) A genetic program promotes C. elegans longevity at cold temperatures via a thermosensitive TRP channel. *Cell*, **152**, 806-817.
118. Ohta, A., Ujisawa, T., Sonoda, S. and Kuhara, A. (2014) Light and pheromone-sensing neurons regulates cold habituation through insulin signalling in Caenorhabditis elegans. *Nat Commun*, **5**, 4412.
119. Robinson, J.D. and Powell, J.R. (2016) Long-term recovery from acute cold shock in Caenorhabditis elegans. *BMC Cell Biol*, **17**, 2.
120. Zevian, S.C. and Yanowitz, J.L. (2014) Methodological considerations for heat shock of the nematode Caenorhabditis elegans. *Methods*, **68**, 450-457.
121. Jovic, K., Sterken, M.G., Grilli, J., Bevers, R.P.J., Rodriguez, M., Riksen, J.A.G., Allesina, S., Kammenga, J.E. and Snoek, L.B. (2017) Temporal dynamics of gene expression in heat-stressed Caenorhabditis elegans. *PLoS One*, **12**, e0189445.
122. Kuramochi, M., Takanashi, C., Yamauchi, A., Doi, M., Mio, K., Tsuda, S. and Sasaki, Y.C. (2019) Expression of Ice-Binding Proteins in Caenorhabditis elegans Improves the Survival Rate upon Cold Shock and during Freezing. *Sci Rep*, **9**, 6246.
123. Murray, P., Hayward, S.A., Govan, G.G., Gracey, A.Y. and Cossins, A.R. (2007) An explicit test of the phospholipid saturation hypothesis of acquired cold tolerance in Caenorhabditis elegans. *Proc Natl Acad Sci U S A*, **104**, 5489-5494.
124. Okahata, M., Motomura, H., Ohta, A. and Kuhara, A. (2022) Molecular physiology regulating cold tolerance and acclimation of Caenorhabditis elegans. *Proc Jpn Acad Ser B Phys Biol Sci*, **98**, 126-139.
125. Horikawa, M., Sural, S., Hsu, A.L. and Antebi, A. (2015) Co-chaperone p23 regulates C. elegans Lifespan in Response to Temperature. *PLoS Genet*, **11**, e1005023.
126. Lee, H.J., Noormohammadi, A., Koyuncu, S., Calculli, G., Simic, M.S., Herholz, M., Trifunovic, A. and Vilchez, D. (2019) Prostaglandin signals from adult germ stem cells delay somatic aging of Caenorhabditis elegans. *Nat Metab*, **1**, 790-810.
127. Ujisawa, T., Ohta, A., Ii, T., Minakuchi, Y., Toyoda, A., Ii, M. and Kuhara, A. (2018) Endoribonuclease ENDU-2 regulates multiple traits including cold tolerance via cell autonomous and nonautonomous controls in Caenorhabditis elegans. *Proc Natl Acad Sci U S A*, **115**, 8823-8828.
128. Takagaki, N., Ohta, A., Ohnishi, K., Kawanabe, A., Minakuchi, Y., Toyoda, A., Fujiwara, Y. and Kuhara, A. (2020) The mechanoreceptor DEG-1 regulates cold tolerance in Caenorhabditis elegans. *EMBO Rep*, **21**, e48671.

129. Miller, E.V., Grandi, L.N., Giannini, J.A., Robinson, J.D. and Powell, J.R. (2015) The Conserved G-Protein Coupled Receptor FSHR-1 Regulates Protective Host Responses to Infection and Oxidative Stress. *PLoS One*, **10**, e0137403.
130. Tandara, L. and Salamunic, I. (2012) Iron metabolism: current facts and future directions. *Biochem Med (Zagreb)*, **22**, 311-328.
131. Romney, S.J., Newman, B.S., Thacker, C. and Leibold, E.A. (2011) HIF-1 regulates iron homeostasis in Caenorhabditis elegans by activation and inhibition of genes involved in iron uptake and storage. *PLoS Genet*, **7**, e1002394.
132. Zeidan, R.S., Han, S.M., Leeuwenburgh, C. and Xiao, R. (2021) Iron homeostasis and organismal aging. *Ageing Res Rev*, **72**, 101510.
133. Galaris, D., Barbouti, A. and Pantopoulos, K. (2019) Iron homeostasis and oxidative stress: An intimate relationship. *Biochim Biophys Acta Mol Cell Res*, **1866**, 118535.
134. Wang, J. and Pantopoulos, K. (2011) Regulation of cellular iron metabolism. *Biochem J*, **434**, 365-381.
135. Dev, S. and Babitt, J.L. (2017) Overview of iron metabolism in health and disease. *Hemodial Int*, **21 Suppl 1**, S6-S20.
136. Valentini, S., Cabreiro, F., Ackerman, D., Alam, M.M., Kunze, M.B., Kay, C.W. and Gems, D. (2012) Manipulation of in vivo iron levels can alter resistance to oxidative stress without affecting ageing in the nematode C. elegans. *Mech Ageing Dev*, **133**, 282-290.
137. Anderson, C.P. and Leibold, E.A. (2014) Mechanisms of iron metabolism in Caenorhabditis elegans. *Front Pharmacol*, **5**, 113.
138. Ren, Y., Yang, S., Tan, G., Ye, W., Liu, D., Qian, X., Ding, Z., Zhong, Y., Zhang, J., Jiang, D., Zhao, Y. and Lu, J. (2012) Reduction of mitoferrin results in abnormal development and extended lifespan in Caenorhabditis elegans. *PLoS One*, **7**, e29666.
139. Muckenthaler, M.U., Rivella, S., Hentze, M.W. and Galy, B. (2017) A Red Carpet for Iron Metabolism. *Cell*, **168**, 344-361.
140. Shaw, G.C., Cope, J.J., Li, L., Corson, K., Hersey, C., Ackermann, G.E., Gwynn, B., Lambert, A.J., Wingert, R.A., Traver, D., Trede, N.S., Barut, B.A., Zhou, Y., Minet, E., Donovan, A., Brownlie, A., Balzan, R., Weiss, M.J., Peters, L.L., Kaplan, J., Zon, L.I. and Paw, B.H. (2006) Mitoferrin is essential for erythroid iron assimilation. *Nature*, **440**, 96-100.
141. Huang, J., Chen, S., Hu, L., Niu, H., Sun, Q., Li, W., Tan, G., Li, J., Jin, L., Lyu, J. and Zhou, H. (2018) Mitoferrin-1 is Involved in the Progression of Alzheimer's Disease Through Targeting Mitochondrial Iron Metabolism in a Caenorhabditis elegans Model of Alzheimer's Disease. *Neuroscience*, **385**, 90-101.
142. Rao, A.U., Carta, L.K., Lesuisse, E. and Hamza, I. (2005) Lack of heme synthesis in a free-living eukaryote. *Proc Natl Acad Sci U S A*, **102**, 4270-4275.
143. Chakraborti, S. and Chakrabarti, P. (2019) Self-Assembly of Ferritin: Structure, Biological Function and Potential Applications in Nanotechnology. *Adv Exp Med Biol*, **1174**, 313-329.
144. Gourley, B.L., Parker, S.B., Jones, B.J., Zumbrennen, K.B. and Leibold, E.A. (2003) Cytosolic aconitase and ferritin are regulated by iron in Caenorhabditis elegans. *J Biol Chem*, **278**, 3227-3234.
145. Kim, Y.I., Cho, J.H., Yoo, O.J. and Ahnn, J. (2004) Transcriptional regulation and life-span modulation of cytosolic aconitase and ferritin genes in C.elegans. *J Mol Biol*, **342**, 421-433.
146. Wilkinson, N. and Pantopoulos, K. (2014) The IRP/IRE system in vivo: insights from mouse models. *Front Pharmacol*, **5**, 176.

147. Lee, J.H., Pooley, N.J., Mohd-Adnan, A. and Martin, S.A. (2014) Cloning and characterisation of multiple ferritin isoforms in the Atlantic salmon (Salmo salar). *PLoS One*, **9**, e103729.
148. Chiou, B. and Connor, J.R. (2018) Emerging and Dynamic Biomedical Uses of Ferritin. *Pharmaceuticals (Basel)*, **11**.
149. Zhang, N., Yu, X., Xie, J. and Xu, H. (2021) New Insights into the Role of Ferritin in Iron Homeostasis and Neurodegenerative Diseases. *Mol Neurobiol*, **58**, 2812-2823.
150. Andrews, S.C. (2010) The Ferritin-like superfamily: Evolution of the biological iron storeman from a rubrerythrin-like ancestor. *Biochim Biophys Acta*, **1800**, 691-705.
151. Melman, A. and Bou-Abdallah, F. (2020) Iron mineralization and core dissociation in mammalian homopolymeric H-ferritin: Current understanding and future perspectives. *Biochim Biophys Acta Gen Subj*, **1864**, 129700.
152. Cha'on, U., Valmas, N., Collins, P.J., Reilly, P.E., Hammock, B.D. and Ebert, P.R. (2007) Disruption of iron homeostasis increases phosphine toxicity in Caenorhabditis elegans. *Toxicol Sci*, **96**, 194-201.
153. James, S.A., Roberts, B.R., Hare, D.J., de Jonge, M.D., Birchall, I.E., Jenkins, N.L., Cherny, R.A., Bush, A.I. and McColl, G. (2015) Direct in vivo imaging of ferrous iron dyshomeostasis in ageing Caenorhabditis elegans. *Chem Sci*, **6**, 2952-2962.
154. Goujon, M., McWilliam, H., Li, W., Valentin, F., Squizzato, S., Paern, J. and Lopez, R. (2010) A new bioinformatics analysis tools framework at EMBL-EBI. *Nucleic Acids Res*, **38**, W695-699.
155. Sievers, F., Wilm, A., Dineen, D., Gibson, T.J., Karplus, K., Li, W., Lopez, R., McWilliam, H., Remmert, M., Soding, J., Thompson, J.D. and Higgins, D.G. (2011) Fast, scalable generation of high-quality protein multiple sequence alignments using Clustal Omega. *Mol Syst Biol*, **7**, 539.
156. Kelley, L.A., Mezulis, S., Yates, C.M., Wass, M.N. and Sternberg, M.J. (2015) The Phyre2 web portal for protein modeling, prediction and analysis. *Nat Protoc*, **10**, 845-858.
157. Yin, R., Zhang, J., Xu, S., Kong, Y., Wang, H. and Gao, Y. (2022) Resistance to disuse-induced iron overload in Daurian ground squirrels (Spermophilus dauricus) during extended hibernation inactivity. *Comp Biochem Physiol B Biochem Mol Biol*, **257**, 110650.
158. Biggar, K.K., Wu, C.W., Tessier, S.N., Zhang, J., Pifferi, F., Perret, M. and Storey, K.B. (2015) Modulation of Gene Expression in Key Survival Pathways During Daily Torpor in the Gray Mouse Lemur, Microcebus murinus. *Genomics Proteomics Bioinformatics*, **13**, 111-118.
159. Faherty, S.L., Villanueva-Canas, J.L., Blanco, M.B., Alba, M.M. and Yoder, A.D. (2018) Transcriptomics in the wild: Hibernation physiology in free-ranging dwarf lemurs. *Mol Ecol*, **27**, 709-722.
160. Pizanis, N., Gillner, S., Kamler, M., de Groot, H., Jakob, H. and Rauen, U. (2011) Cold-induced injury to lung epithelial cells can be inhibited by iron chelators - implications for lung preservation. *Eur J Cardiothorac Surg*, **40**, 948-955.
161. Bartels-Stringer, M., Verpalen, J.T., Wetzels, J.F., Russel, F.G. and Kramers, C. (2007) Iron chelation or anti-oxidants prevent renal cell damage in the rewarming phase after normoxic, but not hypoxic cold incubation. *Cryobiology*, **54**, 258-264.
162. Rauen, U., Kerkweg, U., Wusteman, M.C. and de Groot, H. (2006) Cold-induced injury to porcine corneal endothelial cells and its mediation by chelatable iron: implications for corneal preservation. *Cornea*, **25**, 68-77.

163. Huang, H., He, Z., Roberts, L.J., 2nd and Salahudeen, A.K. (2003) Deferoxamine reduces cold-ischemic renal injury in a syngeneic kidney transplant model. *Am J Transplant*, **3**, 1531-1537.
164. Knovich, M.A., Storey, J.A., Coffman, L.G., Torti, S.V. and Torti, F.M. (2009) Ferritin for the clinician. *Blood Rev*, **23**, 95-104.
165. Kell, D.B. and Pretorius, E. (2014) Serum ferritin is an important inflammatory disease marker, as it is mainly a leakage product from damaged cells. *Metallomics*, **6**, 748-773.
166. Mahroum, N., Alghory, A., Kiyak, Z., Alwani, A., Seida, R., Alrais, M. and Shoenfeld, Y. (2022) Ferritin - from iron, through inflammation and autoimmunity, to COVID-19. *J Autoimmun*, **126**, 102778.
167. Kappert, K., Jahic, A. and Tauber, R. (2020) Assessment of serum ferritin as a biomarker in COVID-19: bystander or participant? Insights by comparison with other infectious and non-infectious diseases. *Biomarkers*, **25**, 616-625.
168. Kaushal, K., Kaur, H., Sarma, P., Bhattacharyya, A., Sharma, D.J., Prajapat, M., Pathak, M., Kothari, A., Kumar, S., Rana, S., Kaur, M., Prakash, A., Mirza, A.A., Panda, P.K., Vivekanandan, S., Omar, B.J., Medhi, B. and Naithani, M. (2022) Serum ferritin as a predictive biomarker in COVID-19. A systematic review, meta-analysis and meta-regression analysis. *J Crit Care*, **67**, 172-181.
169. Celma Nos, F., Hernandez, G., Ferrer-Cortes, X., Hernandez-Rodriguez, I., Navarro-Almenzar, B., Fuster, J.L., Bermudez Cortes, M., Perez-Montero, S., Tornador, C. and Sanchez, M. (2021) Hereditary Hyperferritinemia Cataract Syndrome: Ferritin L Gene and Physiopathology behind the Disease-Report of New Cases. *Int J Mol Sci*, **22**.
170. Muhoberac, B.B. and Vidal, R. (2013) Abnormal iron homeostasis and neurodegeneration. *Front Aging Neurosci*, **5**, 32.
171. Muhoberac, B.B. and Vidal, R. (2019) Iron, Ferritin, Hereditary Ferritinopathy, and Neurodegeneration. *Front Neurosci*, **13**, 1195.
172. Ndayisaba, A., Kaindlstorfer, C. and Wenning, G.K. (2019) Iron in Neurodegeneration - Cause or Consequence? *Front Neurosci*, **13**, 180.
173. Biasiotto, G., Di Lorenzo, D., Archetti, S. and Zanella, I. (2016) Iron and Neurodegeneration: Is Ferritinophagy the Link? *Mol Neurobiol*, **53**, 5542-5574.
174. Ayton, S., Faux, N.G., Bush, A.I. and Alzheimer's Disease Neuroimaging, I. (2015) Ferritin levels in the cerebrospinal fluid predict Alzheimer's disease outcomes and are regulated by APOE. *Nat Commun*, **6**, 6760.
175. Zhang, C., Zhang, X. and Zhao, G. (2020) Ferritin Nanocage: A Versatile Nanocarrier Utilized in the Field of Food, Nutrition, and Medicine. *Nanomaterials (Basel)*, **10**.
176. Rodrigues, M.Q., Alves, P.M. and Roldao, A. (2021) Functionalizing Ferritin Nanoparticles for Vaccine Development. *Pharmaceutics*, **13**.
177. Brenner, S. (1974) The genetics of Caenorhabditis elegans. *Genetics*, **77**, 71-94.
178. Frokjaer-Jensen, C., Davis, M.W., Hopkins, C.E., Newman, B.J., Thummel, J.M., Olesen, S.P., Grunnet, M. and Jorgensen, E.M. (2008) Single-copy insertion of transgenes in Caenorhabditis elegans. *Nat Genet*, **40**, 1375-1383.
179. Petersen, L.K. and Stowers, R.S. (2011) A Gateway MultiSite recombination cloning toolkit. *PLoS One*, **6**, e24531.
180. Cheo, D.L., Titus, S.A., Byrd, D.R., Hartley, J.L., Temple, G.F. and Brasch, M.A. (2004) Concerted assembly and cloning of multiple DNA segments using in vitro site-specific recombination: functional analysis of multi-segment expression clones. *Genome Res*, **14**, 2111-2120.
181. Cozzi, A., Corsi, B., Levi, S., Santambrogio, P., Albertini, A. and Arosio, P. (2000) Overexpression of wild type and mutated human ferritin H-chain in HeLa cells: in vivo role of ferritin ferroxidase activity. *J Biol Chem*, **275**, 25122-25129.

182. Torti, F.M. and Torti, S.V. (2002) Regulation of ferritin genes and protein. *Blood*, **99**, 3505-3516.
183. Oh, S.I., Park, J.K. and Park, S.K. (2015) Lifespan extension and increased resistance to environmental stressors by N-acetyl-L-cysteine in Caenorhabditis elegans. *Clinics (Sao Paulo)*, **70**, 380-386.
184. Savion, N., Levine, A., Kotev-Emeth, S., Bening Abu-Shach, U. and Broday, L. (2018) S-allylmercapto-N-acetylcysteine protects against oxidative stress and extends lifespan in Caenorhabditis elegans. *PLoS One*, **13**, e0194780.
185. De Magalhaes Filho, C.D., Henriquez, B., Seah, N.E., Evans, R.M., Lapierre, L.R. and Dillin, A. (2018) Visible light reduces C. elegans longevity. *Nat Commun*, **9**, 927.
186. Schulz, T.J., Zarse, K., Voigt, A., Urban, N., Birringer, M. and Ristow, M. (2007) Glucose restriction extends Caenorhabditis elegans life span by inducing mitochondrial respiration and increasing oxidative stress. *Cell Metab*, **6**, 280-293.
187. Ewald, C.Y., Hourihan, J.M., Bland, M.S., Obieglo, C., Katic, I., Moronetti Mazzeo, L.E., Alcedo, J., Blackwell, T.K. and Hynes, N.E. (2017) NADPH oxidase-mediated redox signaling promotes oxidative stress resistance and longevity through memo-1 in C. elegans. *Elife*, **6**.
188. Rual, J.F., Ceron, J., Koreth, J., Hao, T., Nicot, A.S., Hirozane-Kishikawa, T., Vandenhaute, J., Orkin, S.H., Hill, D.E., van den Heuvel, S. and Vidal, M. (2004) Toward improving Caenorhabditis elegans phenome mapping with an ORFeome-based RNAi library. *Genome Res*, **14**, 2162-2168.
189. Savory, F.R., Sait, S.M. and Hope, I.A. (2011) DAF-16 and Delta9 desaturase genes promote cold tolerance in long-lived Caenorhabditis elegans age-1 mutants. *PLoS One*, **6**, e24550.
190. Davis, C.A., Hitz, B.C., Sloan, C.A., Chan, E.T., Davidson, J.M., Gabdank, I., Hilton, J.A., Jain, K., Baymuradov, U.K., Narayanan, A.K., Onate, K.C., Graham, K., Miyasato, S.R., Dreszer, T.R., Strattan, J.S., Jolanki, O., Tanaka, F.Y. and Cherry, J.M. (2018) The Encyclopedia of DNA elements (ENCODE): data portal update. *Nucleic Acids Res*, **46**, D794-D801.
191. Sammarco, M.C., Ditch, S., Banerjee, A. and Grabczyk, E. (2008) Ferritin L and H subunits are differentially regulated on a post-transcriptional level. *J Biol Chem*, **283**, 4578-4587.
192. He, L., He, T., Farrar, S., Ji, L., Liu, T. and Ma, X. (2017) Antioxidants Maintain Cellular Redox Homeostasis by Elimination of Reactive Oxygen Species. *Cell Physiol Biochem*, **44**, 532-553.
193. Theil, E.C. (2010) Ferritin iron minerals are chelator targets, antioxidants, and coated, dietary iron. *Ann N Y Acad Sci*, **1202**, 197-204.
194. Miranda-Vizuete, A. and Veal, E.A. (2017) Caenorhabditis elegans as a model for understanding ROS function in physiology and disease. *Redox Biol*, **11**, 708-714.
195. Song, S., Zhang, X., Wu, H., Han, Y., Zhang, J., Ma, E. and Guo, Y. (2014) Molecular basis for antioxidant enzymes in mediating copper detoxification in the nematode Caenorhabditis elegans. *PLoS One*, **9**, e107685.
196. Olahova, M., Taylor, S.R., Khazaipoul, S., Wang, J., Morgan, B.A., Matsumoto, K., Blackwell, T.K. and Veal, E.A. (2008) A redox-sensitive peroxiredoxin that is important for longevity has tissue- and stress-specific roles in stress resistance. *Proc Natl Acad Sci U S A*, **105**, 19839-19844.
197. Wang, Y., Branicky, R., Noe, A. and Hekimi, S. (2018) Superoxide dismutases: Dual roles in controlling ROS damage and regulating ROS signaling. *J Cell Biol*, **217**, 1915-1928.

198. Doonan, R., McElwee, J.J., Matthijssens, F., Walker, G.A., Houthoofd, K., Back, P., Matscheski, A., Vanfleteren, J.R. and Gems, D. (2008) Against the oxidative damage theory of aging: superoxide dismutases protect against oxidative stress but have little or no effect on life span in Caenorhabditis elegans. *Genes Dev*, **22**, 3236-3241.
199. Neutelings, T., Lambert, C.A., Nusgens, B.V. and Colige, A.C. (2013) Effects of mild cold shock (25 degrees C) followed by warming up at 37 degrees C on the cellular stress response. *PLoS One*, **8**, e69687.
200. Henderson, S.T. and Johnson, T.E. (2001) daf-16 integrates developmental and environmental inputs to mediate aging in the nematode Caenorhabditis elegans. *Curr Biol*, **11**, 1975-1980.
201. Morris, C., Foster, O.K., Handa, S., Peloza, K., Voss, L., Somhegyi, H., Jian, Y., Vo, M.V., Harp, M., Rambo, F.M., Yang, C. and Hermann, G.J. (2018) Function and regulation of the Caenorhabditis elegans Rab32 family member GLO-1 in lysosome-related organelle biogenesis. *PLoS Genet*, **14**, e1007772.
202. Jeltsch, K.M., Hu, D., Brenner, S., Zoller, J., Heinz, G.A., Nagel, D., Vogel, K.U., Rehage, N., Warth, S.C., Edelmann, S.L., Gloury, R., Martin, N., Lohs, C., Lech, M., Stehklein, J.E., Geerlof, A., Kremmer, E., Weber, A., Anders, H.J., Schmitz, I., Schmidt-Supprian, M., Fu, M., Holtmann, H., Krappmann, D., Ruland, J., Kallies, A., Heikenwalder, M. and Heissmeyer, V. (2014) Cleavage of roquin and regnase-1 by the paracaspase MALT1 releases their cooperatively repressed targets to promote T(H)17 differentiation. *Nat Immunol*, **15**, 1079-1089.
203. Sobanska, D., Komur, A.A., Chabowska-Kita, A., Gumna, J., Kumari, P., Pachulska-Wieczorek, K. and Ciosk, R. (2022) The silencing of ets-4 mRNA relies on the functional cooperation between REGE-1/Regnase-1 and RLE-1/Roquin-1. *Nucleic Acids Res*, **50**, 8226-8239.
204. Ruzzenenti, P., Asperti, M., Mitola, S., Crescini, E., Maccarinelli, F., Gryzik, M., Regoni, M., Finazzi, D., Arosio, P. and Poli, M. (2015) The Ferritin-Heavy-Polypeptide-Like-17 (FTHL17) gene encodes a ferritin with low stability and no ferroxidase activity and with a partial nuclear localization. *Biochim Biophys Acta*, **1850**, 1267-1273.
205. Rucker, P., Torti, F.M. and Torti, S.V. (1996) Role of H and L subunits in mouse ferritin. *J Biol Chem*, **271**, 33352-33357.
206. Levi, S., Ripamonti, M., Dardi, M., Cozzi, A. and Santambrogio, P. (2021) Mitochondrial Ferritin: Its Role in Physiological and Pathological Conditions. *Cells*, **10**.
207. Smith, J.L. (2004) The physiological role of ferritin-like compounds in bacteria. *Crit Rev Microbiol*, **30**, 173-185.
208. Calhoun, L.N. and Kwon, Y.M. (2011) Structure, function and regulation of the DNA-binding protein Dps and its role in acid and oxidative stress resistance in Escherichia coli: a review. *J Appl Microbiol*, **110**, 375-386.
209. de Llanos, R., Martinez-Garay, C.A., Fita-Torro, J., Romero, A.M., Martinez-Pastor, M.T. and Puig, S. (2016) Soybean Ferritin Expression in Saccharomyces cerevisiae Modulates Iron Accumulation and Resistance to Elevated Iron Concentrations. *Appl Environ Microbiol*, **82**, 3052-3060.
210. Martins, T.S., Costa, V. and Pereira, C. (2018) Signaling pathways governing iron homeostasis in budding yeast. *Mol Microbiol*, **109**, 422-432.
211. Mandilaras, K., Pathmanathan, T. and Missirlis, F. (2013) Iron absorption in Drosophila melanogaster. *Nutrients*, **5**, 1622-1647.
212. Mehta, A., Deshpande, A., Bettedi, L. and Missirlis, F. (2009) Ferritin accumulation under iron scarcity in Drosophila iron cells. *Biochimie*, **91**, 1331-1334.

213. Tang, X. and Zhou, B. (2013) Ferritin is the key to dietary iron absorption and tissue iron detoxification in Drosophila melanogaster. *FASEB J*, **27**, 288-298.
214. Lee, J.-H., Wan, K.-L., Mohd-Adnan, A. and Gabaldón, T. (2012) Evolution of the ferritin family in vertebrates. *Trends in Evolutionary Biology*, **4**, p. e3.
215. Zielinska-Dawidziak, M. (2015) Plant ferritin--a source of iron to prevent its deficiency. *Nutrients*, **7**, 1184-1201.
216. Dunkov, B.C. and Georgieva, T. (1999) Organization of the ferritin genes in Drosophila melanogaster. *DNA Cell Biol*, **18**, 937-944.
217. Ruan, P., Hayashida, M., Akutsu, T. and Vert, J.P. (2018) Improving prediction of heterodimeric protein complexes using combination with pairwise kernel. *BMC Bioinformatics*, **19**, 39.
218. Smyth, M.S. and Martin, J.H. (2000) x ray crystallography. *Mol Pathol*, **53**, 8-14.
219. Romero-Afrima, L., Zelmanovich, V., Abergel, Z., Zuckerman, B., Shaked, M., Abergel, R., Livshits, L., Smith, Y. and Gross, E. (2020) Ferritin is regulated by a neuro-intestinal axis in the nematode Caenorhabditis elegans. *Redox Biol*, **28**, 101359.
220. McElwee, J.J., Schuster, E., Blanc, E., Thomas, J.H. and Gems, D. (2004) Shared transcriptional signature in Caenorhabditis elegans Dauer larvae and long-lived daf-2 mutants implicates detoxification system in longevity assurance. *J Biol Chem*, **279**, 44533-44543.
221. James, S.A., Hare, D.J., Jenkins, N.L., de Jonge, M.D., Bush, A.I. and McColl, G. (2016) phiXANES: In vivo imaging of metal-protein coordination environments. *Sci Rep*, **6**, 20350.
222. Kirkwood, T.B. and Kowald, A. (2012) The free-radical theory of ageing--older, wiser and still alive: modelling positional effects of the primary targets of ROS reveals new support. *Bioessays*, **34**, 692-700.
223. Levi, S. and Arosio, P. (2004) Mitochondrial ferritin. *Int J Biochem Cell Biol*, **36**, 1887-1889.
224. Halaschek-Wiener, J., Khattra, J.S., McKay, S., Pouzyrev, A., Stott, J.M., Yang, G.S., Holt, R.A., Jones, S.J., Marra, M.A., Brooks-Wilson, A.R. and Riddle, D.L. (2005) Analysis of long-lived C. elegans daf-2 mutants using serial analysis of gene expression. *Genome Res*, **15**, 603-615.
225. Ma, Y.C., Dai, L.L., Qiu, B.B., Zhou, Y., Zhao, Y.Q., Ran, Y., Zhang, K.Q. and Zou, C.G. (2021) TOR functions as a molecular switch connecting an iron cue with host innate defense against bacterial infection. *PLoS Genet*, **17**, e1009383.
226. Weinkove, D., Halstead, J.R., Gems, D. and Divecha, N. (2006) Long-term starvation and ageing induce AGE-1/PI 3-kinase-dependent translocation of DAF-16/FOXO to the cytoplasm. *BMC Biol*, **4**, 1.
227. Wanby, P., Berglund, J., Brudin, L., Hedberg, D. and Carlsson, M. (2016) Increased ferritin levels in patients with anorexia nervosa: impact of weight gain. *Eat Weight Disord*, **21**, 411-417.
228. Palmer, L.D. and Skaar, E.P. (2016) Transition Metals and Virulence in Bacteria. *Annu Rev Genet*, **50**, 67-91.
229. Ganz, T. and Nemeth, E. (2015) Iron homeostasis in host defence and inflammation. *Nat Rev Immunol*, **15**, 500-510.
230. Kernan, K.F. and Carcillo, J.A. (2017) Hyperferritinemia and inflammation. *Int Immunol*, **29**, 401-409.
231. van den Ecker, D., Hoffmann, M., Muting, G., Maglioni, S., Herebian, D., Mayatepek, E., Ventura, N. and Distelmaier, F. (2015) Caenorhabditis elegans ATAD-3 modulates mitochondrial iron and heme homeostasis. *Biochem Biophys Res Commun*, **467**, 389-394.

232. Catoire, H., Dion, P.A., Xiong, L., Amari, M., Gaudet, R., Girard, S.L., Noreau, A., Gaspar, C., Turecki, G., Montplaisir, J.Y., Parker, J.A. and Rouleau, G.A. (2011) Restless legs syndrome-associated MEIS1 risk variant influences iron homeostasis. *Ann Neurol*, **70**, 170-175.
233. Hsu, A.L., Murphy, C.T. and Kenyon, C. (2003) Regulation of aging and age-related disease by DAF-16 and heat-shock factor. *Science*, **300**, 1142-1145.
234. Quach, T.K., Chou, H.T., Wang, K., Milledge, G.Z. and Johnson, C.M. (2013) Genome-wide microarrray analysis reveals roles for the REF-1 family member HLH-29 in ferritin synthesis and peroxide stress response. *PLoS One*, **8**, e59719.
235. Yanase, S., Yasuda, K. and Ishii, N. (2020) Interaction between the ins/IGF-1 and p38 MAPK signaling pathways in molecular compensation of sod genes and modulation related to intracellular ROS levels in C. elegans. *Biochem Biophys Rep*, **23**, 100796.
236. Eleftheriadis, T., Pissas, G., Liakopoulos, V. and Stefanidis, I. (2019) Factors that May Protect the Native Hibernator Syrian Hamster Renal Tubular Epithelial Cells from Ferroptosis Due to Warm Anoxia-Reoxygenation. *Biology (Basel)*, **8**.
237. Zhang, Y., Fan, B.Y., Pang, Y.L., Shen, W.Y., Wang, X., Zhao, C.X., Li, W.X., Liu, C., Kong, X.H., Ning, G.Z., Feng, S.Q. and Yao, X. (2020) Neuroprotective effect of deferoxamine on erastininduced ferroptosis in primary cortical neurons. *Neural Regen Res*, **15**, 1539-1545.
238. Kletkiewicz, H., Klimiuk, M., Wozniak, A., Mila-Kierzenkowska, C., Dokladny, K. and Rogalska, J. (2020) How to Improve the Antioxidant Defense in Asphyxiated Newborns-Lessons from Animal Models. *Antioxidants (Basel)*, **9**.